

**PRELIMINARY UPDATED GROUNDWATER FLOW AND  
TRANSPORT MODELING REPORT FOR BELEWS CREEK  
STEAM STATION, BELEWS CREEK, NORTH CAROLINA**

**October 2018**

Prepared for  
Duke Energy Carolinas, LLC

Investigators

Ronald W. Falta, Ph.D. – Falta Environmental, LLC  
Regina Graziano, M.S. – SynTerra Corporation  
Rong Yu, Ph.D. – SynTerra Corporation  
Lawrence C. Murdoch, Ph.D. – FRx, Inc.

## TABLE OF CONTENTS

<b>EXECUTIVE SUMMARY .....</b>	<b>ES-1</b>
<b>1.0 INTRODUCTION .....</b>	<b>1</b>
1.1 General Setting and Background .....	1
1.2 Study Objectives .....	4
<b>2.0 CONCEPTUAL MODEL .....</b>	<b>5</b>
2.1 Aquifer System Framework .....	5
2.2 Groundwater Flow System .....	5
2.3 Hydrologic Boundaries .....	6
2.4 Hydraulic Boundaries .....	7
2.5 Sources and Sinks .....	7
2.6 Water Budget .....	7
2.7 Modeled Constituents of Interest .....	7
2.8 Constituent Transport.....	8
<b>3.0 COMPUTER MODEL .....</b>	<b>9</b>
3.1 Model Selection .....	9
3.2 Model Description .....	9
<b>4.0 GROUNDWATER FLOW AND TRANSPORT MODEL CONSTRUCTION .....</b>	<b>10</b>
4.1 Model Domain and Grid .....	10
4.2 Hydraulic Parameters.....	12
4.3 Flow Model Boundary Conditions.....	13
4.4 Flow Model Sources and Sinks.....	14
4.5 Flow Model Calibration Targets .....	15
4.6 Transport Model Parameters.....	16
4.7 Transport Model Boundary Conditions .....	18
4.8 Transport Model Sources and Sinks .....	18
4.9 Transport Model Calibration Targets.....	19
<b>5.0 MODEL CALIBRATION TO CURRENT CONDITIONS .....</b>	<b>20</b>
5.1 Flow Model.....	20
5.2 Flow Model Sensitivity Analysis.....	24
5.3 Historical Transport Model Calibration.....	24
5.4 Transport Model Sensitivity .....	25

## TABLE OF CONTENTS

<b>6.0</b>	<b>PREDICTIVE SIMULATIONS OF CLOSURE SCENARIOS.....</b>	<b>27</b>
6.1	Interim Period with Ash Basin Pond Decanted .....	28
6.2	Excavation Scenario.....	29
6.3	Final Cover Scenario.....	30
6.4	Hybrid Design Scenario.....	33
6.5	Conclusions Drawn from the Predictive Simulations.....	35
<b>7.0</b>	<b>REFERENCES.....</b>	<b>37</b>

## LIST OF TABLES

Table 5-1. Comparison of observed and computed heads for the calibrated flow model.

Table 5-2. Calibrated hydraulic parameters.

Table 5-3. Flow model sensitivity.

Table 5-4. Ash basin boron source concentrations (ug/L) used in historical transport model.

Table 5-5. Comparison of observed and simulated boron (ug/L) in monitoring wells.

Table 5-6. Transport model sensitivity to the boron  $K_d$  values.

## LIST OF FIGURES

Figure ES-1 Simulated boron concentrations transition zone excavation, final cover system, and hybrid simulations

Figure ES-2 Simulated boron concentrations transition zone excavation, final cover system, and hybrid simulations

Figure ES-3 Boron time verse concentration plots transition zone excavation, final cover system, and hybrid simulation

Figure 1-1. Site location map, Belews Creek Steam Station, Stokes County, NC.

Figure 4-1. Numerical model domain.

Figure 4-2. Fence diagram of the 3D hydrostratigraphic model used to construct the model grid.

Figure 4-3. Numerical grid used for flow and transport modeling.

Figure 4-4. Hydraulic conductivity measured in slug tests performed in coal ash at 14 sites in North Carolina.

Figure 4-5. Hydraulic conductivity measured in slug tests performed in saprolite at 10 Piedmont sites in North Carolina.

Figure 4-6. Hydraulic conductivity measured in slug tests performed in the transition zone at 10 Piedmont sites in North Carolina.

Figure 4-7. Hydraulic conductivity measured in slug tests performed in bedrock at 10 Piedmont sites in North Carolina.

Figure 4-8. Distribution of recharge zones in the model.

Figure 4-9. Surface water features included in the model outside of the ash basin area.

Figure 4-10. Surface water features included in the model in the ash basin area.

Figure 4-11. Location of water supply wells in the model area.

Figure 5-1. Zones used to define horizontal hydraulic conductivity and horizontal to vertical anisotropy in the ash basins (model layer 3 shown).

Figure 5-2. Cross-section through ash basin dam showing hydraulic conductivity (colors) and hydraulic heads (lines).

Figure 5-3. Zones used to define horizontal hydraulic conductivity and horizontal to vertical anisotropy in the saprolite, model layers 10-12.

Figure 5-4. Zones used to define horizontal hydraulic conductivity and horizontal to vertical anisotropy in the saprolite, model layers 13-14.

Figure 5-5. Zones used to define horizontal hydraulic conductivity and horizontal to vertical anisotropy in the transition zone, model layer 15.

Figure 5-6. Zones used to define horizontal hydraulic conductivity and horizontal to vertical anisotropy in the fractured bedrock, model layers 16-20.

Figure 5-7. Zones used to define horizontal hydraulic conductivity and horizontal to vertical anisotropy in the deep bedrock, model layers 21-27.

Figure 5-8. Comparison of observed and computed heads from the calibrated steady state flow model.

Figure 5-9. Simulated heads in the transition zone (model layer 15).

Figure 5-10. Simulated heads in the second fractured bedrock model layer (model layer 17)

Figure 5-11. Closeup view of simulated hydraulic heads near the ash basin dam.

Figure 5-12. Groundwater divide and flow directions under current conditions at the BCSS.

Figure 5-13. Approximate groundwater budget under current conditions in the ash basin area.

Figure 5-14. COI source zones for the historical transport model.

Figure 5-15a. Simulated December 2017 boron concentrations ( $\mu\text{g/L}$ ) in the transition zone (layer 15).

Figure 5-15b. Simulated December 2017 boron concentrations ( $\mu\text{g/L}$ ) in the upper bedrock (layer 16).

Figure 6-1. Location of current accelerated remediation wells

Figure 6-2. Simulated hydraulic heads in the transition zone after ash basin pond drainage.

Figure 6-3. Simulated boron concentrations in the transition zone in 2032 for a simulation where the ash basin pond has been decanted, and 10 interim action groundwater extraction wells are operating.

Figure 6-4. Drain network used in excavation simulations to represent springs and streams that may form.

Figure 6-5. Simulated hydraulic heads for excavation scenario with 10 interim action groundwater extraction wells.

Figure 6-6 a,b,c,d. Simulated boron concentrations in the transition zone (layer 15) in 2050 (a), 2100 (b), 2150 (c), and 2200 (d) for the excavation scenario with 10 interim action groundwater extraction wells.

Figure 6-7 a,b,c,d. Simulated boron concentrations in the upper bedrock (layer 16) in 2050 (a), 2100 (b), 2150 (c), and 2200 (d) for the excavation scenario with 10 interim action extraction wells.

Figure 6-8. Locations for boron time-series plots.

Figure 6-9. Predicted boron concentrations at location 1 along Middleton Loop Road for the excavation scenario with 10 interim action groundwater extraction wells.

Figure 6-10. Predicted boron concentrations at location 2 below the ash basin dam for the excavation scenario with 10 interim action groundwater extraction wells.

Figure 6-11. Predicted boron concentrations at location 3 near the Dan River for the excavation scenario with 10 interim action groundwater extraction wells.

Figure 6-12. Proposed ash basin underdrain system for the final cover simulations.

Figure 6-13. Simulated hydraulic heads for the final cover scenario with 10 interim action groundwater extraction wells.

Figure 6-14 a,b,c,d. Simulated boron concentrations in the transition zone (layer 15) in 2050 (a), 2100 (b), 2150 (c), 2200 (d) for the final cover scenario with 10 interim action groundwater extraction wells.

Figure 6-15 a,b,c,d. Simulated boron concentrations in the upper bedrock (layer 16) in 2050 (a), 2100 (b), 2150 (c), 2200 (d) for the final cover scenario with 10 interim action groundwater extraction wells.

Figure 6-16. Predicted boron concentrations at location 1 along Middleton Loop Road for the final cover scenario with 10 interim action groundwater extraction wells.

Figure 6-17. Predicted boron concentrations at location 2 below the ash basin dam for the final cover scenario with 10 interim action groundwater extraction wells.

Figure 6-18. Predicted boron concentrations at location 3 near the Dan River for the final cover scenario with 10 interim action groundwater extraction wells.

Figure 6-19. Hybrid closure design used in simulations

Figure 6-20. Drains used in the hybrid design simulation.

Figure 6-21. Simulated hydraulic heads for the hybrid scenario with 10 interim action groundwater extraction wells.

Figure 6-22 a,b,c,d. Simulated boron concentrations in the transition zone (layer 15) in 2050 (a), 2100 (b), 2150 (c), 2200 (d) for the hybrid scenario with 10 interim action groundwater extraction wells.

Figure 6-23 a,b,c,d. Simulated boron concentrations in the upper bedrock (layer 16) in 2050 (a), 2100 (b), 2150 (c), 2200 (d) for the hybrid scenario with 10 interim action groundwater extraction wells.

Figure 6-24. Predicted boron concentrations at location 1 along Middleton Loop Road for the hybrid scenario with 10 interim action groundwater extraction wells.

Figure 6-25. Predicted boron concentrations at location 2 below the ash basin dam for the hybrid scenario with 10 interim action groundwater extraction wells.

Figure 6-26. Predicted boron concentrations at location 3 near the Dan River for the hybrid scenario with 10 interim action groundwater extraction wells.

Figure 6-27. Comparison of closure options for the transition flow zone - Model years 2050 and 2100

Figure 6-28. Comparison of closure options for the transition flow zone - Model years 2150 and 2200

Figure 6-29. Comparison of closure options for the upper bedrock flow zone - Model years 2050 and 2100

Figure 6-30. Comparison of closure options for the upper bedrock flow zone - Model years 2150 and 2220

## EXECUTIVE SUMMARY

Duke Energy Carolinas, LLC (Duke Energy) owns and operates the Belews Creek Steam Station (BCSS, Plant or Site) in Belews Creek, Stokes County, North Carolina. BCSS is a two-unit coal-fired electricity generating plant with a combined capacity of 2,240 megawatts (MW). The station began commercial operations in 1974 with Unit 1 (1,120 MW) followed by Unit 2 (1,120 MW) in 1975. Cooling water for BCSS is provided by Belews Reservoir which was built for this purpose. Coal combustion residuals (CCR) have historically been managed in the Site's ash basin, on-site landfills and a structural fill. Inorganic compounds in the ash have dissolved and transported in groundwater in the vicinity of the ash basin.

Preliminary numerical simulations of groundwater flow and transport have been calibrated to current conditions and used to evaluate different scenarios being considered as options for closure of the ash basin. The predictive simulations presented herein are not intended to represent a final detailed closure design. These simulations use conceptual designs that are subject to change as the closure plans are finalized. The simulations are intended to show the key characteristics of groundwater flow and mobile constituent transport that are expected to result from the closure actions. This preliminary model report is intended to provide basic model development information and simulations of conceptual basin closure designs. A more detailed model report is planned for inclusion in the groundwater corrective action plan (CAP) scheduled for completion in December 2019.

The model simulations were developed using flow and transport models MODFLOW and MT3DMS. Boron was the constituent of interest (COI) selected to estimate the time to achieve compliance because it is highly mobile in groundwater and tends to have the largest extent of migration. The less mobile, more reactive constituents (i.e. arsenic, selenium, chromium, etc.) will follow the same flow path as boron; however, they generally are not present at concentrations greater than 2L beyond the compliance boundary.



The results of the model simulations indicate the boron plume configuration over time is similar for the three closure scenarios: Excavation, Final Cover and Hybrid<sup>1</sup>. The differences are due primarily to differing locations of potential, closure-specific, compliance boundaries. Three closure-specific compliance boundaries were used to evaluate the results:

- Final Cover scenario is evaluated using a compliance boundary that is 500 ft from the current waste boundary.
- Excavation scenario is evaluated using a compliance boundary that is 250 ft from the current waste boundary.
- Hybrid scenario is evaluated using a compliance boundary 250 ft from the final waste boundary.

The transition zone flow regime future boron concentration comparisons indicate the closure scenarios are equally effective in reducing plume migration for the excavation, final cover system, and hybrid design (Figure ES-1 and ES-2). The time to achieve compliance with the 2L standard at the compliance boundary is approximately 100 to 200 years for the excavation, final cover, and hybrid design scenarios.

Reference locations near the compliance boundary were also used to evaluate changes in boron concentrations with time for the three closure designs. The boron concentrations exceed the 2L standard at the reference locations during historical operation of the ash basin (Figure ES-3). The boron concentrations decrease over the next 150 years with compliance achieved at Point 1 by 2200 with no apparent difference noted between the three closure options. At Point 2, the boron concentrations decrease below the 2L standard relatively quickly by 2050 with no significant difference in the three closure options. The simulation assumptions and the predicted distributions of boron concentration with time are described in the report.

A notable result of the model simulation for year 2020 after the ash basin is decanted, but before closure action construction is complete, is that the natural groundwater divide along

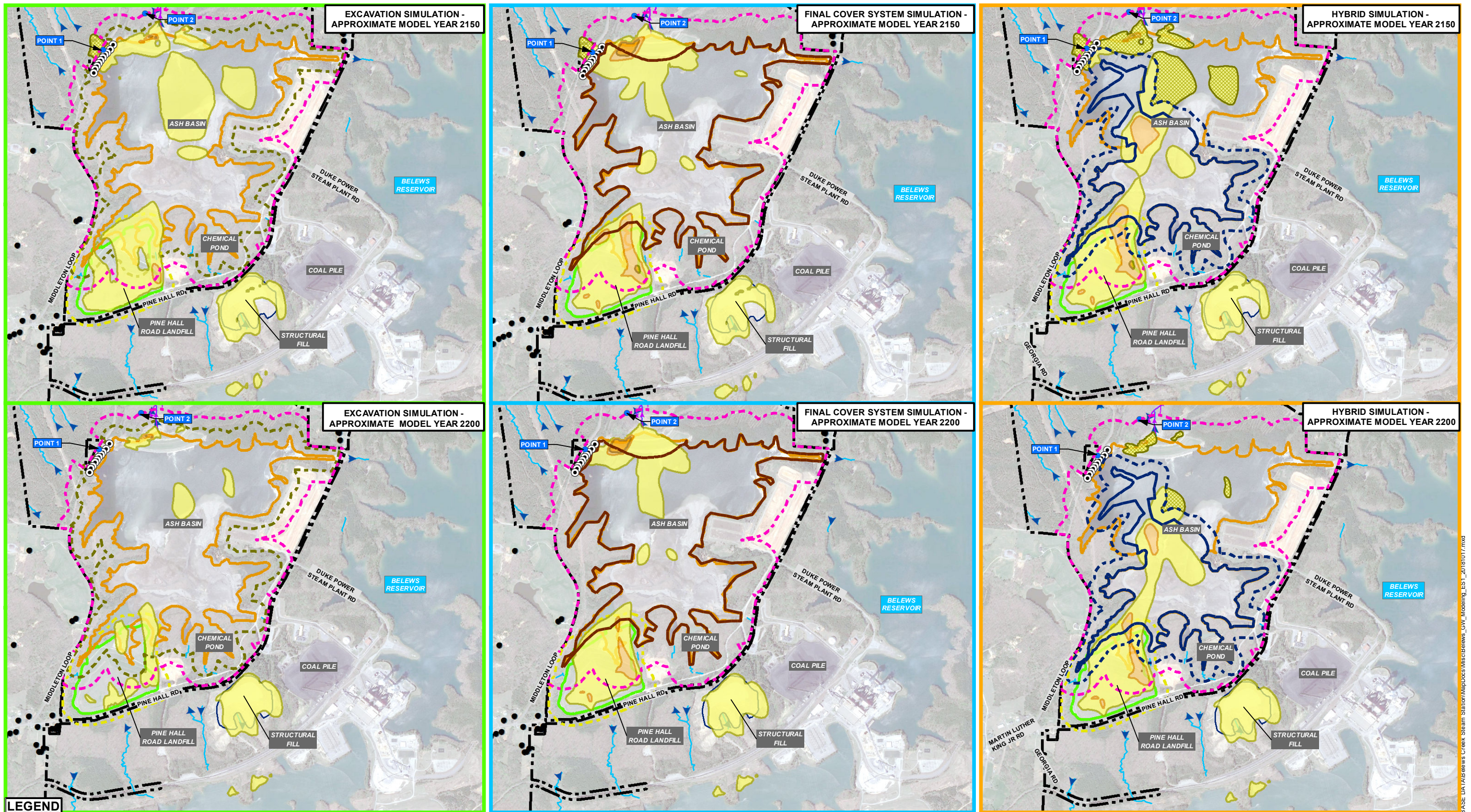
---

<sup>1</sup> It is noted that these modeled scenarios do not include any active form of groundwater remediation with the exception of the interim action groundwater extraction system currently in place. The relative benefits of various groundwater remediation alternatives will be addressed in the CAP. However, preliminary modeling of corrective action (e.g., groundwater extraction) indicates that the relative effectiveness and timeframes required to achieve the applicable standards at the compliance boundaries will not be significantly different between the three closure scenarios considered with those corrective actions; therefore, the comparison of the performance of the closure scenarios via the groundwater modeling presented in this report (without corrective actions) is valid.

Middleton Loop Road, west of the ash basin, will be re-established. The flow from the current interim action groundwater extraction system located in the area will be reduced from approximately 20 gpm to about 4 gpm due to the lower hydraulic head. Boron concentrations greater than the 2L standard are similar beyond the property boundary in the area under all three basin closure scenarios.

Data from recent ash basin and underlying saprolite pumping tests and planned deep bedrock wells within the ash basin dam will reduce model uncertainty, and these results will be incorporated into the next version of this model. The new data are unlikely to change the conclusion that ash basin closure by excavation, a final cover system, and the hybrid closure result in similar boron transport predictions near and beyond the 2L compliance boundary.

The simulations indicate that there are no exposure pathways between the groundwater flow through the ash basin and the pumping wells used for water supply in the vicinity of the Belews Creek site. Domestic and public water supply wells are outside, or upgradient of the groundwater flow system containing the ash basin. Domestic and public water supply wells are not affected by constituents released from the ash basin or by the different closure options, according to the simulations.



**LEGEND**

BORON CONCENTRATION RANGE (>10,000 µg/L)	ASH BASIN WASTE BOUNDARY (CURRENT)	LANDFILL BOUNDARY
BORON CONCENTRATION RANGE (4,000 - 10,000 µg/L)	FINAL COVER SYSTEM EXTENT (AECOM)	STRUCTURAL FILL BOUNDARY
BORON CONCENTRATION RANGE (700 - 4,000 µg/L)	HYBRID SIMULATION WASTE BOUNDARY (AECOM)	DUKE ENERGY CAROLINAS BELEWS CREEK PLANT SITE BOUNDARY
SIMULATED BORON CONCENTRATIONS OUTSIDE CURRENT OR POTENTIAL FUTURE COMPLIANCE BOUNDARY	ASH BASIN COMPLIANCE BOUNDARY (CURRENT)	DESIGNATED EFFLUENT CHANNEL
ACCELERATED REMEDIATION WELL	POTENTIAL COMPLIANCE BOUNDARY ASSOCIATED WITH EXCAVATION	STREAM (AMEC NRTR 2015)
TIME-SERIES PLOT POINT	POTENTIAL COMPLIANCE BOUNDARY ASSOCIATED WITH HYBRID OPTION	
WATER SUPPLY WELL	LANDFILL COMPLIANCE BOUNDARY	

**NOTES:**

THE MODELED TIME TO RETURN TO COMPLIANCE WITH 2L GROUNDWATER STANDARDS IS APPROXIMATELY 100 TO 200 YEARS FOR BOTH THE EXCAVATION AND FINAL COVER SYSTEM OPTIONS USING BORON IN THE TRANSITION ZONE AS THE BASIS FOR THE ESTIMATE.

TRANSITION ZONE RESULTS SHOWN SINCE THIS REPRESENTS THE MOST TRANSMISSIVE ZONE.

THE THREE MODEL SIMULATIONS ARE BASED ON THE COMPLETION DATES FOR THOSE ACTIVITIES. THESE DATES ARE: EXCAVATION - YEAR 2032, FINAL COVER SYSTEM - YEAR 2025, HYBRID - YEAR 2032.

SEE FIGURE 3 FOR TIME VS. CONCENTRATION PLOTS OF BORON AT POINT 1 AND POINT 2.

FINAL COVER SYSTEM EXTENT AND HYBRID WASTE BOUNDARY PROVIDED BY AECOM, INC.

POTENTIAL COMPLIANCE BOUNDARY ASSOCIATED WITH CLOSURE IS 250 FEET FROM WASTE BOUNDARY OR 50 FEET WITHIN THE PROPERTY BOUNDARY, WHICHEVER IS CLOSER TO THE WASTE.

AERIAL PHOTOGRAPHY OBTAINED FROM GOOGLE EARTH PRO ON AUGUST 17, 2017. IMAGE COLLECTED ON APRIL 8, 2017.

DRAWING HAS BEEN SET WITH A PROJECTION OF NORTH CAROLINA STATE PLANE COORDINATE SYSTEM FIPS 3200 (NAD83).

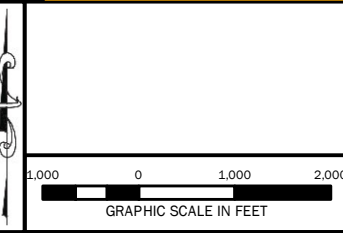
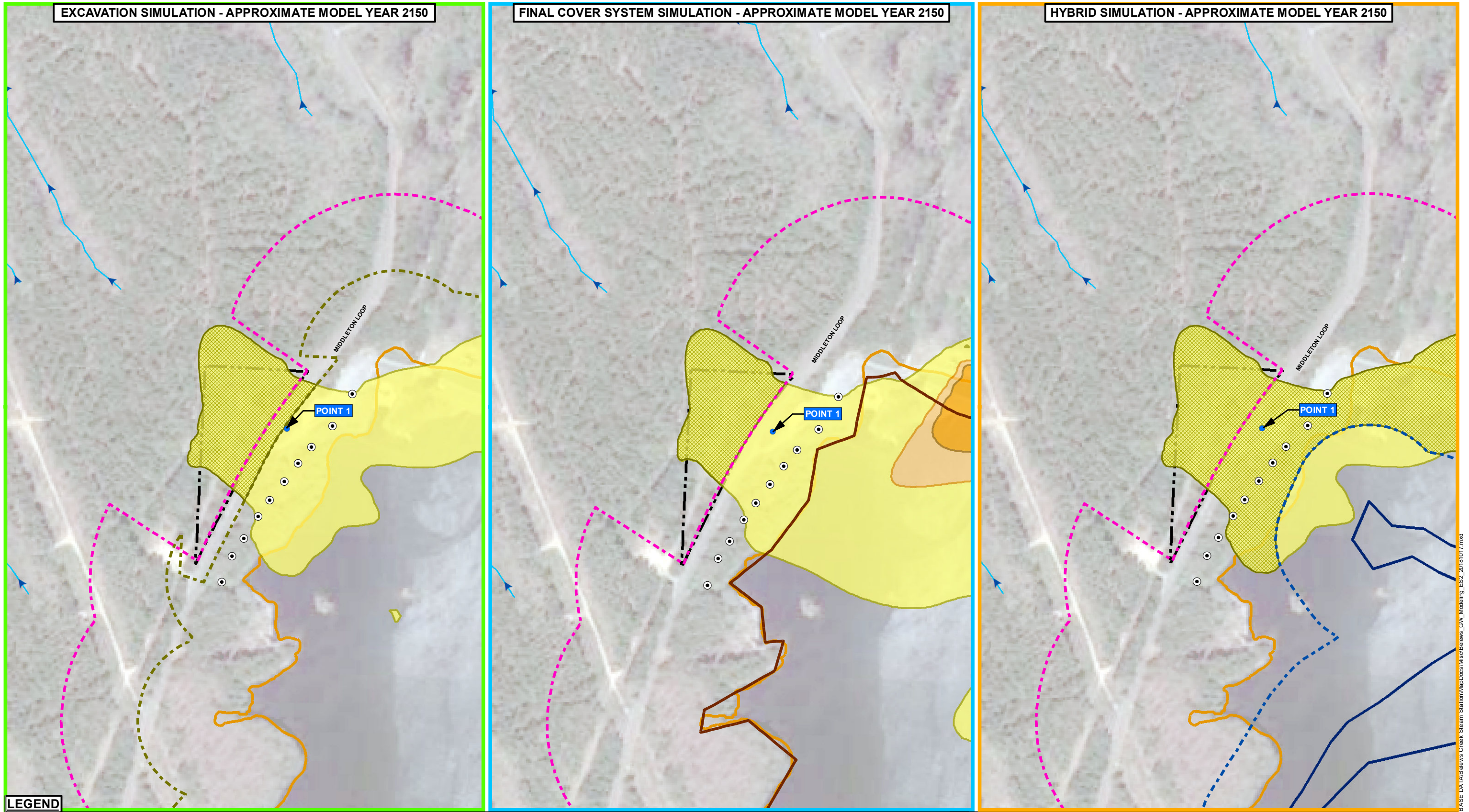


**FIGURE ES-1  
SIMULATED BORON CONCENTRATIONS  
TRANSITION ZONE  
EXCAVATION, FINAL COVER SYSTEM,  
AND HYBRID SIMULATIONS  
BELEWS CREEK STEAM STATION  
DUKE ENERGY CAROLINAS, LLC  
BELEWS CREEK, NORTH CAROLINA**

**EXCAVATION SIMULATION - APPROXIMATE MODEL YEAR 2150**

**FINAL COVER SYSTEM SIMULATION - APPROXIMATE MODEL YEAR 2150**

**HYBRID SIMULATION - APPROXIMATE MODEL YEAR 2150**



**LEGEND**

BORON CONCENTRATION RANGE (>10,000 µg/L)	ASH BASIN WASTE BOUNDARY (CURRENT)
BORON CONCENTRATION RANGE (4,000 - 10,000 µg/L)	FINAL COVER SYSTEM EXTENT (AECOM)
BORON CONCENTRATION RANGE (700 - 4,000 µg/L)	HYBRID SIMULATION WASTE BOUNDARY (AECOM)
SIMULATED BORON CONCENTRATIONS OUTSIDE CURRENT OR POTENTIAL FUTURE COMPLIANCE BOUNDARY	ASH BASIN COMPLIANCE BOUNDARY (CURRENT)
ACCELERATED REMEDIATION WELL	POTENTIAL COMPLIANCE BOUNDARY ASSOCIATED WITH EXCAVATION
TIME-SERIES PLOT POINT	POTENTIAL COMPLIANCE BOUNDARY ASSOCIATED WITH HYBRID OPTION
STREAM (AMEC NRTR 2015)	DUKE ENERGY CAROLINAS BELEWS CREEK PLANT SITE BOUNDARY

**NOTES:**  
 THE MODELED TIME TO RETURN TO COMPLIANCE WITH 2L GROUNDWATER STANDARDS IS APPROXIMATELY 100 TO 200 YEARS FOR BOTH THE EXCAVATION AND FINAL COVER SYSTEM OPTIONS USING BORON IN THE TRANSITION ZONE AS THE BASIS FOR THE ESTIMATE. TRANSITION ZONE RESULTS SHOWN SINCE THIS REPRESENTS THE MOST TRANSMISSIVE ZONE.  
 THE THREE MODEL SIMULATIONS ARE BASED ON THE COMPLETION DATES FOR THOSE ACTIVITIES. THESE DATES ARE: EXCAVATION - YEAR 2032, FINAL COVER SYSTEM - YEAR 2025, HYBRID - YEAR 2032.  
 SEE FIGURE 3 FOR TIME VS. CONCENTRATION PLOTS OF BORON AT POINT 1 AND POINT 2.  
 FINAL COVER SYSTEM EXTENT AND HYBRID WASTE BOUNDARY PROVIDED BY AECOM, INC.  
 POTENTIAL COMPLIANCE BOUNDARY ASSOCIATED WITH CLOSURE IS 250 FEET FROM WASTE BOUNDARY OR 50 FEET WITHIN THE PROPERTY BOUNDARY, WHICHEVER IS CLOSER TO THE WASTE.  
 AERIAL PHOTOGRAPHY OBTAINED FROM GOOGLE EARTH PRO ON AUGUST 17, 2017. IMAGE COLLECTED ON APRIL 8, 2017.  
 DRAWING HAS BEEN SET WITH A PROJECTION OF NORTH CAROLINA STATE PLANE COORDINATE SYSTEM FIPS 3200 (NAD83).

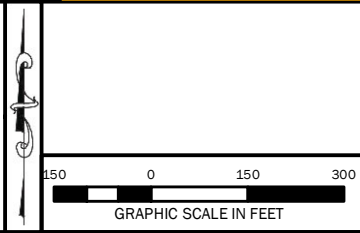
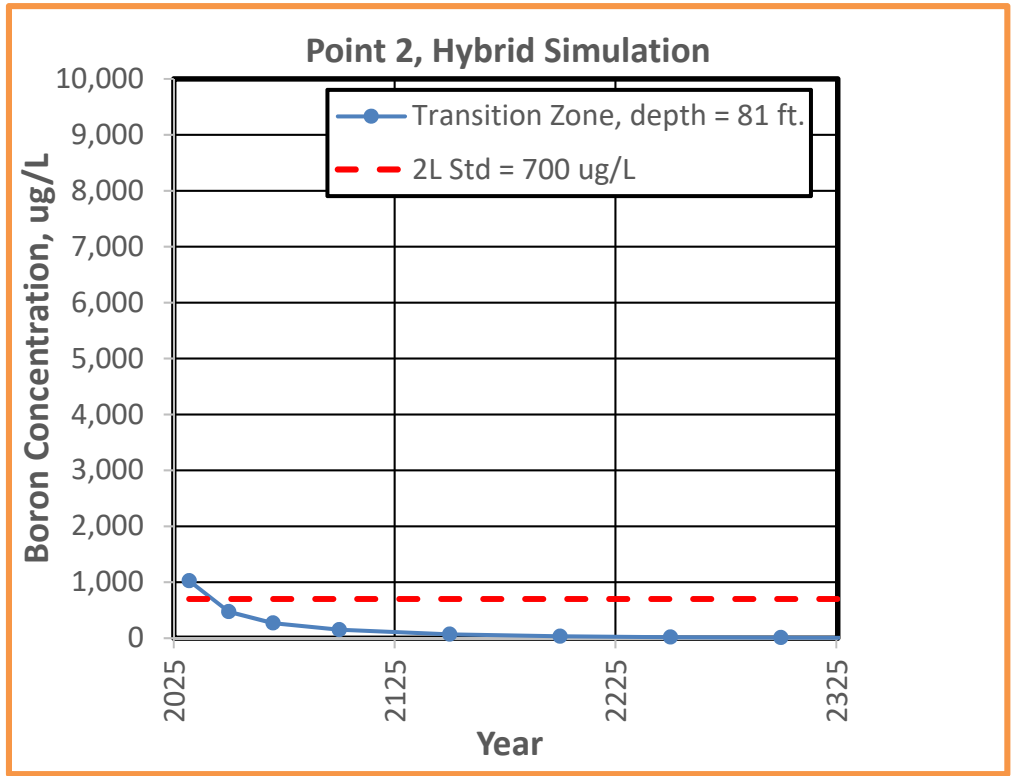
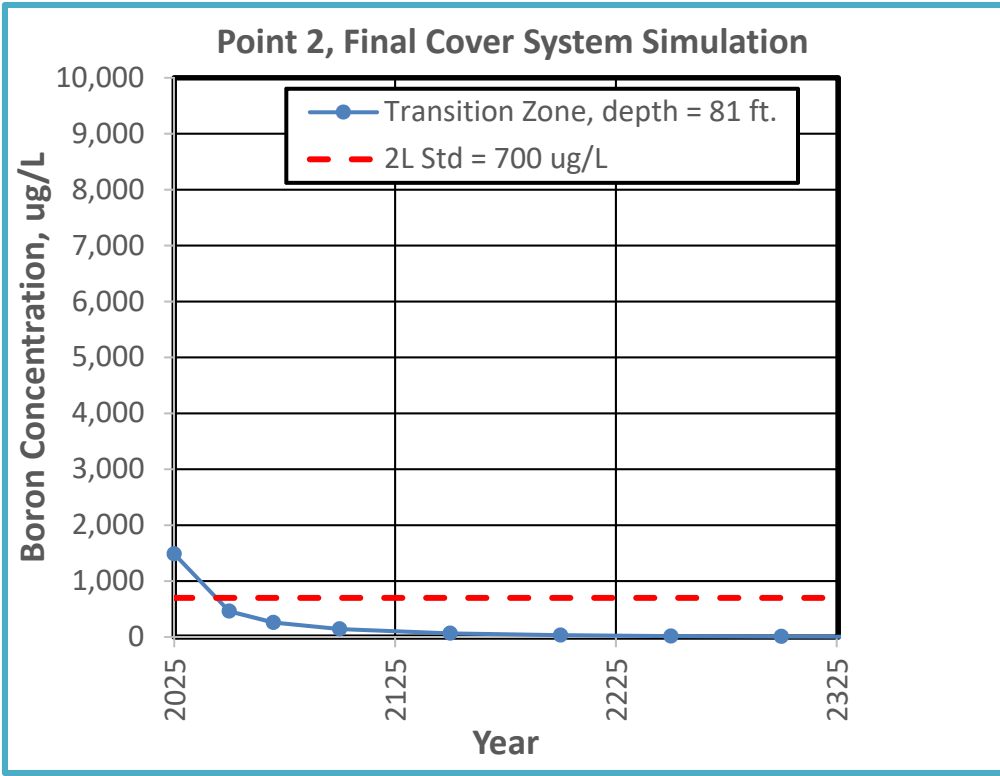
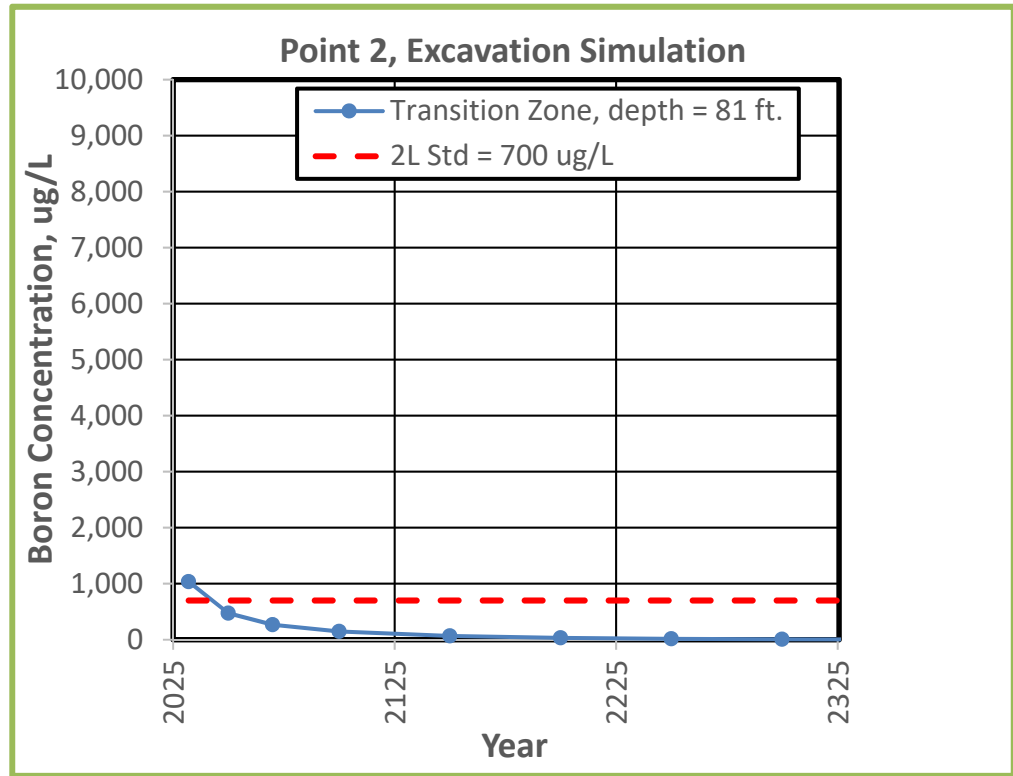
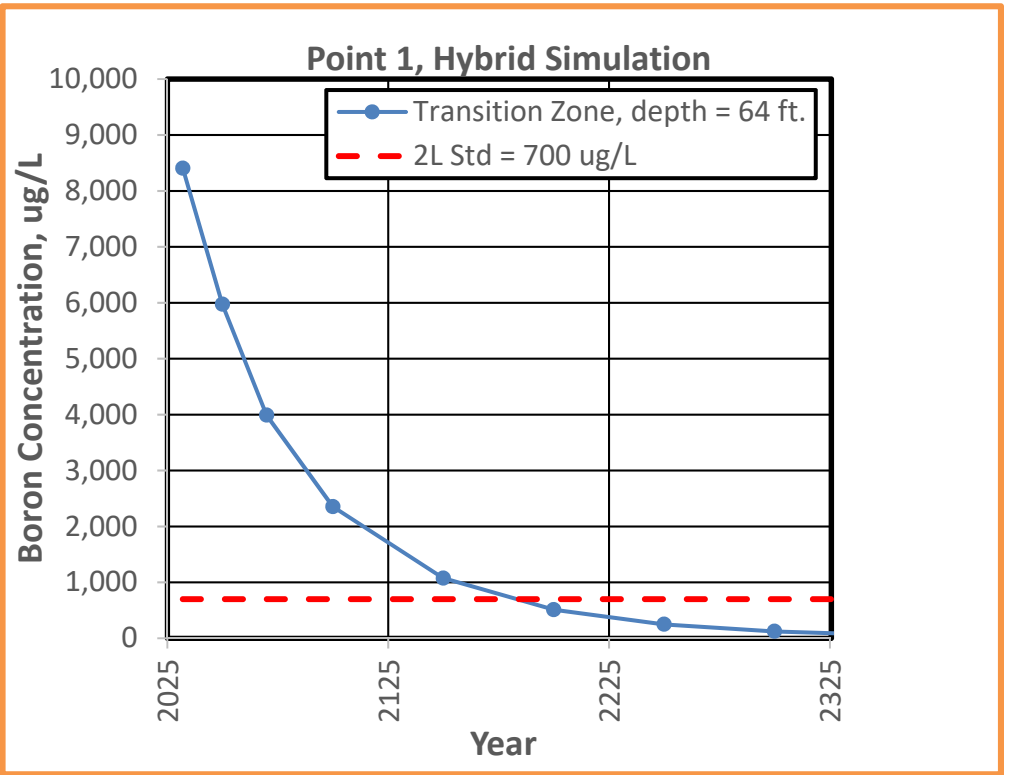
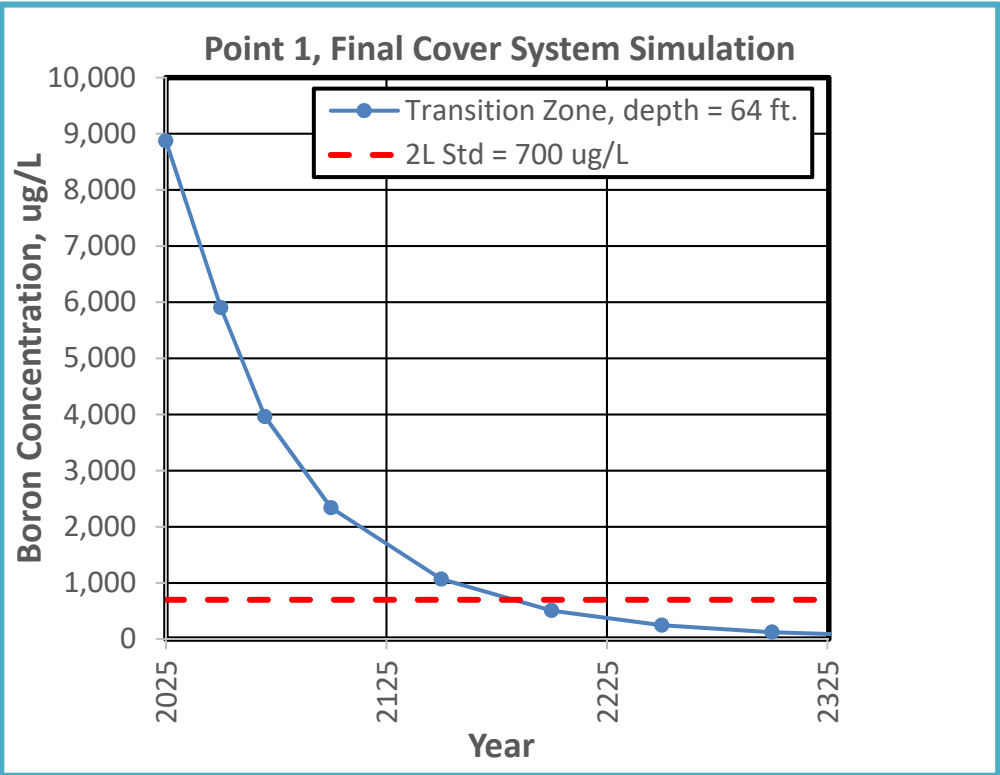
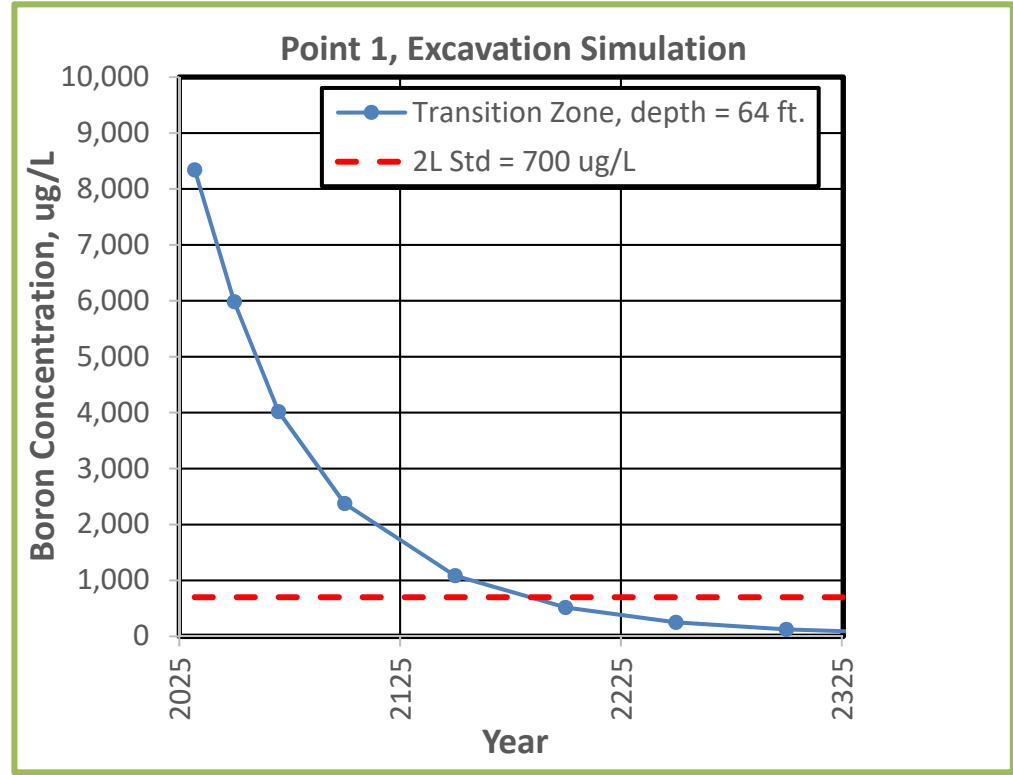


**FIGURE ES-2  
 SIMULATED BORON CONCENTRATIONS  
 TRANSITION ZONE  
 EXCAVATION, FINAL COVER SYSTEM,  
 AND HYBRID SIMULATIONS  
 BELEWS CREEK STEAM STATION  
 DUKE ENERGY CAROLINAS, LLC  
 BELEWS CREEK, NORTH CAROLINA**

P:\Duke Energy Progress\1026300 GIS BASE DATA\Belews Creek Steam Station\MapDocs\Misc\Belews\_GW\_Modeling\_ES2\_20181017.mxd



**NOTES:**  
 THE START DATES FOR THE THREE MODEL SCENARIOS ARE BASED ON THE COMPLETION DATES FOR THOSE ACTIVITIES. THESE DATES ARE:  
 • EXCAVATION – YEAR 2032  
 • FINAL COVER SYSTEM – YEAR 2025  
 • HYBRID – YEAR 2032

ALL THREE SCENARIOS CONSIDER THE OPERATION OF THE 10 EXTRACTION WELLS CURRENTLY IN OPERATION NORTHWEST OF THE ASH BASIN.  
 TRANSITION ZONE RESULTS SHOWN SINCE THIS REPRESENTS THE MOST TRANSMISSIVE ZONE.

**FIGURE ES-3**  
**BORON TIME VS. CONCENTRATION PLOTS**  
**TRANSITION ZONE**  
**EXCAVATION, FINAL COVER SYSTEM, AND HYBRID SIMULATIONS**  
**BELEWS CREEK STEAM STATION**  
**DUKE ENERGY CAROLINAS, LLC**  
**BELEWS CREEK, NORTH CAROLINA**

## 1.0 INTRODUCTION

Duke Energy Carolinas, LLC (Duke Energy) owns and operates the Belews Creek Steam Station (BCSS, Plant or Site) in Belews Creek, Stokes County, North Carolina (Figure 1-1). BCSS is a two-unit coal-fired electricity generating plant with a combined capacity of 2,240 megawatts (MW). The station began commercial operations in 1974 with Unit 1 (1,120 MW) followed by Unit 2 (1,120 MW) in 1975. Cooling water for BCSS is provided by Belews Reservoir, created to serve this purpose. Coal combustion residuals (CCR), composed primarily of fly ash and bottom ash, have historically been managed in the Site's ash basin located north of Pine Hall Road to the west-northwest of the Plant. Inorganic compounds in the ash have dissolved and been transported in groundwater in the vicinity of the ash basin. Preliminary numerical simulations of groundwater flow and transport have been calibrated to current conditions and used to evaluate different scenarios being considered as options for closure of the ash basin. The methods and results of those simulations are described in this report.

### 1.1 General Setting and Background

The BCSS is located in the Piedmont region of North Carolina. The topography in the area is hilly with elevations ranging from a high of about 878 feet<sup>2</sup> near the intersection of Pine Hall Road and Middleton Loop Road, to a low of about 578 feet at the Dan River north of the station. Belews Reservoir, which serves as the cooling lake for the Station has a pool elevation of about 725 feet. The ash basin is located across Pine Hall Road to the northwest of the Plant and is generally bounded by an earthen dam and a natural ridge to the northeast, Middleton Loop Road to the west, and Pine Hall Road to the south and east. Middleton Loop Road and Pine Hall Road are located along topographic ridges that act as groundwater divides that affect groundwater flow within an area approximately 0.5 mile northeast, east, south, and west of the ash basin. The topography slopes downward toward the Dan River north of the earthen dam and natural ridge and west of Middleton Loop Road. To the south and east of Pine Hall Road, the topography generally slopes downward toward Belews Reservoir. The ash basin pond water level is typically maintained at level of 750 feet.

---

<sup>2</sup> The datum for all elevation information presented in the report is NAVD88.

Coal combustion residuals (CCR) were historically sluiced to the ash basin. In 1984, BCSS converted to a dry fly ash handling system, but the ability to sluice fly ash to the ash basin remained available. In accordance with the requirements in CAMA, the units were converted to a 100% dry fly ash disposal system in March 2018 and a dry bottom ash disposal system in May 2018. The most significant volume of wastewater streams placed in the ash basin is FGD wastewater and until recently, sluiced bottom ash. The volume of wastewater discharge to the ash basin has been reduced over the years owing to less runtime for generating units since the units are reserved to provide electricity during peak periods. Wastewater from the ash basin is discharged to the Dan River under NPDES permit NC0024406 from the North Carolina Department of Environmental Quality (NCDEQ) Division of Water Resources (DWR).

The Pine Hall Road (PHR) Landfill, located near the southern edge of the ash basin, began operation in late 1984 after the BCSS converted to dry handling of fly ash and was closed in 2008. The original landfill, which encompassed 37.9 acres, was unlined and was permitted with a soil cap 1-foot-thick on the side slopes and 2 feet thick on flatter areas. A synthetic cap was applied to this area at closure in 2008. A subsequent expansion (Phase I Expansion), which encompassed 14.5 acres, was permitted in 2003. This phase was also unlined and is not covered with a synthetic cap. The total area of the PHR Landfill is 52 acres, and this landfill is located in the watershed that drains to the ash basin.

An unlined structural fill consisting of compacted fly ash was constructed between 2004 and 2009 immediately south of Pine Hall Road. An engineered cover system was installed over the structural fill in 2012. The structural fill is located south of a divide that separates the watershed that includes the ash basin from the Belews Reservoir watershed.

The subsurface at the Site is composed of residual soil/saprolite, a transition zone, and bedrock. Typically, the residual soil/saprolite is partially saturated and the water table fluctuates within it. Water movement is generally preferential through the weathered/fractured and fractured bedrock of the transition zone (i.e., enhanced permeability zone). Groundwater within the Site area exists under unconfined, or water table, conditions within the saprolite, transition zone and in fractures and joints of the underlying bedrock. The shallow water table and bedrock water-bearing zones are interconnected. The saprolite, where saturated thickness is sufficient, acts as a reservoir for supplying groundwater to the fractures and joints in the bedrock. Shallow

groundwater generally flows from local recharge zones in topographically high areas, such as ridges, toward groundwater discharge zones, such as stream valleys.

The groundwater flow and transport model for the BCSS has been under development since 2015. The development process began with a steady-state groundwater flow model and a transient model of constituent transport that were calibrated to field observations resulting from an intensive drilling campaign in early and mid-2015. The first set of simulations were completed in December 2015 (HDR, 2015) and revised in March 2016 (HDR, 2016). The present model domain has been greatly expanded compared to the 2015 model (HDR, 2015), and the number of model layers has been tripled. The earlier model was calibrated to hydraulic heads and COI concentrations measured in 2015. Since that time, significant site activities have taken place including the installation of many additional monitoring wells. The current model has been accordingly revised with respect to the 2015 model. These additional data have further improved the predictive capability and reduce uncertainty in the model results. To take advantage of this potential, the model was recalibrated using data from both the new and existing groundwater wells.

The following data sources were used during calibration of the revised groundwater flow and fate and transport model:

- Average site-wide water levels measured in CAMA/CCR/Compliance groundwater monitoring wells through November 2017.
- Groundwater quality data obtained from CAMA/CCR/Compliance sampling events conducted in November 2017.
- Concentration sources in Pine Hall Road (PHR) Landfill
- Surface water elevations, as described in the CSA Update report (SynTerra, 2017).
- Estimated recharge, as described in the CSA Update report (SynTerra, 2017).

The study consists of three main activities: developing a calibrated steady-state flow model of current conditions, developing historical transient model of boron transport that is calibrated to current conditions, and performing predictive simulations of the possible closure actions at the Site. The predictive simulations include consideration of complete excavation of the coal ash basin at the Site, consideration of a final cover system over the coal ash in the basin,



and a hybrid design that involves excavating ash in the northern part of the basin and placing it in the southern part of the basin with a final engineered cover system.

## **1.2 Study Objectives**

The overall objective of the groundwater flow and transport modeling effort is to predict the performance of three closure scenarios. The goal is for these predictions to guide decisions during the selection of closure actions. The flow and transport models have been undergoing a process of continuous improvement and refinement by including new field data. The continuous improvement process is designed to increase the accuracy and reliability of the performance predictions.

The objective of this model is to describe a subset of the overall results of simulations of boron transport in saprolite, the transition zone, and the underlying fractured rock. The predictive simulations shown here are not intended to represent a final detailed closure design. These simulations use conceptual designs that are subject to change as the closure plans are finalized. The simulations are intended to show the key characteristics of groundwater flow and mobile constituent transport that are expected to result from the closure actions.

## **2.0 CONCEPTUAL MODEL**

The site conceptual model for the BCSS Site is primarily based on the 2015 Comprehensive Site Assessment report (HDR, 2015a), and the 2017 Comprehensive Site Assessment Update (2017 CSA) for the BCSS (SynTerra, 2017). The 2017 CSA Update report contains extensive detail and data related to most aspects of the site conceptual model that are used here.

### **2.1 Aquifer System Framework**

The aquifer system at the Site consists of an unconfined aquifer. Depending on the local topography and hydrogeology, the water table surface may exist in the saprolite, the transition zone, or in the fractured bedrock. At some isolated locations along streambeds, the upper units (saprolite and transition zone) are absent. At other locations, the upper units may be unsaturated, with the water table located in deeper units (fractured bedrock).

The hydraulic conductivity at the BCSS Site has been measured in a series of slug tests in the different units. Fifteen slug tests were performed in the coal ash, with conductivities ranging from 0.08 ft/d to 35 ft/d.

Ten slug tests performed in saprolite wells yielded hydraulic conductivities ranging from 0.22 ft/d to 7.7 ft/d. Eighteen slug tests performed in transition zone wells gave results ranging from 0.002 ft/d to 32 ft/d. Eighteen slug tests conducted in bedrock wells gave hydraulic conductivity values ranging from 0.0008 ft/d to 2.5 ft/d. It should be noted that the bedrock wells are screened near the top of the bedrock surface, and the conductivity of the deeper bedrock would be expected to be lower. The range of observed conductivity in the transition zone and bedrock wells (from nearly zero to 32 ft/d) highlights the very large degree of heterogeneity in the multi-unit system.

### **2.2 Groundwater Flow System**

The unconfined groundwater system at the BCSS is currently dominated by flow from the ash basin pond, which is maintained at an elevation of 750 ft. The basin was constructed by damming the northern side of a former stream valley that is encircled by natural ridges. It is expected that the groundwater and surface water flow system within the valley-basin is separated

from surrounding properties by Middleton Loop Road and Pine Hall Road, which define the topographic ridges. Groundwater flow from the ash basin is generally towards the north and northwest, towards the Dan River with an elevation approximately 578 ft. A groundwater divide exists south and east of the ash basin, approximately along Pine Hall Road. To the south and east of this divide, groundwater flows toward Belews Reservoir at an elevation of 725 ft. A second groundwater divide approximately follows Middleton Loop Road north from the intersection with Pine Hall Road. This groundwater divide is not present in the Middleton Loop Road area near the ash basin dam. Inside the groundwater divides, groundwater flows towards the ash basin.

The groundwater system is recharged from infiltrating rainwater, and from water that infiltrates from the ash basin pond. The average value of recharge in the vicinity of the BCSS was estimated at 8 inches per year. The North Carolina map of recharge by Haven (2003) does not show values for Stokes County, but the average value in adjacent counties is consistent with this estimate. A reduced rate of recharge (1 inch per year) was assumed for the power plant, and an infiltration rate of zero was assumed for the former constructed wetland areas (currently the lined retention basin). The capped areas of the PHR Landfill and structural fill were assigned very low infiltration rates of .00054 in/yr based on results from landfill cover simulations.

There is one public supply well and 50 private water wells that have been identified within one-half mile of the ash basin compliance boundary (SynTerra, 2017). Most of these wells are located northeast of the ash basin along Pine Hall Road and Middleton Loop, and west and southwest of the ash basin along Middleton Loop, Old Plantation Road, Pine Hall Road, and Martin Luther King Jr. Road. Pumping rates for the private wells were not available, and completion depths were only available for a few wells. The wells are situated in distinct drainage basins/slope-aquifer systems separate and/or upgradient relative to groundwater flow from the Plant area and the ash basin.

### **2.3 Hydrologic Boundaries**

The major discharging locations for the shallow water system serve as hydrologic boundaries to the shallow groundwater system. Belews Reservoir and the Dan River serve as major hydrologic boundaries in the area.

## **2.4 Hydraulic Boundaries**

The shallow groundwater system does not appear to contain impermeable barriers or boundaries in the study area, but it does include hydraulic boundaries between zones of different hydraulic conductivity. The degree of fracturing, and thus the hydraulic conductivity, is expected to decrease with depth in metamorphic rock. This will result in blocks of unfractured rock where the hydraulic conductivity is quite low to negligible. However, isolated fractures may occur that result in large local hydraulic conductivities, and the locations of these fractures is difficult to predict or to comprehensively map. It was assumed that the rock was impermeable below the depth of the bottom modeled layer, and a no-flow boundary was used to represent this condition.

## **2.5 Sources and Sinks**

Groundwater flow out of the ash basin pond and areal recharge (rainfall infiltration) are sources of water to the groundwater system. Groundwater discharges to the Dan River, Belews Reservoir, and to numerous small streams. The private water wells within the model area remove only a small amount of water from the overall hydrologic system.

## **2.6 Water Budget**

Over the long term, the rate of water inflow to the study area is equal to the rate of water outflow from the study area. Water enters the groundwater system from the ash basin pond and recharge. Water leaves the system through discharge to the Dan River, Belews Reservoir, several small creeks and through private wells.

## **2.7 Modeled Constituents of Interest**

Antimony, arsenic, barium, beryllium boron, cadmium, chloride, chromium (hexavalent and total), cobalt, iron, manganese, molybdenum, pH, selenium, strontium, sulfate, TDS (total dissolved solids), thallium, and vanadium have been identified as constituents of interest (COIs) for groundwater at the BCSS (SynTerra, 2017).

The COIs that were initially selected for modeling at the BCSS were boron, chloride, and TDS. Selenium was considered, but early simulation results produced poor matches with the observed selenium concentrations in monitoring wells, likely due to the geochemical reactivity of selenium. Boron is the best (most conservative, or proxy) constituent for tracking historical

and future plume migration because it is almost always present in plumes from CCR releases at concentrations higher than background. Boron is also not subject to chemical attenuation under normal aquifer conditions (low reactivity, low  $K_d$ ).

Boron is present at relatively high concentrations in the ash basin, near and beneath the PHR Landfill, and near the structural fill. A boron plume extends to monitoring wells north and west of the ash basin. Boron is found in monitoring wells screened in the saprolite, the transition zone, and the bedrock. Boron concentrations in background monitoring wells are far below 2L standards, and are generally less than the laboratory detection limit. Other conservative constituents have similar  $K_d$  values but are not present in such large concentrations in the source area or are present naturally in regional groundwater. Attenuation for these conservative COIs primarily occurs through physical means (i.e., dispersion, dilution, and diffusion). This preliminary model report will focus exclusively on boron because boron is the dominant mobile constituent.

The remaining constituents were not considered for the modeling exercise for one or more of the following reasons: 1) concentrations in the ash pore water do not greatly exceed likely background levels; and 2) there is no discernable plume of the constituent extending downgradient from the ash basin. The reactive, non-conservative parameters subject to chemical attenuation have relatively high  $K_d$  (i.e., greater than 10 L/kg) under all probable pH and  $E_H$  conditions at BCSS. The relatively high  $K_d$  values are due to sorption, ion exchange, and (co)precipitation. Therefore, their migration potential is significantly limited, meaning that the plume is small and sometimes discontinuous.

## **2.8 Constituent Transport**

The COIs that are present in the coal ash dissolve into the ash pore water. As water infiltrates through the ash, water containing COIs can enter the groundwater system. Once in the groundwater system, the COIs are transported by advection and dispersion, subject to retardation due to sorption to solids. If the COIs reach a hydrologic boundary or water sink, they are removed from the groundwater system, and they enter the surface water system, where in general, they are greatly diluted.

## 3.0 COMPUTER MODEL

### 3.1 Model Selection

The numerical groundwater flow model was developed using MODFLOW (McDonald and Harbaugh, 1988), a three-dimensional (3D) finite difference groundwater model created by the United States Geological Survey (USGS). The chemical transport model is a new version the Modular 3-D Transport Multi-Species (MT3DMS) model (Zheng and Wang, 1999). MODFLOW and MT3DMS are widely used in industry and government, and are considered to be industry standards. The models were assembled using the Aquaveo GMS 10.3 graphical user interface (<http://www.aquaveo.com/>).

### 3.2 Model Description

MODFLOW uses Darcy's law and the conservation of mass to derive water balance equations for each finite difference cell. MODFLOW considers 3D transient groundwater flow in confined and unconfined heterogeneous systems, and it can include dynamic interaction with pumping wells, recharge, evapotranspiration, rivers, streams, springs, lakes, and swamps.

This study uses the MODFLOW-NWT version (Niswonger, et al., 2011). The NWT version of MODFLOW provides improved numerical stability and accuracy for modeling problems with variable water tables. That improved capability is helpful in the present work where the position of the water table in the ash basin can fluctuate depending on the conditions under which the basin is operated and the various closure scenario simulations.

Some of the Belews Creek flow models were challenging to run due to the topography and layers that become unsaturated in the model. It was found that using the NWT solver options "MODERATE" with the xMD matrix solver could overcome these difficulties.

MT3DMS uses the groundwater flow field from MODFLOW to simulate 3D advection and dispersion of the dissolved COIs including the effects of retardation due to COI adsorption on the soil and rock matrix.

## **4.0 GROUNDWATER FLOW AND TRANSPORT MODEL CONSTRUCTION**

The flow and transport model for this site was built through a series of steps.

- Step 1: Build a 3D model of the site hydrostratigraphy based on field data.
- Step 2: Determine the model domain and construction of the numerical grid.
- Step 3: Populate the numerical grid with flow parameters
- Step 4: Calibrate the steady-state flow model to current hydraulic heads with adjustments of the flow parameters
- Step 5: Develop a transient model of historical flow and transport to provide time-dependent constituent transport development.
- Step 6: Calibration to recent boron concentration field data to ensure the model reproduces the observed boron plumes.

The process of revising the model involved using the initial updated model as a starting point and following an iterative process of adjusting parameters until the model adequately predicted the observed heads and concentrations.

### **4.1 Model Domain and Grid**

The initial steps in the model grid generation process were the determination of the model domain, and the construction of a 3D hydrostratigraphic model. The model has dimensions of about 13,000 ft by 13,000 ft and it is oriented in a North-South orientation. (Figure 4-1). The model is generally bounded to the north by the Dan River and Town Fork Creek. It is also bounded by Belews Reservoir to the south and east. The model boundary is located several deep creek drainages away from the ash basin to the west and the northeast. The distance to the boundary from the ash basin is large enough to prevent boundary conditions from artificially affecting the results near the basin.

The ground surface of the model was developed by HDR and was interpolated from the North Carolina Floodplain Mapping Program's 2010 Light Detection and Ranging (LiDAR) elevation data. These data were supplemented by on-site surveys conducted by Duke Energy in 2014. The elevations used for the top of the ash surface in the ash basin pond were modified

from the bathymetric data to provide a model surface that can accommodate planned regrading of ash for the final cover or hybrid closure options. For current conditions simulations, this part of the ash in the model is given a large hydraulic conductivity to represent the open water conditions in the basin pond.

The hydrostratigraphic model (called a solids model in GMS) consists of five units: ash, saprolite, transition zone, upper fractured bedrock, and deeper bedrock. The contact elevations between these units were determined from boring logs from previous studies by HDR (2015a, 2016). The contact elevations were estimated by HDR for locations where well logs were not available by extrapolation of the borehole data using the Leapfrog Hydro geologic modeling tool. This program was used by HDR to develop surfaces defining the top of the saprolite, transition zone, and bedrock. While the contact between the upper units (ash, saprolite, transition zone, bedrock) are well defined, the division of the bedrock into an upper fractured zone and deeper bedrock was subjective. For the purposes of model construction, the upper fractured zone is approximately 180 feet thick. The deeper bedrock extends another 530 feet below the upper zone for a total bedrock thickness of 710 feet in the model. The upper bedrock zone in the model was given a heterogeneous hydraulic conductivity distribution to represent more and less fractured zones.

Figure 4-2 shows a fence diagram of the 3D hydrostratigraphic unit viewed from the northwest, with a vertical exaggeration of 2x. The light grey material corresponds to the ash in the basin, the light tan material is the saprolite, the orange material is the transition zone, the brown hatched material is the upper fractured part of the bedrock, and the dark grey material is the deep bedrock.

The numerical model grid is shown in Figure 4-3. The grid is discretized in the vertical direction using the solids model (Figure 4-2) to define the numerical model layers. The top 9 model layers represent the ash basin, including the dams that form the basin, the PHR Landfill, and the structural fill. Model layers 10-14 represent the saprolite. Model layer 15 represents the transition zone. Model layers 16-20 represent the upper fractured part of the bedrock, while model layers 21 to 27 represent deeper parts of the bedrock (which also may be fractured). The model varies in thickness from about 730 ft to 810 ft.



The discretization in the horizontal direction is variable with smaller grid cells in and around the ash basin area. The minimum horizontal grid spacing in the finely divided areas is about 20 ft, while the maximum grid spacing near the outer edges of the model is about 150 ft. The grid contains a total of 987,192 active cells in 27 layers.

#### **4.2 Hydraulic Parameters**

The horizontal hydraulic conductivity and the horizontal to vertical hydraulic conductivity anisotropy ratio are the main hydraulic parameters in the model. The distribution of these parameters is based primarily on the model hydrostratigraphy, with additional horizontal and vertical variation. Most of the hydraulic parameter distributions in the model were heterogeneous across a model layer. The geometries and parameter values of the heterogeneous distributions were determined during the flow model calibration process. Initial estimates of parameters were based on literature values, results of slug and core tests, and simulations performed using a preliminary flow model. The hydraulic parameter values were adjusted during the flow model calibration process described in Section 5.0 to provide a best fit to observed water levels in observation wells. Slug test data from hundreds of wells at the Duke Energy coal ash basin sites in North Carolina are shown in Figures 4-4 through 4-7.

The hydraulic conductivity of coal ash measured at 14 sites in North Carolina ranges over about 4 orders of magnitude, with a median value of about 1.6 ft/d (Figure 4-4). Ash hydraulic conductivity values measured in slug tests at Belews Creek ranged from 0.07 ft/d to 35 ft/d. The current conditions flow model is insensitive to the ash conductivity, but the predicted heads in the final cover simulations are sensitive to the ash hydraulic conductivity. Two pumping tests were recently conducted within the ash basin including the underlying saprolite from 9/10/2018 to 9/12/2018 and in the ash material within the basin from 9/26/2018 to 9/27/2018 to help refine the value of these unit specific parameters. Results of these tests are expected to yield an estimate of the ash properties that is more representative of site conditions. The simulations will be revised when the data from the pumping tests have been evaluated. Results from the revised simulations will be presented in future versions of the flow and transport model.

The hydraulic conductivities from hundreds of slug tests performed in saprolite wells at 10 Piedmont sites are shown in Figure 4-5. These also range over 4 or more orders of magnitude, and have a median value of 1.0 ft/d. Saprolite slug tests performed at Belews Creek

ranged from 0.2 ft/d to 7.7 ft/d. Transition zone hydraulic conductivities from hundreds of slug tests at 10 Piedmont sites are shown in Figure 4-6. These range over 6 orders of magnitude, with a median value of 0.97 ft/d. The measured values at Belews Creek range from 0.002 ft/d to 32 ft/d.

Slug test results from bedrock from hundreds of wells at 10 Piedmont sites in North Carolina (Figure 4-7) range over more than 6 orders of magnitude, with a median value of 0.5 ft/d. It is possible that this median value is larger than the true average value for bedrock for three reasons. First, the bedrock wells are almost all screened in the uppermost few tens of feet of the bedrock, which is expected to be more highly fractured than deeper bedrock zones. Second, the wells are normally screened in zones with visible flowing fractures, rather than in zones with intact unfractured rock. Finally, wells that do not produce water are not slug tested. These factors likely bias the slug test data to higher values than may be representative of the bedrock as a whole. At Belews Creek, the measured values from slug tests in shallow bedrock ranged from 0.0008 ft/d to 2.5 ft/d.

### **4.3 Flow Model Boundary Conditions**

Belews Reservoir forms a hydraulic boundary south and east of the ash basin. The lake is treated as a specified constant head boundary in the uppermost active model layer with an elevation of 725 ft. The Dan River and Town Fork Creek are located north and northeast of the ash basin, and these are treated as specified head boundaries in the uppermost active model layer. The water elevations here range from a maximum of 590 ft in the western part of Town Fork Creek, to 575 ft in the eastern part of the Dan River.

The western model boundary does not align with any clearly defined hydraulic features. This boundary is located almost a mile from the ash basin, and there are several deep creek valleys between the model boundary and the basin. Most of the western boundary is treated as a general head boundary with the head set to an elevation of 20 feet below the top of the saprolite, except in stream valleys, where a no flow boundary is used perpendicular to the streams. The flow in these valleys is dominated by flow towards the streams, which are modeled as drains. The northeastern boundary is treated as a no flow boundary as it crosses several stream valleys approximately perpendicular to the streams, which are treated as drains in the model. This boundary is also almost a mile away from the ash basin.

#### 4.4 Flow Model Sources and Sinks

The flow model sources and sinks consist of Belews Reservoir, the Dan River and Town Fork Creek, the ash basin pond, recharge, streams, and wet areas that are assumed to directly drain into the ash basin pond.

Recharge is a significant hydrologic parameter in the model, and the distribution of recharge zones in the model is shown in Figure 4-8. As described in Section 2.2, the recharge rate for the BCSS Site was estimated to be 8 inches/year. The recharge rate for the BCSS Plant was set to 1 inch per year due to the large areas of roof and pavement. The ash basin pond is treated as a specified head boundary and has zero rainfall recharge, but the part of the basin south of the pond has a reduced rate of 4 inches per year except near the pond, where the rate was set to zero. The water table in this location is very close to the ground surface, and heavy rain events likely result in runoff to the basin pond rather than in infiltration to the groundwater system. The use of higher recharge rates in the model in this area resulted in unrealistic flooding of the top of the model. The recharge rate in the dam was set to 2 inches per year, and it was set to zero in the stream valley below the dam, which is a groundwater discharge area. The recharge rate was set to zero in the former constructed wetlands areas (currently the lined retention basin). The recharge rate through the PHR Landfill and structural fill covers was set to 0.00054 inches per year based on landfill cover simulations.

Belews Reservoir, the Dan River, Town Fork Creek, and the ash basin pond were treated as specified head zones in the model (Figures 4-9 and 4-10). Belews Reservoir is maintained at an elevation of 725 ft and the ash basin is maintained at an elevation of 750 ft. Town Fork Creek and the Dan River range from an elevation of 590 ft in the upstream part of Town Fork Creek, to an elevation of 575 ft in the downstream part of Dan River.

The many creeks exert a significant local control on the hydrology in the model. These features are shown as green lines in Figure 4-9. The position of these creeks was determined mainly from the topographic map (Figure 1-1), supplemented by two site visits where each drainage feature near the ash basin was inspected. The elevation of locations along the creeks were determined from the surface LiDAR elevations, and were assumed to be 2 feet below the ground surface. The creeks were simulated using the DRAIN feature in MODFLOW with a high conductance value ( $500 \text{ ft}^2/\text{d}/\text{ft}$ ).

The southern part of the ash basin contains several areas of standing water, along with two main sluicing channels. Inspection of these wet areas suggests that they drain to the main ash basin pond during periods of high water. These wet areas and the sluice channels were treated as drains in the current conditions model (Figure 4-10). The ash basin dam contains a blanket drain at an approximate elevation of 648 feet, and this is included in the model (Figure 4-9).

Figure 4-11 shows the location of public and private water supply wells in the model area. There is one public supply well in the model domain, located in the northeastern part of the model, along Pine Hall Road at the Withers Chapel United Methodist Church. The average flow rate from this well is not known, and was assumed to be 7,500 gallons per day in the model based on available well records for the public supply well (HDR, 2015a). The depth of this well is not known and the well was assumed to draw from the upper bedrock model layer (layer 16).

There are 64 private wells inside the model boundary. Of those, there were 50 wells that were identified within a 0.5 mile radius of the ash basin compliance boundary (SynTerra, 2017) due to the fact that the model extends about a mile beyond the ash basin waste boundary. Where depth data were available, the private wells were screened over the known depth. In most cases, the well depths were unknown, and the wells were assumed to be screened in the upper part of the bedrock in model layer 16. The pumping rates from the wells were unknown, but the model simulated a pumping rate of 280 gals/day, which is an average water use for a family of four (Treece et al. 1990; North Carolina Water Use, 1987, and 1995). Septic return was assumed to be 94% of the pumping rate, based on Treece et al. (1990), Daniels et al. (1997) and Radcliffe et al. (2006). The septic return was injected into layer 10 (saprolite) in the model.

#### **4.5 Flow Model Calibration Targets**

The steady state flow model calibration targets were the 130 water level measurements made in observations wells in the 4<sup>th</sup> quarter of 2017 and the flow rate of water through and immediately underneath the ash basin dam. This flow is measured at location S-11 in the channel just downstream from the dam. The flow rate measured at S-11 appears to be variable in time, with an average rate of about 180 gpm. All sampled wells are included in the calibration. These wells include wells screened in each of the hydrostratigraphic units, including many sets of nested wells.

#### 4.6 Transport Model Parameters

The transport model uses a time-dependent MODFLOW simulation to provide the time-dependent groundwater velocity field. The MODFLOW simulation started January 1974, and it continued through December 2017. The transient flow field is approximated as a series of flow fields that correspond to conditions at different times as the PHR Landfill and the structural fill were capped with an engineered cover system for closure of those units. The transient flow field was modeled as three successive steady state flow fields; one corresponding to the site conditions before the PHR Landfill and structural fill locations were capped (1974-2008), one corresponding to conditions after the PHR Landfill was capped, but before the structural fill was capped (2008-2012), and one after both were capped (2012-2017). Capping of the PHR Landfill and the structural fill were simulated by reducing the recharge rate from 8 inches per year to 0.00054 inches per year in those areas.

The key transport model parameters (besides the flow field) are the boron source concentrations in the ash, and the boron soil-water distribution coefficient ( $K_d$ ). Other parameters are the longitudinal, transverse, and vertical dispersivity, and the effective porosity. The boron source concentrations in the ash basin, PHR Landfill, and structural fill were initially estimated from the ash pore water concentrations and from concentrations in nearby wells. During the transport model calibration process, the basin and other areas were subdivided, and different concentrations were assigned to different zones at different times. The timing of boron sources appearing in the PHR Landfill and structural fill locations correspond to the time when they became active (1985 and 2004, respectively). Source concentrations of the boron are held constant at the specified levels in the ash layers during the historical transport simulation, but they are allowed to vary in time during the predictive simulations that follow.

The numerical treatment of adsorption in the model requires special consideration because part of the system is a porous media (ash, saprolite, and transition zone) with a relatively high porosity, while the bedrock is a fractured media with very low matrix porosity and permeability. As a result, transport in the fractured bedrock occurs almost entirely through the fractures. The MODFLOW and MT3DMS flow and transport models used here simulated the fractured bedrock as an equivalent porous media. With this approach, an effective hydraulic conductivity is assigned to the fractured rock zones so that it produces the correct Darcy flux

(volume of water per area of media per time) for a given hydraulic gradient. However, because the water flows almost entirely through the fractures, this approach requires that a small effective porosity value (~0.01 or less) be used for the transport calculations to compute a realistic flow velocity.

The COI retardation factor is computed internally in the MT3DMS code using a conventional approach:

$$R = 1 + \frac{\rho_b K_d}{\phi}$$

Where  $\rho_b$  is the bulk density and  $\phi$  is the porosity. If typical porous media values are used for the bulk density and  $K_d$ , the resulting retardation factor in the fractured media becomes unrealistically large due to the low porosity value. In the current model, the calibrated boron  $K_d$  value was 0.4 mL/g for the saprolite and transition zone. Considering the fractured bedrock, with a conservative bulk density of 1.6 g/mL and a porosity of 0.01, a  $K_d$  value of 0.4 mL/g results in a retardation factor is 65, which is unrealistically high for boron transport. To avoid this problem, the boron was assigned a much lower  $K_d$  value in the bedrock layers of the model so that it would have a reasonable retardation factor during transport through the fractured media.

Ash leaching tests were performed on 5 samples from the Belews Creek ash basin using US EPA (LEAF) Method 1316. The leaching data were analyzed to develop a  $K_d$  (partition coefficient) value for boron in the coal ash. The average of those test values was 0.46 mL/g. The modeling approach for the predictive simulations of future boron transport allow the boron concentration in the ash to vary with time in response to flushing by groundwater. Using the  $K_d$  value that is derived from ash leaching tests ensures that the model response of the boron in the ash to groundwater flushing is realistic.

The  $K_d$  value for the boron outside of the ash basin was treated as a calibration parameter. Boron is expected to be mobile, and to have a low  $K_d$  value. The calibrated  $K_d$  values for the saprolite and transition zone layers were 0.4 mL/g. In the fractured bedrock, a much lower value was used as described above of 0.02 mL/g.

The longitudinal dispersivity was assigned a value of 20 ft, the transverse dispersivity was set to 2 ft, and the vertical dispersivity was set to 0.2 ft. The effective porosity was set to a value of 0.3 in the unconsolidated layers, and to 0.01 in all of the bedrock layers. The soil dry bulk density was set to 1.6 g/mL.

#### **4.7 Transport Model Boundary Conditions**

The transport model boundary conditions are no flow on the exterior edges of the model except where constant or general head boundaries exist, where they are specified as a concentration of zero. All of the constant head water bodies (lakes, river, and pond), have a fixed concentration of zero. As water containing dissolved constituents enters these zones, the dissolved mass is removed from the model. The infiltrating rainwater is assumed to be clean, and enters from the top of the model. The ash basin pond receives special treatment, where the water level is maintained using a constant head hydraulic boundary, but the boron concentration is specified in model cells below the water surface.

The initial condition for the current conditions transport model (back in 1974) is one of zero concentration of boron everywhere in the model. No background concentrations are considered.

#### **4.8 Transport Model Sources and Sinks**

The ash basin, PHR Landfill, and structural fill are the sources of boron in the model. During the historical transport simulation, these sources are simulated by holding the boron concentration constant in cells located inside the ash in these zones. The boron concentrations from the historical transport simulation form the initial condition for the predictive simulations of future transport at the Site. The predictive simulations do not hold the boron concentrations constant in the ash source zones, and this mobile constituent can wash out of the ash over time. The boron  $K_d$  value used for the ash was measured in ash leaching tests using ash from the Site to ensure that the simulated boron leaching rate is realistic.

Impacted soil and rock at the Site can continue to serve as a source for groundwater contamination by the boron at the site. This potential is fully accounted for in the model by continuously tracking the boron concentrations in time in the saprolite, transition zone, and rock materials throughout the model. The historical transport model simulates the migration of boron

through the soil and rock from the ash basin, and these results are used as the starting concentrations for the predictive simulations. Therefore, even if all of the coal ash is excavated, the transport model predicts ongoing impacts to groundwater from the contaminated soil beneath the ash.

The transport model sinks are the constant head lakes, river, ponds, creeks, and drains. As groundwater enters these features, it is removed along with any dissolved constituent mass. Similarly, if water containing a constituent were to encounter a pumping well, the constituent is removed with the water.

#### **4.9 Transport Model Calibration Targets**

The transport model calibration targets are boron concentrations measured in 142 monitoring wells in the 4<sup>th</sup> quarter of 2017. All sampled wells are included in the calibration.



## 5.0 MODEL CALIBRATION TO CURRENT CONDITIONS

### 5.1 Flow Model

The flow model was calibrated in stages starting with a relatively simple layered model. All calibration was done by trial and error, simultaneously matching the recent water levels measured in observation wells (Table 5-1), and matching the flow through and immediately under the ash basin dam that is measured at S-11. Additional flow model calibration was required to also match the current conditions boron distribution. The primary calibration parameters are the three-dimensional distribution of hydraulic conductivity. Each model layer has been subdivided into hydraulic conductivity zones. These model conductivity zones are shown in Figures 5-1 through 5-7, and the calibrated hydraulic conductivity values assigned to each zone in each layer are listed in Table 5-2.

Starting at the top, in layers 1-9, the layers represent both the coal ash and the ash basin dam. It was important to calibrate the conductivity of the dam fill material in these layers (Figures 5-1 and 5-2) in order to match the high head values in wells located in and near the dam, and to match the substantial flow through the dam. The dam fill material is thicker in deeper layers to approximate a 3:1 dam slope (Figure 5-2), and it has a calibrated conductivity of 0.8 ft/d. This relatively high value for the conductivity of the dam fill was required in order to simultaneously match hydraulic heads of wells in and below the dam, and the leakage through and immediately under the dam.

In the current steady-state flow model, a high hydraulic conductivity (200 ft/d) was applied to the ash basin pond to represent open water (Figure 5-2). The hydraulic conductivity of the ash was assumed to be 2.0 ft/d. The current conditions flow model is insensitive to the ash conductivity because the water levels around the ash basin are controlled by the ash basin pond elevation. The value of 2.0 ft/d that was used is close to the median of more than 200 slug tests performed at 14 coal ash basin sites in North Carolina shown in Figure 4-4, and it falls within the range of values measured at Belews Creek. Although the current conditions model is insensitive to this parameter, the predictive final cover simulations are more sensitive to the ash conductivity. Pumping tests in the Belews Creek ash basin were performed in late 2018 to improve the understanding of the coal ash hydraulic conductivity at the BCSS. The simulations

will be revised when the data from the pumping tests have been evaluated. Results from the revised simulations will be presented in a future report revision.

The calibrated background hydraulic conductivity for the saprolite (layers 10-14) was 0.5 ft/d, which falls near the average value for slug tests performed in saprolite at 10 coal ash basin sites in the Piedmont of North Carolina, and for slug tests performed at Belews Creek (Figure 4-5). This material is heterogeneous and zones of both higher and lower conductivity were required to match the hydraulic heads, flow under the dam, and boron transport near the dam (Figures 5-3 and 5-4, and Table 5-2). The range of saprolite conductivity in the model goes from 0.05 ft/d to 4.0 ft/d, which falls within the range of values measured in slug tests in the 10 Piedmont Sites shown in Figure 4-5.

The conductivity of the saprolite (and transition zone) below the dam appears to be relatively high. These units are thin below the center of the dam. Flows at S-11 likely represent flows through the embankment material as well as through the foundation. Just south and west of the dam, zones of high conductivity were required in order to recreate the observed boron transport in this area. To the east of the dam, a zone of low permeability was needed to match the low boron concentrations seen in wells in this area. To the south, a zone of very low conductivity was needed along the Pine Hall Road ridge to recreate the high hydraulic heads observed here.

The calibrated background conductivity for the transition zone (layer 15) was 1.0 ft/d. This value falls near the average value for slug tests performed in the transition zone at 10 Piedmont Sites in North Carolina (Figure 4-6). The transition zone is heterogeneous, with values ranging from 0.04 ft/d to 7.0 ft/d (Figure 5-5 and Table 5-2). The highest conductivity zone is located below the center of the dam along the former drainage area, where it contributes to leakage of water under the dam. The lowest conductivity zone, present below the Pine Hall Road ridge south of the ash basin, was required to match the high hydraulic heads seen there. Another low conductivity zone is located below the ridge west of the dam and was needed to simulate the low boron concentrations observed there.

The upper bedrock zone in the model includes layers 16-20, and it is 180 feet thick. There are relatively fewer wells in the bedrock at the BCSS, and almost all of these are in the upper few tens of feet of the bedrock. The background conductivity value used in the model of

0.04 ft/d falls within the range of values measured from slug tests at 10 Piedmont sites in North Carolina, and in slug tests performed at Belews Creek (Figure 4-7). The background conductivity value used in the model is somewhat lower than the median value measured in slug tests, but for reasons described in Section 4.2, the slug test values may be biased towards higher values that occur in shallow fracture zones.

The upper bedrock conductivity ranges from 0.0005 ft/d to 0.7 ft/d in the model (Figure 5-6 and Table 5-2). The very low value was used to better match the low boron concentrations observed in three wells (GWA-19BR, GWA-20BR, and GWA-27BR) west of the ash basin dam. Other shallow bedrock wells in the area, such as AB-01BR, have high boron levels, and the uncertain nature of fracture flow transport makes it difficult to determine if boron is absent in the shallow bedrock around GWA-19BR, GWA-20BR, and GWA-27BR.

The deep bedrock layer extends 530 feet (layers 21-27) below the upper bedrock, and was assigned a uniform value of 0.006 ft/d. The flow model calibration is insensitive to this value, but the model conductivity is high enough to allow some water flow in the deep bedrock. Combined with the low rock porosity (0.01), and the high mobility of boron, this combination results in deep predicted migration of boron beneath the ash basin dam. There are no deep bedrock wells in this area currently to confirm this prediction, so it is subject to uncertainty. Additional deeper bedrock wells are planned in the vicinity of the ash basin dam and hydraulic and COI concentration data from those wells will be used to refine the calibration of shallow and deeper bedrock parameters in a future version of the flow and transport model.

The final calibrated flow model has a mean head residual of -0.81 ft., a root mean squared error (RMSE) of 4.34 ft, and a normalized root mean square error (NRMSE) of 2.13%. The range of heads at the site is about 204 ft with a maximum of 819.61 ft and a minimum of 615.88 ft. A comparison of the observed and simulated water levels is listed in Table 5-1 and the observed and simulated levels are cross-plotted in Figure 5-8. Table 5-2 lists the best-fit hydraulic parameters from the calibration effort.

The computed heads in the transition zone (model layer 15) are shown in Figure 5-9. Figure 5-10 shows the simulated heads in the second fractured bedrock model layer (model layer 17). These are similar to the shallower heads. The calibration wells are also shown in this figure (many of the nested wells plot on top of each other). The green and yellow bars indicate the

magnitude of model error at each well. The green color indicates that the difference is less than 10 ft and the yellow color indicates a difference of 10 to 20 ft. The head gradients become extremely steep below the ash basin dam, but are almost flat across the ash basin.

A closer view of the heads around the ash basin dam is shown in Figure 5-11. The green lines in this figure show the blanket drain that is installed in the dam at an elevation of about 648 ft, a seep near the western abutment of the dam, and the channel that forms below the dam. The flow of water that flows through and immediately under the dam is measured at location S-11 near well MW-200S, and averages roughly 180 gpm. The value calculated by the calibrated flow model is 185 gpm.

The groundwater flow divide around the ash basin under current, steady state, conditions is shown in Figure 5-12 as the red line. This divide wraps around the west, south, east and part of the northern side of the basin area. Inside of this divide, groundwater flows towards the ash basin (blue arrows), while outside of the divide, groundwater flows away from the ash basin. Groundwater from the ash basin flows to the north and northwest near the dam and the northwestern corner of the ash basin (yellow arrows). Mobile COIs are transported from the ash basin in this area.

The approximate groundwater flow budget in the ash basin watershed is shown in Figure 5-13. The size of the watershed that contributes to groundwater flow towards the ash basin depends on the locations of the groundwater divides that can change over time (for example if the ash basin is excavated or capped) and that vary with depth. Under current conditions, the watershed area contributing flow towards the basin is estimated at approximately 620 acres. Removing the areas that are capped (PHR Landfill, former constructed wetlands area (current lined retention basin)) and the ash basin pond, the remaining area is about 270 acres, resulting in about 112 gpm of groundwater flow from recharge. Additional recharge in the southern part of the ash basin adds another 20 gpm of flow, and the drains in this area remove about 68 gpm. Water leakage from the ash basin pond to the groundwater system is calculated to be 229 gpm, while flow through and immediately under the dam is about 185 gpm. Completing this water balance, we estimate that about 108 gpm flows through the ridge to the northwest and deep under the dam to the north. This estimate is subject to uncertainty related to the subsurface hydraulic conductivity distribution.

## 5.2 Flow Model Sensitivity Analysis

A parameter sensitivity analysis was performed by varying the main hydraulic parameters (recharge, ash conductivity, saprolite conductivity, transition zone conductivity, and upper and lower bedrock conductivity) in the current conditions flow model. Starting with the calibrated model, each parameter was halved and doubled to evaluate the model sensitivity. Only the main background conductivity values were varied in this study. Table 5-3 shows the results of the flow parameter sensitivity study. The model is very sensitive to the recharge rate, and is moderately sensitive to the saprolite, transition zone, and upper bedrock conductivities. The model is insensitive to the ash conductivity and to the conductivity of the deeper bedrock. As discussed earlier, additional testing of the ash and deeper bedrock units from pumping tests and geophysical testing will take place in late fall 2018. The results will be incorporated into a later version of this model.

## 5.3 Historical Transport Model Calibration

The transient flow model used for transport consisted of a series of three steady-state flow fields: 1) the period after the ash basin was built, but before the PHR Landfill was capped (1974-2008), 2) when the PHR Landfill was capped but the structural fill was not capped (2008-2012), and 3) after the structural fill was capped (2012-2017).

The transport simulations used five spatial zones of specified boron source concentration (Figure 5-14 and Table 5-4). The ash basin was split into 2 zones: one zone that represents the northern part of the ash basin, and one that represents the southern part of the basin. These zones were assigned very similar boron concentrations. The PHR Landfill was divided into a northern and a southern section in an attempt to improve the transport model calibration. The structural fill was treated as a separate boron source zone. The concentration of boron was held constant in the ash material in these zones during the historical transport simulations.

The calibrated  $K_d$  values for the boron was 0.4 in the saprolite and transition zone materials, and 0.02 respectively in the bedrock. The effective porosity was set to 0.3 in the unconsolidated layers, and 0.01 in the bedrock layers.

Table 5-5 compares measured (4<sup>th</sup> quarter, 2017) and simulated current conditions boron concentrations. The simulated boron concentrations in the transition zone (model layer 15) and

the upper part of the bedrock (model layer 16), are shown in Figure 5-15. The model predicts boron transport above the 2L standard from the ash basin to the west and north of the compliance boundary near the ash basin dam. This boron migration appears to mainly occur in the transition zone and saprolite, but transport in the bedrock is also predicted, including some transport in deeper bedrock. There are no wells this deep in the area to confirm this simulation result. Several deep wells are planned to be installed in the ash basin dam to help improve the understanding of possible boron transport in the bedrock near the ash basin dam. Some boron migration from the structural fill occurs in the simulation, but the model is not able to reproduce the high observed boron concentrations in wells GWA-23S and GWA-23D. These wells are located cross-gradient from the structural fill, and there is a deeply cut stream valley between these wells and the structural fill. Overall, the simulated boron concentrations appear to reasonably match the observed concentrations in most areas, and the model simulated boundary where the 2L standard is exceeded is similar to the observed locations.

#### 5.4 Transport Model Sensitivity

The most important transport model parameter for the boron is the  $K_d$ . The effective porosity affects transport velocity, but it also appears in the denominator of the retardation factor equation. Considering a Darcy velocity of  $V$ , the actual COI velocity,  $V_c$  is affected by both the porosity and the retardation factor:

$$V_c = \frac{V}{\phi R} = \frac{V}{\phi + \rho_b K_d}$$

The denominator of this relationship tends to be dominated by the  $K_d$  term unless it is very small. This is the reason why a small  $K_d$  value is assigned to the bedrock, where the effective porosity is due to the fractures, and is low. The transport model sensitivity to the  $K_d$  values was evaluated by running the boron transport simulation with  $K_d$  values that were 5 times smaller, and 5 times larger than the calibrated values (0.4 mL/g in the saprolite and transition zone, and 0.02 mL/g in the bedrock). The results of this study are shown in Table 5-6. The simulation results are seen to be fairly sensitive to the  $K_d$  value range tested here. The calibrated value produces a normalized root mean square error of 12.5%. This increases to 14.0% and 15.1% for the low  $K_d$  and high  $K_d$  cases, respectively. In terms of the boron plume behavior, the

low  $K_d$  simulation over-predicts the extent of boron migration, while the high  $K_d$  simulation under-predicts the extent of boron migration.

## 6.0 PREDICTIVE SIMULATIONS OF CLOSURE SCENARIOS

The simulated December 2017 boron distribution was used as the initial condition in closure simulations of future flow and transport at the BCSS. There are three main simulated scenarios: one in which all of the ash in the ash basin is excavated and removed from the Site; one in which a final cover system is installed over the ash basin; and a possible hybrid design where part of the ash is excavated and moved to the southern part of the ash basin where it is capped with a final cover system.

The current plans call for the BCSS ash basin pond to be decanted (drained of free-standing water) beginning in 2019. The decanting of the ash basin pond is expected to take one to two years. Ash basin pond decanting will have a major effect on the groundwater flow field, because the pond level will be lowered by about 70 feet, removing free-standing water. This will result in the re-creation of a strong groundwater divide along Middleton Loop Road to the west of the ash basin dam, and it will greatly reduce the hydraulic driving force for COI transport.

After the ash basin pond decanting, the final site closure activities will start and will continue for several years. It is assumed that final cover construction can be completed in 5 years and that excavation and the hybrid design construction can be completed in 12 years.

The predictive simulations are run in two steps. The first step is a simulation that starts in 2020, and uses the groundwater flow field after the ash basin pond is decanted. The starting boron distribution for this simulation is the simulated December 2017 concentration distribution. This simulation step continues for a period of 12 years (for excavation and the hybrid design) or 5 years (for the final cover system) ending in either 2032 or 2025. The second step assumes that construction activities have been completed and uses the final excavation, hybrid, or final cover system flow field for transport simulations. These simulations start in 2032 or 2025, and continue for over 1,000 years or until the boron concentrations beyond the current compliance boundary decrease below 2L standards. New potential compliance boundaries have recently been developed for the excavation and hybrid closure actions, and these potential boundaries are shown on the related figures in this report. These potential compliance boundaries for the excavation and hybrid scenarios are located at 250 feet from the waste, or at 50 feet inside the



property line, whichever is closer to the waste. For the final cover scenario, the existing '500 foot' compliance boundary remains unchanged.

An accelerated (interim action) remediation system consisting of 10 extraction wells was recently installed along the edge of Middleton Loop Road just west of the ash basin dam at the northwest corner of the ash basin. These wells started operating in March 2018, and are currently pumping at a combined rate of about 20 gpm. Figure 6-1 shows the locations of the current extraction wells. A flow simulation performed using the current ash basin pond level predicted that the 10 existing accelerated remediation wells could remove water at a rate of about 20 gpm, which is close to the observed value. These well flow rates are predicted to decrease dramatically as the ash basin is decanted, and groundwater levels decrease.

The extraction well screens extend to the top of the bedrock surface in the model, and they are operated in the simulation so that the water level is maintained 5 feet above the top of the bedrock using the DRAIN feature in MODFLOW.

### **6.1 Interim Period with Ash Basin Pond Decanted**

This simulation represents an interim period after the pond is decanted, but before closure action construction is completed. Decanting of the pond is simulated by removing the specified head zone that represents the pond in the current conditions flow simulation, and replacing it with a small drain area at an elevation of 680 ft, which is 70 feet below the current ash basin free water surface. The drain area is located in the deepest part of the current ash basin pond. Recharge at a rate of 8 inches per year is added to the ash basin, and boron initial conditions come from the historical transport simulation. Boron concentrations in the ash are no longer held constant, and the boron can leach from the ash according to its  $K_d$  value (which was derived from ash leaching tests). Boron present in the underlying soil and rock is mobile, and moves in response to the groundwater flow with adsorption occurring according to the soil or rock  $K_d$  value. The surface drains in the southern part of the ash basin remain in this simulation. Figure 6-2 shows the simulated steady-state hydraulic heads after the pond is decanted. The simulated hydraulic heads following decanting indicate the natural groundwater divide along the northwest side of the ash basin is re-established. The COI transport near the northwest corner of the basin will be to the east, northeast following decanting compared to the northwest prior to decanting.

This case includes the 10 well extraction system, but the well flow rates are reduced due to the much lower groundwater levels following pond decanting. The 10 accelerated remediation wells are now only removing a total of about 4 gpm in the simulation. The low flow rate from these wells reduces their effectiveness, and they are seen to have very little effect in the transport simulations. Figure 6-3 shows the simulated boron distribution in the transition zone in 2032 with the ash basin decanted.

## **6.2 Excavation Scenario**

These simulations begin in 2032 using the boron distribution from the decanted pond simulation described above. Excavation is simulated by setting the boron concentration in the ash layers in the ash basin to zero. The concentrations of boron in the remaining impacted soil underneath the ash basin are set to the values from the decanted pond simulation. The ash layers and dam are given a very high hydraulic conductivity (they are now excavated), and the previous ash basin surface water features are removed. Recharge occurs in the ash basin footprint at the background level of 8 inches per year. A small stream network is added to the ash basin, following the original drainages along the top of the saprolite surface. This drain network simulates the springs and streams that will form in the basin, and it connects to the stream below the dam (Figure 6-4). The water from the stream network may need to be collected and treated and discharged per NPDES permit requirements.

The steady-state hydraulic heads in the transition zone are shown in Figure 6-5 for the excavation scenario with 10 extraction wells operating. The groundwater levels are now at or below the original ground surface, and there is a strong groundwater divide along Middleton Loop Road, west of the ash basin similar to the interim period following ash pond decanting. An approximate water balance was calculated from the excavation flow model. The watershed that contributes groundwater flow to the basin area increases in size to about 678 acres due to the lower water levels that cause the groundwater divides to move outward somewhat. The capped areas inside this watershed include the constructed wetland areas (currently the lined retention basin) and the Pine Hall Road Landfill, so the net area contributing recharge is about 611 acres. This area contributes about 254 gpm to the basin. The stream network inside the basin removes most of this water, about 239 gpm, and an additional 6 gpm discharges to the stream immediately downstream from the former dam location. The cumulative discharge from the newly created

stream network will be collected, treated and discharged per the NPDES permit for a period of time. The 10 extraction wells remove a total of about 4 gpm. Therefore, the net deep groundwater flow is calculated to be only a few gpm in this case.

The simulated boron concentrations in the transition zone (model layer 15) are shown for the years 2050, 2100, 2150, and 2200 for the excavation case with 10 extraction wells in Figure 6-6. The predicted boron concentrations in the shallow bedrock (model layer 16) are shown for the years 2050, 2100, 2150, and 2200 in Figure 6-7. The outer red line in these figures is the current 2L compliance boundary while the inner red line is the potential compliance boundary following ash basin excavation. These simulations suggest that boron may continue to migrate beyond the current compliance boundary at Middleton Loop Road and north of the ash basin dam for over 100 years. As discussed earlier, there is substantial uncertainty with respect to predicted transport in the deeper bedrock because no wells currently monitor that zone. Deep bedrock wells are planned to be installed in the ash basin dam to help reduce this uncertainty, and the simulations will be revised accordingly at a later date.

Three locations were chosen to produce boron concentration versus time (time-series) plots (Figure 6-8). Location 1 is located at the compliance boundary at Middleton Loop Road west of the ash basin. Location 2 is on the compliance boundary north of the ash basin dam, and location 3 is located at the Dan River at the farthest extent of predicted boron transport.

The predicted concentrations in the transition zone and shallow bedrock at location 1 are shown in Figure 6-9. The concentrations are predicted to gradually decrease over time. Similar behavior is observed at location 2, shown in Figure 6-10. The simulated concentrations at location 3 at the edge of the Dan River are shown in Figure 6-11.

### **6.3 Final Cover Scenario**

The final cover simulations begin in 2025 using the boron distribution from the decanted basin simulations described above. The ash basin cover design used in the model is based on a draft closure plan design developed by AECOM. Following ash basin pond decanting, this draft design calls for the ash basin dam to be lowered to an elevation of 700 ft, and for the ash to be regraded inside the basin to form a gentle slope from south to north towards the dam. Shallow swales are built that approximately trace the original surface water drainage patterns in the basin

footprint, with ditches at the center of each swale. The cover system consists of an impermeable geomembrane, covered with about 2 feet of soil and a grass surface. The surface drainage ditches follow the centers of the final cover swales, and converge to a single channel near the dam. An underdrain system is proposed to collect water in the ash below the cap. The current conceptual design for this subsurface drainage system calls for the installation of drains 5 feet below the elevation of the cover system in a network that corresponds to the cover surface water drainage system. Figure 6-12 shows the drain network that was used in the final cover simulation to simulate this underdrain system. The numbered nodes along the drain arcs are locations where the drain elevation was specified using the draft design from AECOM. Drain elevations between these nodes were interpolated along the arcs. The drains are simulated using the MODFLOW DRAIN feature, using a relatively high conductance of 10.0 ft<sup>2</sup>/d/ft. Groundwater flow into these drains is removed from the model. If this closure option is selected, the discharge from the drain system may need to be collected, treated and discharged per the NPDES permit.

The final cover system is simulated by removing all of the original ash basin surface water features, and replacing them with this underdrain network. The ash properties are adjusted to reflect regrading of the ash in the area near the dam, and the recharge rate through the cover is set to 0.00054 inches per year. This value is based on landfill cover simulations performed using the Hydrologic Evaluation of Landfill Performance program (HELP) by AECOM, and it is also assumed that the PHR Landfill cover system will be extended to the north to cover the entire landfill. The boron initial conditions come from the dewatered ash basin pond simulation in the year 2025. The boron concentrations in the ash are variable in time, and the  $K_d$  value in the ash was set to value measured in ash leaching tests performed with ash from the basin (0.46 mL/g). The simulation includes the 10 well accelerated remediation system. These wells are predicted to only be capable of low flow rates due to the lower groundwater levels compared to current conditions. As before, the wells are assumed to extend to the bedrock surface, and the water level in the simulation is maintained 5 feet about the top of bedrock.

The steady-state hydraulic heads in the transition zone are shown in Figure 6-13. This design creates a strong groundwater divide along Middleton Loop Road, west of the ash basin, similar to the interim condition following ash basin pond decanting. An approximate water

balance was calculated from the final cover flow model. The watershed that contributes groundwater flow to the basin area for this case is about 654 acres. The cover system over the ash basin occupies about 283 acres, the former constructed wetlands areas (currently the lined retention basin) have an area of about 27 acres, and the enlarged cover over the PHR Landfill has an area of about 53 acres. This results in a net area of about 291 acres that contributes recharge to the groundwater system in the ash basin area at an average rate of about 120 gpm. The underdrain system beneath the ash basin cover removes 71 gpm, and the flow through the remaining part of the dam, and immediately underneath the dam is 36 gpm. The extraction wells remove a total of about 4 gpm. This balance indicates that the deep groundwater flow in the ash basin area is only a few gpm, which is a reduction by about a factor of ten from the current conditions simulation.

The simulated boron concentrations in the transition zone (model layer 15) are shown for the years 2050, 2100, 2150, and 2200 for the final cover simulation in Figure 6-14. The predicted boron concentrations in the shallow bedrock (model layer 16) are shown for the years 2050, 2100, 2150, and 2200 in Figure 6-15. Similar to the excavation simulations, the final cover simulations suggest that boron may continue to migrate beyond the current compliance boundary at Middleton Loop Road and north of the ash basin dam for over 100 years.

As before, three locations were used to produce boron concentration versus time plots (see Figure 6-8). Location 1 is located at the compliance boundary at Middleton Loop Road west of the ash basin. Location 2 is on the compliance boundary north of the ash basin dam, and location 3 is located at the Dan River at the farthest extent of predicted boron transport. These are the exact same locations discussed in the previous section.

The predicted concentrations in the transition zone and shallow bedrock at location 1 are shown in Figure 6-16. These time series concentrations are practically the same as for the excavation case. As before, the shallower concentrations are predicted to gradually decrease over time. Similar behavior is seen at location 2, shown in Figure 6-17. The simulated concentrations at location 3 at the edge of the Dan River are shown in Figure 6-18.

## 6.4 Hybrid Design Scenario

The hybrid design simulations begin in 2032 using the boron distributions from the decanted basin simulations described earlier. The hybrid design is based on a draft closure plan option developed by AECOM. This design involves complete excavation of the coal ash from the northern part of the ash basin following decanting of the ash basin pond. This ash would be placed in the southern part of the ash basin, forming a large mound or stack in the center of the southern part of the basin. The design results in a maximum ash stack elevation of 810 ft, and an overall footprint of about 132 acres. The design calls for the ash elevation in the ash basin fingers to be about 10 to 20 feet higher compared to current ash elevations. The ash basin dam is completely removed in this design.

The hybrid design was modified slightly in the current simulation to reflect design changes that are being considered. This model uses the same excavation and ash stack footprint as the design, but the ash elevation in the ash basin fingers is lowered compared to current ash elevations, and the ash stack is taller (845 ft) and steeper than in the design. Compared to the hybrid design, the ash elevations in the ash basin fingers are about 20 feet lower in the present simulation.

The regraded ash would be covered with an impermeable geomembrane, soil, and a grass surface. The center elevated ash stack will have 4:1 final slopes and will be surrounded by a perimeter ditch that drains towards the excavated area. The elevation of the perimeter ditch around the ash stack ranges from about 745 ft on the southern side of the stack to about 725 ft on the northern side of the stack.

The ash in the remaining part of the basin would be graded to maintain slopes of at least 1% towards the perimeter ditch around the ash stack. Shallow swales are built into each finger of the ash basin to direct the surface water. A stabilized ash zone with lower permeability is proposed along the southern edge of the excavated area. This stabilized ash zone could potentially be created using a deep mixing technique, and it is included in the model as a 50 foot wide zone of lower ash conductivity (0.2 ft/d) parallel to the northern slope of the ash stack. This position is approximately where the southern edge of the ash basin pond and ash delta are located.

An underdrain system has been included in this simulation to collect water in the ash below the cap. These drains are located 5 feet below the elevation of the cover system in a network that follows the surface drainage ditches from the ash basin fingers, towards the central perimeter ditch that drains water around the main ash stack (Figure 6-20). The underdrain node elevations were estimated based on discussions with the Duke closure design team. The underdrains along with the reformation of streams in former ash basin footprint will be collected, treated and discharged per the NPDES permit for a period of time.

The cover system over the ash is simulated by setting the recharge rate to 0.00054 inches per year as in the final cover system simulation. The excavated part of the ash basin is simulated by increasing the hydraulic conductivity of the ash to a very high value, by restoring the recharge to the background level of 8 inches per year, and by adding a drain network along the base of the excavation in former valleys. This drain network is intended to simulate springs and streams that will form in the excavated area (Figure 6-20). Boron concentrations in the excavated ash layers are set to zero, while initial boron concentrations in the deeper layers come from the decanted ash basin pond simulation.

The boron initial conditions in the remaining ash also come from the decanted ash basin pond simulation. The boron concentrations in the ash are variable in time, and the  $K_d$  value in the ash is set to the value measured in ash leaching tests performed with ash from the basin (0.46 mL/g). The simulation includes the 10 well accelerated remediation system, but these wells are predicted to only be capable of low flow rates due to the lower groundwater levels compared to current conditions. As before, the wells are assumed to extend to the bedrock surface, and the water level is maintained 5 feet about the top of bedrock.

The steady-state hydraulic heads in the transition zone are shown in Figure 6-21. This design also creates a strong groundwater divide along Middleton Loop Road, west of the ash basin similar to the interim condition following ash basin pond decanting. An approximate water balance was calculated from the hybrid flow model. The watershed that contributes groundwater flow to the basin area for this case is about 651 acres. The cover over the ash basin occupies about 133 acres, the former constructed wetlands areas (now used for wastewater collection in a lined retention basin) have an area of about 27 acres, and the enlarged cover over the PHR Landfill has an area of about 53 acres. This results in a net area of about 438 acres that

contributes recharge to the groundwater system in the ash basin area at an average rate of about 182 gpm. The underdrain system beneath the ash basin cover removes 49 gpm, and the springs and streams in the excavated area and just below the dam remove 126 gpm. The 10 extraction wells remove a total of about 4 gpm. This balance indicates that the deep groundwater flow in the ash basin area is only a few gpm, which is a reduction by about a factor of ten from the current conditions simulation.

The simulated boron concentrations in the transition zone (model layer 15) are shown for the years 2050, 2100, 2150, and 2200 for the hybrid case in Figure 6-22. The predicted boron concentrations in the shallow bedrock (model layer 16) are shown for the years 2050, 2100, 2150, and 2200 in Figure 6-23. The outer red line in these figures is the current 2L compliance boundary and the inner red line is a potential compliance boundary for the hybrid closure action. Similar to the excavation and final cover simulations, the hybrid design simulations suggest that boron may continue to migrate beyond the current compliance boundary at Middleton Loop Road and north of the ash basin dam for over 100 years.

As in the earlier simulations, three locations were used to produce boron concentration versus time plots (see Figure 6-8). Location 1 is located at the compliance boundary at Middleton Loop Road west of the ash basin. Location 2 is on the compliance boundary north of the ash basin dam, and location 3 is located at the Dan River at the farthest extent of predicted boron transport. These are the exact same locations discussed in the previous sections.

The predicted concentrations in the transition zone and shallow bedrock at location 1 are shown in Figure 6-24. These time series concentrations are practically the same as for the excavation case. As before, the concentrations are predicted to gradually decrease over time. Similar behavior is seen at location 2, shown in Figure 6-25. The simulated concentrations at location 3 at the edge of the Dan River are shown in Figure 6-26.

## **6.5 Conclusions Drawn from the Predictive Simulations**

- Ash basin pond decanting will have a major effect on the groundwater flow field, which will result in the re-creation of a strong groundwater divide along Middleton Loop Road to the west of the ash basin dam, and greatly reduce the hydraulic driving force for COI transport regardless of closure options.



- Predicted future boron concentrations at and beyond the current compliance boundary are very similar for the excavation, final cover system, and hybrid design closure simulations. A comparison of the groundwater concentrations over time for the three conceptual closure design simulations are similar as shown on Figures 6-27 through 6-30.
- Boron is predicted to exceed the 2L standard at the current northwest compliance boundary for 100 to 200 years in all 3 cases.
- Recently completed ash basin pumping tests and the planned installation of deep bedrock wells near the ash basin dam will reduce model uncertainty, and results will be incorporated into the next version of this model. The more detailed model report is planned for inclusion in the groundwater corrective action plan (CAP) scheduled for completion in December 2019.
- The new field data are not likely to change the conclusion that excavation, final cover system, and the hybrid closure actions result in a similar boron transport at the current compliance boundary.

## 7.0 REFERENCES

- Daniel, C.C., Douglas G. Smith, and Jo Leslie Eimers, 1997, Hydrogeology and Simulation of Ground-Water Flow in the Thick Regolith-Fractured Crystalline Rock Aquifer System of Indian Creek Basin, North Carolina, USGS Water-Supply 2341.
- Haven, W. T. 2003. Introduction to the North Carolina Groundwater Recharge Map. Groundwater Circular Number 19. North Carolina Department of Environment and Natural Resources. Division of Water Quality, 8 p.
- HDR, 2015a. Comprehensive Site Assessment Report, Belews Creek Steam Station Ash Basin, September, 2015.
- HDR, 2015b. Corrective Action Plan Part 1. Belews Creek Steam Station Ash Basin. December, 2015.
- HDR, 2016. Comprehensive Site Assessment (CSA) Supplement 2, Belews Creek Steam Station Ash Basin, August 11, 2016.
- McDonald, M.G. and A.W. Harbaugh, 1988, A Modular Three-Dimensional Finite-Difference Ground-Water Flow Model, U.S. Geological Survey Techniques of Water Resources Investigations, book 6, 586 p.
- Niswonger, R.G., S. Panday, and I. Motomu, 2011, MODFLOW-NWT, A Newton formulation for MODFLOW-2005, U.S. Geological Survey Techniques and Methods 6-A37, 44-.
- North Carolina Water Supply and Use, in "National Water Summary 1987 - Hydrologic Events and Water Supply and Use". USGS Water-Supply Paper 2350, p. 393-400.
- North Carolina; Estimated Water Use in North Carolina, 1995, USGS Fact Sheet FS-087-97
- Radcliffe, D.E., L.T. West, L.A. Morris, and T. C. Rasmussen. 2006. Onsite Wastewater and Land Application Systems: Consumptive Use and Water Quality, University of Georgia.
- SynTerra, 2017, 2017 Comprehensive Site Assessment Update, October 31, 2017.
- Treece, M.W, Jr., Bales, J.D., and Moreau, D.H., 1990, North Carolina water supply and use, in National water summary 1987 Hydrologic events and water supply and use: U.S. Geological Survey Water-Supply Paper 2350, p. 393-400.
- Zheng, C. and P.P. Wang, 1999, MT3DMS: A Modular Three-Dimensional Multi-Species Model for Simulation of Advection, Dispersion and Chemical Reactions of Contaminants in Groundwater Systems: Documentation and User's Guide, SERDP-99-1, U.S. Army Engineer Research and Development Center, Vicksburg, MS.

## **TABLES**

Table 5-1. Comparison of observed and computed heads for the calibrated flow model.

Well	Observed Head	Computed Head	Residual Head
AB-01D	734.13	739.66	-5.53
AB-01S	732.13	740.64	-8.51
AB-02D	732.63	726.33	6.30
AB-02S	743.05	734.31	8.74
AB-03D	724.66	734.29	-9.63
AB-03S	734.92	737.31	-2.39
AB-04BR	755.17	754.21	0.96
AB-04D	755.30	754.22	1.08
AB-04S	755.33	754.30	1.03
AB-04SL	755.19	754.24	0.95
AB-05D	755.82	755.06	0.76
AB-05S	755.93	755.10	0.83
AB-05SL	756.15	755.06	1.09
AB-06D	758.56	758.04	0.52
AB-06S	759.83	758.17	1.66
AB-06SL	759.74	758.13	1.61
AB-07D	759.62	758.30	1.32
AB-07S	759.40	758.24	1.16
AB-08D	757.73	754.99	2.74
AB-08S	757.95	755.15	2.80
AB-08SL	757.69	755.03	2.66
AB-09BR	758.23	757.17	1.06
AB-09BRD	758.59	757.73	0.86
AB-09D	758.54	755.95	2.59
AB-09S	759.36	755.56	3.80
BG-01D	761.23	764.39	-3.16
BG-02BR	766.03	760.82	5.21
BG-02D	765.51	761.07	4.44
BG-02S	763.78	761.16	2.62
BG-03D	814.16	814.70	-0.54
BG-03S	811.42	815.86	-4.44
GWA-01D	715.19	713.59	1.60
GWA-01S	717.16	712.95	4.21
GWA-02D	748.12	753.31	-5.19
GWA-02S	748.79	753.97	-5.18
GWA-03D	727.90	732.22	-4.32
GWA-06D	753.62	761.52	-7.90
GWA-06S	759.64	761.59	-1.95
GWA-07D	785.57	786.41	-0.84

GWA-08D	801.17	799.63	1.54
GWA-08S	804.67	802.11	2.56
GWA-09D	750.01	753.87	-3.86
GWA-09S	752.80	753.97	-1.17
GWA-10D	741.44	739.90	1.54
GWA-10S	742.43	739.71	2.72
GWA-11D	723.71	730.61	-6.90
GWA-11S	727.01	730.74	-3.73
GWA-12BR	773.19	779.03	-5.84
GWA-12D	781.69	780.96	0.73
GWA-12S	781.37	781.38	-0.01
GWA-16BR	746.30	750.60	-4.30
GWA-16D	748.33	751.01	-2.68
GWA-16S	750.17	751.10	-0.93
GWA-17D	749.92	749.21	0.71
GWA-17S	750.46	749.28	1.18
GWA-18D	748.78	748.43	0.35
GWA-19BR	716.25	721.27	-5.02
GWA-20BR	741.59	745.42	-3.83
GWA-20D	746.73	747.93	-1.20
GWA-21D	717.35	720.80	-3.45
GWA-21S	718.98	722.05	-3.07
GWA-23D	787.88	788.59	-0.71
GWA-23S	785.19	788.61	-3.42
GWA-24BR	615.88	626.81	-10.93
GWA-24D	628.25	625.96	2.29
GWA-30D	717.96	718.07	-0.11
GWA-30S	717.89	718.26	-0.37
GWA-31D	705.22	703.68	1.54
GWA-31S	700.67	703.56	-2.89
GWA-32D	681.12	684.04	-2.92
GWA-32S	688.08	682.06	6.02
MW-01	819.61	821.96	-2.35
MW-01D	811.60	815.33	-3.73
MW-02	815.39	817.43	-2.04
MW-03	802.15	807.15	-5.00
MW-04	752.61	753.65	-1.04
MW-05	760.42	765.25	-4.83
MW-06	804.19	813.71	-9.52
MW-07	808.66	810.63	-1.97
MW-101D	659.54	663.52	-3.98
MW-101S	664.30	663.99	0.31

MW-102D	652.80	646.17	6.63
MW-102S	642.21	646.40	-4.19
MW-103D	678.42	684.35	-5.93
MW-103S	678.45	684.07	-5.62
MW-104BR	757.94	758.13	-0.19
MW-104D	757.24	758.52	-1.28
MW-104S	756.44	758.59	-2.15
MW-200D	629.91	634.46	-4.55
MW-200S	630.48	634.48	-4.00
MW-201D	749.77	753.46	-3.69
MW-202BR	742.41	741.20	1.21
MW-202D	742.41	741.56	0.85
MW-202S	741.54	741.44	0.10
MW-203BR	752.48	754.98	-2.50
MW-203D	752.21	755.08	-2.87
MW-203S	752.61	755.19	-2.58
MW-204D	749.68	750.98	-1.30
MW-204S	749.70	751.00	-1.30
MW2-07	763.42	767.77	-4.35
MW2-09	791.86	787.98	3.88
OB-04	754.67	755.71	-1.04
OB-05	754.76	754.22	0.54
OB-09	761.69	763.17	-1.48
GWA-19SA	734.02	726.18	7.84
CCR-01D	749.30	749.95	-0.65
CCR-01S	749.60	749.97	-0.37
CCR-02D	748.60	747.85	0.75
CCR-02S	748.20	747.76	0.44
CCR-04D	742.80	744.84	-2.04
CCR-04S	740.40	744.73	-4.33
CCR-05D	708.10	717.32	-9.22
CCR-05S	724.10	717.19	6.91
CCR-06D	643.70	648.18	-4.48
CCR-07D	673.70	662.04	11.66
CCR-07S	674.90	662.77	12.13
CCR-08AD	738.20	746.96	-8.76
CCR-08D	703.90	710.57	-6.67
CCR-08S	703.90	710.82	-6.92
CCR-09D	740.80	749.33	-8.53
CCR-09S	749.60	749.51	0.09
CCR-11D	753.00	752.39	0.61
CCR-11S	753.80	752.37	1.43

CCR-12D	751.70	754.12	-2.42
CCR-12S	752.10	754.13	-2.03
SFMW-1D	787.57	784.44	3.13
SFMW-2D	805.12	796.41	8.71
SFMW-3D	748.89	752.61	-3.72
SFMW-4D	756.20	755.27	0.93
SFMW-5D	771.01	760.63	10.38

Table 5-2. Calibrated hydraulic parameters.

Hydrostratigraphic Unit	Model Layers	Spatial Zones (number corresponds to Figures 5-1 through 5-7)	Horizontal Hydraulic Conductivity, ft/d	Anisotropy ratio, $K_h:K_v$
Ash Basin	1-9	#3 coal ash	2.0	10
Ash Basin (pond or excavated)	1-9	#2 lake, excavated coal ash	200	1
Ash Basin Dam	1-9	#1 ash basin dam	0.8	2
Saprolite (upper)	10-12	#11 saprolite main model	0.5	1
	10-12	#1	0.2	1
	10-12	#2	1.0	1
	10-12	#3	0.08	1
	10-12	#4	1.0	1
	10-12	#5	2.0	1
	10-12	#6	2.0	1
	10-12	#7	1.0	1
	10-12	#8	4.0	1
	10-12	#9	4.0	1
	10-12	#10	0.06	1
Saprolite (lower)	13-14	#10 saprolite main model	0.5	1
	13-14	#1	0.2	1
	13-14	#2	1.0	1
	13-14	#3	0.05	1
	13-14	#4	0.1	1
	13-14	#5	2.0	1
	13-14	#6	0.1	1
	13-14	#7	0.1	1
	13-14	#8	2.0	1
	13-14	#9	0.06	1
Transition zone	15	#13 TZ main model	1.0	1
	15	#1	0.5	1
	15	#2	0.5	1
	15	#3	0.08	1
	15	#4	0.05	1
	15	#5	0.1	1
	15	#6	0.1	1
	15	#7	7.0	1
	15	#8	1.0	1
	15	#9	0.1	1
	15	#10	0.3	1
	15	#11	0.05	1
	15	#12	0.04	1
Bedrock (upper)	16-20	#7 main model	0.04	1
	16-20	#1	0.05	1
	16-20	#2	0.005	1
	16-20	#3	0.3	1
	16-20	#4	0.02	1



	16-20	#5	0.0005	1
	10-11	#6	0.7	1
Bedrock (lower)	21-27	#1 main model	0.006	1

Table 5-3. Flow model sensitivity. The normalized root mean square error (NRMSE) is shown.

Parameter	Decrease by 1/2	Calibrated	Increase by 2
Recharge (8 in/yr)	4.57%	2.13%	6.39%
Ash $K_h$ (2.0 ft/d)	2.13%	2.13%	2.14%
Saprolite $K_h$ (0.5 ft/d)	2.39%	2.13%	2.27%
TZ $K_h$ (1.0 ft/d)	2.55%	2.13%	2.30%
Upper Bedrock $K_h$ (0.04 ft/d)	2.50%	2.13%	2.23%
Lower Bedrock $K_h$ (0.006 ft/d)	2.20%	2.13%	2.14%

Table 5-4. Ash basin boron source concentrations (ug/L) used in historical transport model.

Date	Northern AB Poned Area	Southern AB Area	N PHR Landfill	S PHR Landfill	Structural Fill
1974-1985 boron	13,400	13,100	0	0	0
1985-2004 boron	13,400	13,100	40,000	25,000	0
2004-2017 boron	13,400	13,100	40,000	25,000	25,000

Table 5-5. Comparison of observed and simulated boron concentrations (ug/L) in monitoring wells.

Well	Observed Boron (ug/L)	Boron Model (ug/L)
AB-01BR	6540	13407
AB-01D	10000	13417
AB-01S	13400	13454
AB-02D	9190	13393
AB-02S	40.3	11331
AB-03D	3380	13371
AB-03S	11700	13400
AB-04BR	0	0
AB-04BRD	0	0
AB-04D	81.4	0
AB-04S	10600	13100
AB-04SL	13100	13100
AB-05D	0	0
AB-05S	993	13100
AB-05SL	10500	13100
AB-06D	27.5	0
AB-06S	109	54
AB-06SL	177	6
AB-07D	0	0
AB-07S	540	0
AB-08D	0	5
AB-08S	135	13100
AB-08SL	5580	13100
AB-09BR	0	0
AB-09D	76.1	0
AB-09S	0	0
BC-23A	0	0
BG-01D	0	0
BG-02D	0	0
BG-02S	0	0
BG-03D	0	0
BG-03S	0	0
GWA-01D	0	21
GWA-01S	731	609
GWA-02D	0	0
GWA-02S	0	0
GWA-03D	0	0
GWA-06D	0	0

GWA-06S	0	0
GWA-07D	0	0
GWA-08D	0	0
GWA-08S	348	0
GWA-09BR	113	0
GWA-09D	0	0
GWA-09S	0	0
GWA-10DA	0	4
GWA-10S	177	5
GWA-11D	218	1969
GWA-11S	958	426
GWA-12BR	0	0
GWA-12D	0	0
GWA-12S	0	0
GWA-16BR	0	0
GWA-16DA	0	0
GWA-16S	0	0
GWA-17D	0	0
GWA-17S	0	0
GWA-18D	0	10
GWA-18SA	269	61
GWA-19BR	0	673
GWA-19SA	2390	383
GWA-20BR	78.9	3637
GWA-20D	9480	8413
GWA-20SA	10600	8967
GWA-21D	351	999
GWA-21S	306	311
GWA-22D	0	7
GWA-22S	0	1
GWA-23D	6900	0
GWA-23S	2050	0
GWA-24BR	0	80
GWA-24D	0	18
GWA-25BR	0	0
GWA-26BR	0	0
GWA-26D	0	0
GWA-26S	0	0
GWA-27BR	39.7	150
GWA-27D	7140	5275
GWA-27S	4140	2292
GWA-30D	0	2

GWA-30S	0	18
GWA-31D	0	125
GWA-31S	0	3
GWA-32D	38.2	86
GWA-32S	0	20
MW-01	0	0
MW-01D	0	0
MW-02	0	0
MW-03	0	0
MW-04	600	2761
MW-05	0	19
MW-06	0	0
MW-07	2060	1569
MW-104BR	0	0
MW-104D	0	0
MW-104S	0	0
MW-200BR	123	48
MW-200D	183	62
MW-200S	39.6	55
MW-201BR	0	2
MW-201D	0	4
MW-202BR	0	0
MW-202D	0	0
MW-202S	0	0
MW-203BR	0	0
MW-203D	0	0
MW-203S	0	0
MW-204D	0	0
MW-204S	0	0
MW2-07	19000	7757
MW2-09	330	403
OB-04	10800	13100
OB-05	0	321
OB-09	25000	11724
BG-02BRA	0	0
GWA-07SA	67	0
CCR-01D	0	0
CCR-01S	0	0
CCR-02D	3620	1759
CCR-02S	2750	7838
CCR-04D	5930	8639
CCR-04S	6790	7940

CCR-05D	69.7	13378
CCR-05S	8320	13312
CCR-06D	10100	11174
CCR-07D	4960	6963
CCR-07S	55.8	1812
CCR-08AD	8820	9399
CCR-08D	9240	13189
CCR-08S	9180	11836
CCR-09D	144	18
CCR-09S	0	2
CCR-11D	0	0
CCR-11S	0	0
CCR-12D	0	0
CCR-12S	0	0
GWA-16D	39.5	0
SFMW-1D	6640	2371
SFMW-2D	0	1
SFMW-3D	0	214
SFMW-4D	1530	1167
SFMW-5D	98.4	53

Table 5-6. Transport model sensitivity to the boron  $K_d$  values. The calibrated model has a normalized root mean square error (NRMSE) of 12.5%. Boron concentrations are shown for the calibrated model, and for models where the  $K_d$  is increased and decreased by a factor of 5.

Well	Boron (ug/L)	Boron model calibrated	Model, low $K_d$	Model, high $K_d$
	<b>NRMSE</b>	<b>12.5%</b>	<b>14.0%</b>	<b>15.1%</b>
AB-01BR	6540	13407	13413	13069
AB-01D	10000	13417	13418	13289
AB-01S	13400	13454	13455	13236
AB-02D	9190	13393	13396	13349
AB-02S	40.3	11331	11331	11331
AB-03D	3380	13371	13395	12928
AB-03S	11700	13400	13400	13400
AB-04BR	0	0	0	0
AB-04BRD	0	0	0	0
AB-04D	81.4	0	0	0
AB-04S	10600	13100	13100	13100
AB-04SL	13100	13100	13100	13100
AB-05D	0	0	1	0
AB-05S	993	13100	13100	13100
AB-05SL	10500	13100	13100	13100
AB-06D	27.5	0	0	0
AB-06S	109	54	54	54
AB-06SL	177	6	6	6
AB-07D	0	0	0	0
AB-07S	540	0	0	0
AB-08D	0	5	53	0
AB-08S	135	13100	13100	13100
AB-08SL	5580	13100	13100	13100
AB-09BR	0	0	0	0
AB-09D	76.1	0	0	0
AB-09S	0	0	0	0
BC-23A	0	0	0	0
BG-01D	0	0	0	0
BG-02D	0	0	0	0
BG-02S	0	0	0	0
BG-03D	0	0	0	0
BG-03S	0	0	0	0
GWA-01D	0	21	499	0
GWA-01S	731	609	1603	3
GWA-02D	0	0	0	0



GWA-02S	0	0	0	0
GWA-03D	0	0	0	0
GWA-06D	0	0	0	0
GWA-06S	0	0	0	0
GWA-07D	0	0	0	0
GWA-08D	0	0	0	0
GWA-08S	348	0	0	0
GWA-09BR	113	0	0	0
GWA-09D	0	0	0	0
GWA-09S	0	0	0	0
GWA-10DA	0	4	89	0
GWA-10S	177	5	29	0
GWA-11D	218	1969	8524	0
GWA-11S	958	426	1399	0
GWA-12BR	0	0	0	0
GWA-12D	0	0	0	0
GWA-12S	0	0	0	0
GWA-16BR	0	0	0	0
GWA-16DA	0	0	0	0
GWA-16S	0	0	0	0
GWA-17D	0	0	0	0
GWA-17S	0	0	0	0
GWA-18D	0	10	153	0
GWA-18SA	269	61	192	1
GWA-19BR	0	673	1888	3
GWA-19SA	2390	383	757	3
GWA-20BR	78.9	3637	9669	67
GWA-20D	9480	8413	12053	734
GWA-20SA	10600	8967	9176	5985
GWA-21D	351	999	5618	0
GWA-21S	306	311	1335	0
GWA-22D	0	7	12	0
GWA-22S	0	1	2	0
GWA-23D	6900	0	0	0
GWA-23S	2050	0	0	0
GWA-24BR	0	80	854	0
GWA-24D	0	18	110	0
GWA-25BR	0	0	0	0
GWA-26BR	0	0	0	0
GWA-26D	0	0	0	0
GWA-26S	0	0	0	0
GWA-27BR	39.7	150	3137	0

GWA-27D	7140	5275	8853	32
GWA-27S	4140	2292	3319	48
GWA-30D	0	2	216	0
GWA-30S	0	18	274	0
GWA-31D	0	125	574	0
GWA-31S	0	3	37	0
GWA-32D	38.2	86	1006	0
GWA-32S	0	20	348	0
MW-01	0	0	0	0
MW-01D	0	0	0	0
MW-02	0	0	13	0
MW-03	0	0	0	0
MW-04	600	2761	13538	10
MW-05	0	19	23	1
MW-06	0	0	0	0
MW-07	2060	1569	3087	0
MW-104BR	0	0	0	0
MW-104D	0	0	0	0
MW-104S	0	0	0	0
MW-200BR	123	48	235	0
MW-200D	183	62	263	0
MW-200S	39.6	55	239	0
MW-201BR	0	2	2	0
MW-201D	0	4	4	0
MW-202BR	0	0	0	0
MW-202D	0	0	0	0
MW-202S	0	0	0	0
MW-203BR	0	0	0	0
MW-203D	0	0	0	0
MW-203S	0	0	0	0
MW-204D	0	0	0	0
MW-204S	0	0	0	0
MW2-07	19000	7757	12885	1667
MW2-09	330	403	1004	13
OB-04	10800	13100	13100	13100
OB-05	0	321	347	254
OB-09	25000	11724	11688	3823
BG-02BRA	0	0	0	0
GWA-07SA	67	0	0	0
CCR-01D	0	0	0	0
CCR-01S	0	0	0	0
CCR-02D	3620	1759	5917	16

CCR-02S	2750	7838	8711	3517
CCR-04D	5930	8639	10673	738
CCR-04S	6790	7940	9043	2156
CCR-05D	69.7	13378	13398	11927
CCR-05S	8320	13312	13358	9952
CCR-06D	10100	11174	12552	4925
CCR-07D	4960	6963	10322	522
CCR-07S	55.8	1812	3246	34
CCR-08AD	8820	9399	11957	1121
CCR-08D	9240	13189	13315	11616
CCR-08S	9180	11836	12038	9597
CCR-09D	144	18	33	0
CCR-09S	0	2	5	0
CCR-11D	0	0	11	0
CCR-11S	0	0	3	0
CCR-12D	0	0	0	0
CCR-12S	0	0	0	0
GWA-16D	39.5	0	0	0
SFMW-1D	6640	2371	9513	41
SFMW-2D	0	1	11	0
SFMW-3D	0	214	2032	0
SFMW-4D	1530	1167	5067	12
SFMW-5D	98.4	53	443	1

## FIGURES

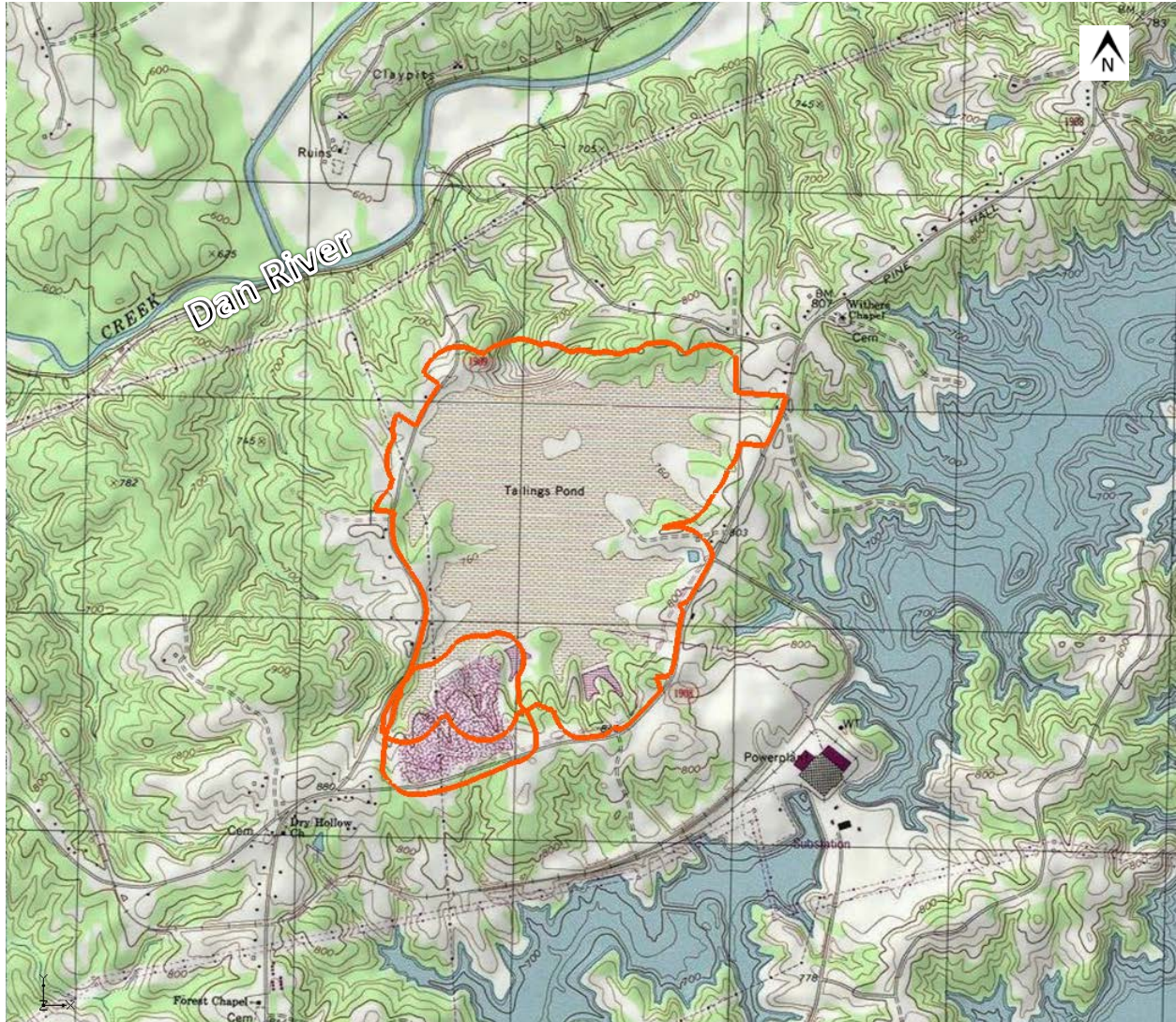
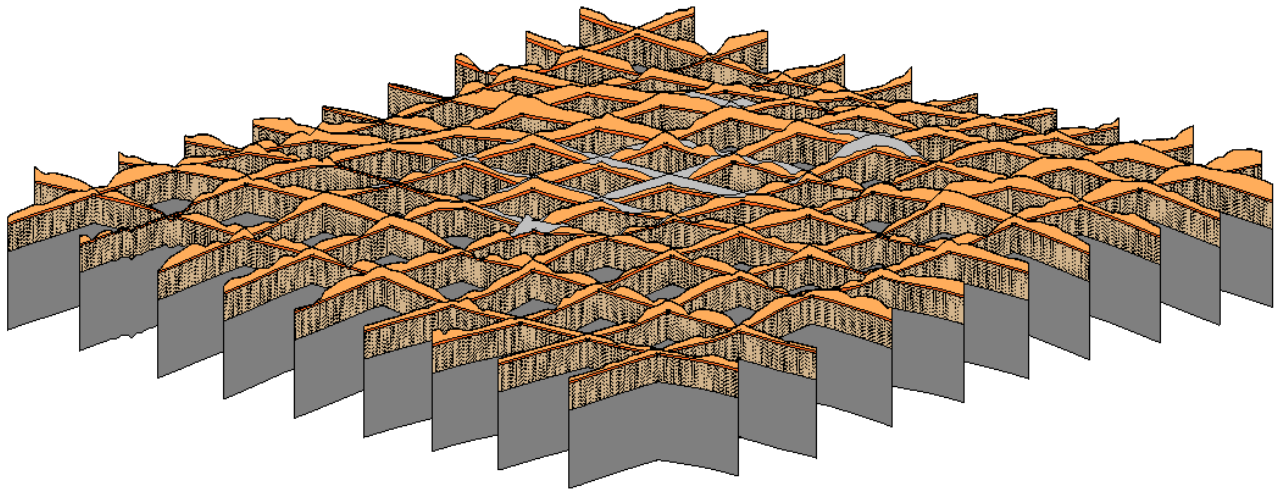


Figure 1-1. Site location map, Belews Creek Steam Station, Stokes County, NC. The larger orange outline is the ash basin compliance boundary and the smaller orange outline is Pine Hall Road Landfill.



Figure 4-1. Numerical model domain. Domain is represented as the red square. The larger orange outline is the ash basin compliance boundary and the smaller orange outline is Pine Hall Road Landfill.



18

Figure 4-2. Fence diagram of the 3D hydrostratigraphic model used to construct the model grid. The view is from the northwest, with 2x vertical exaggeration. The light grey in the upper portion of the model represents ash, the orange layer is saprolite, red is the transition zone, brown with black stripes is the fractured bedrock, and dark grey is competent bedrock.

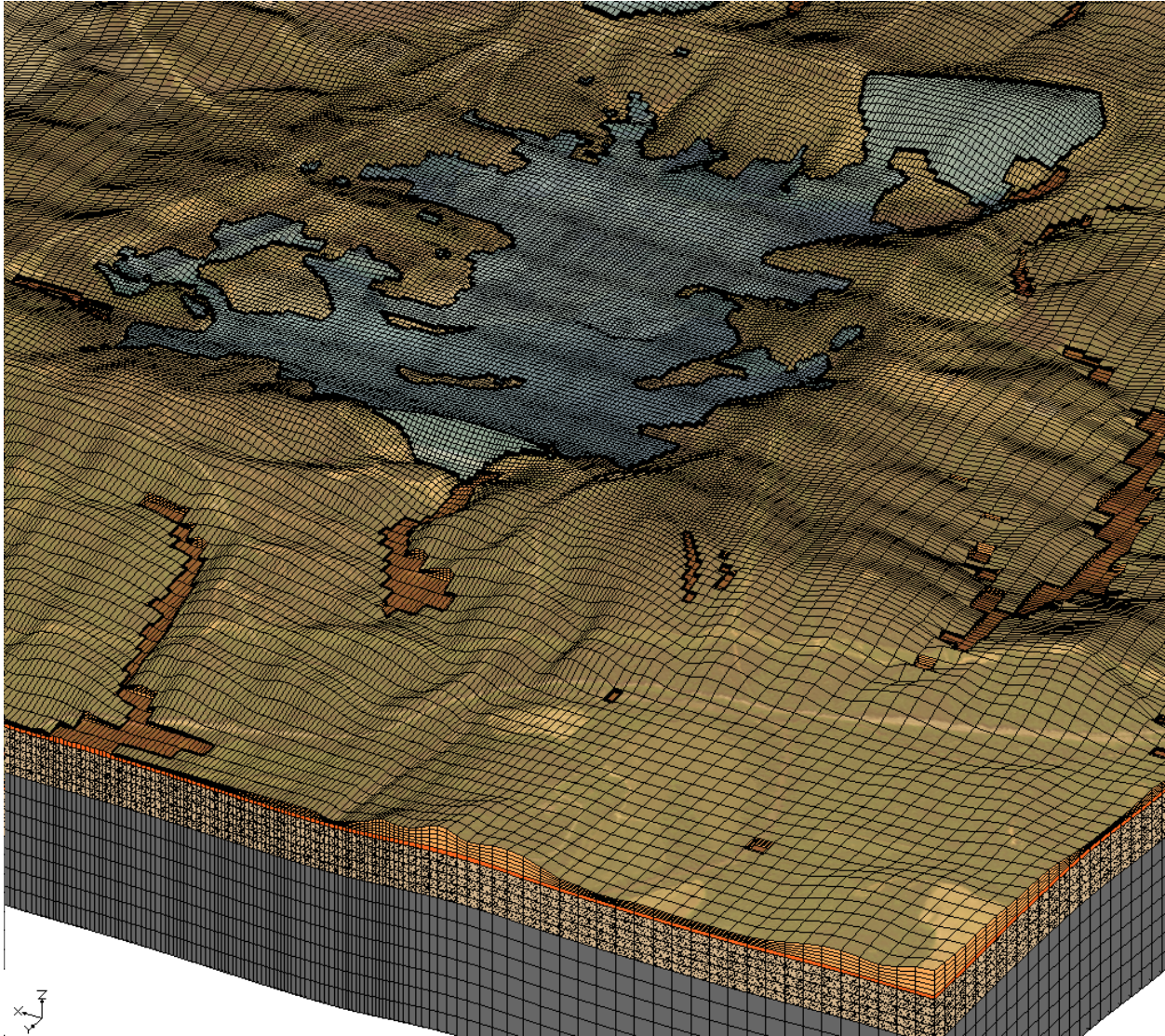


Figure 4-3. Numerical grid used for flow and transport modeling. Vertical exaggeration is 2x. Perspective of site looking south. Numerical grid used for flow and transport modeling.



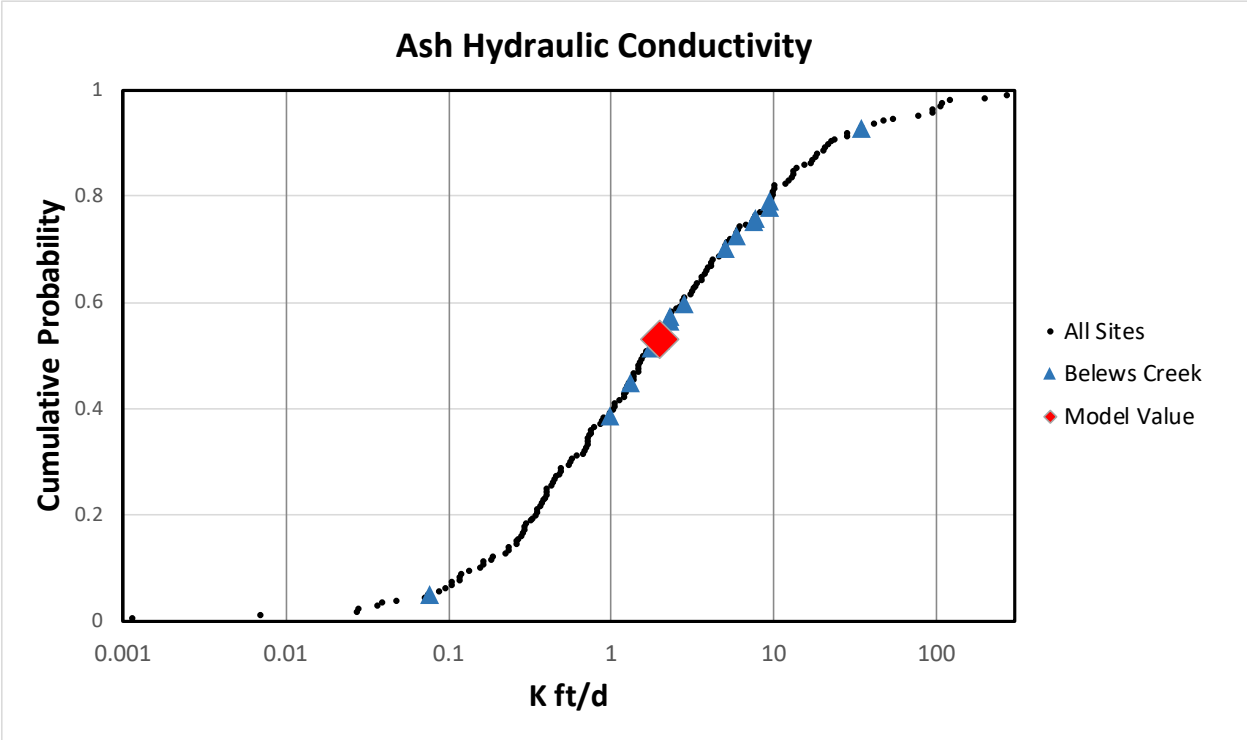


Figure 4-4. Hydraulic conductivity measured in slug tests performed in coal ash at 14 sites in North Carolina.

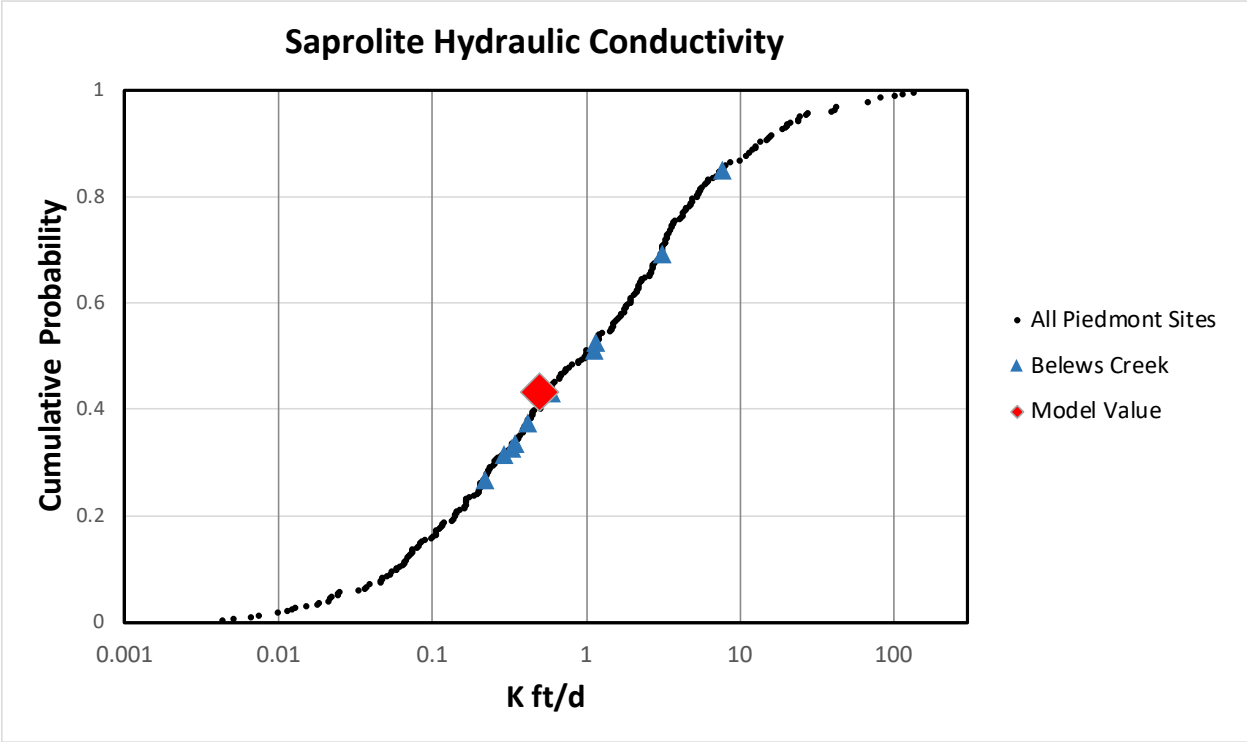


Figure 4-5. Hydraulic conductivity measured in slug tests performed in saprolite at 10 Piedmont sites in North Carolina.

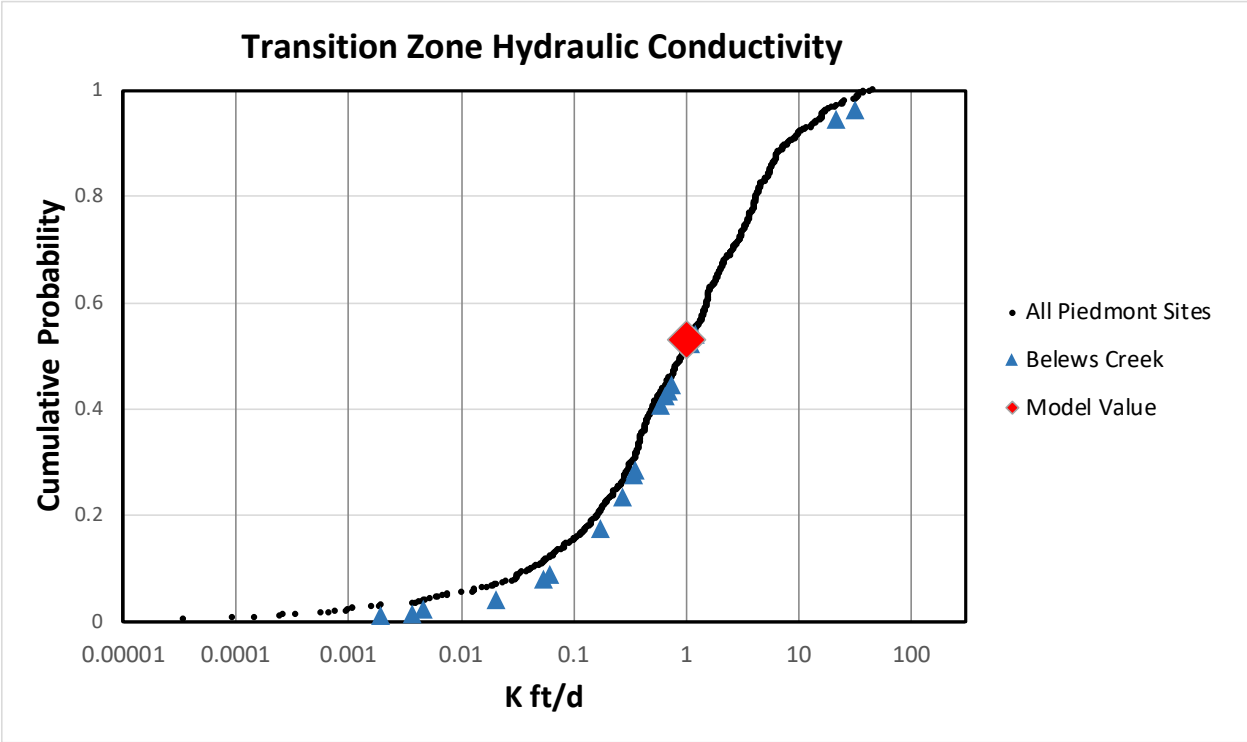


Figure 4-6. Hydraulic conductivity measured in slug tests performed in the transition zone at 10 Piedmont sites in North Carolina.

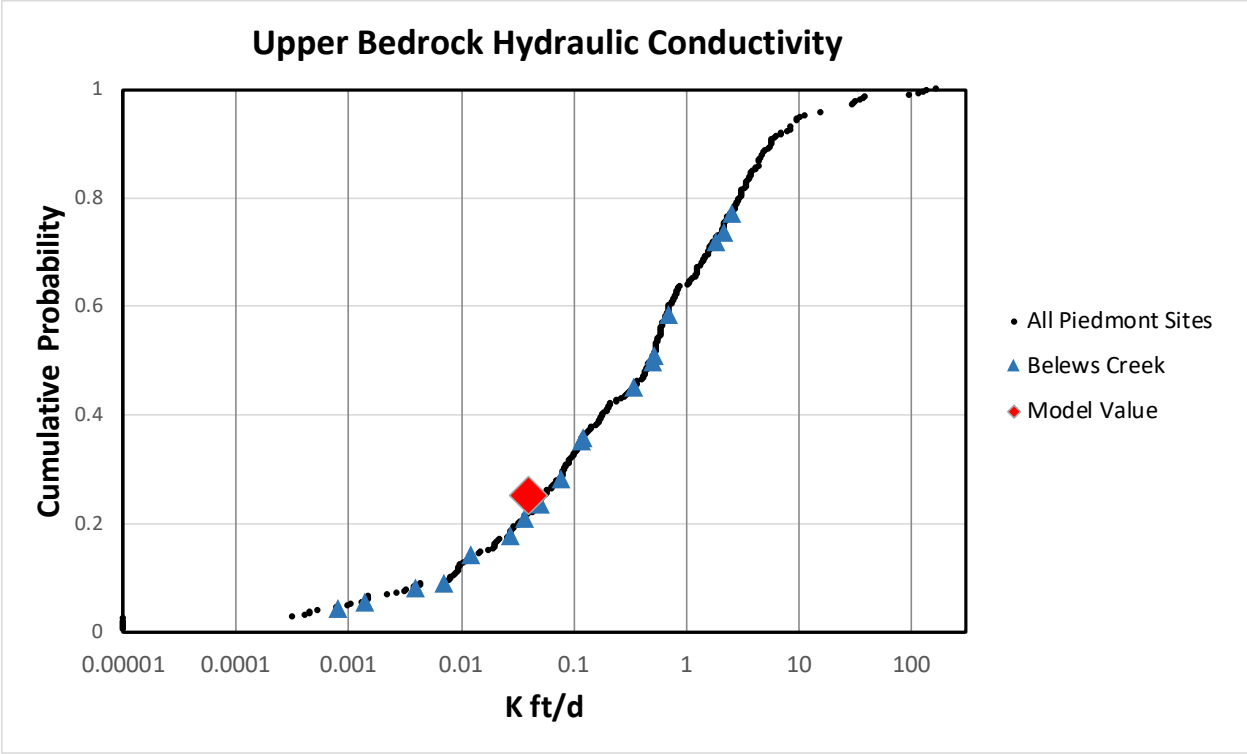


Figure 4-7. Hydraulic conductivity measured in slug tests performed in bedrock at 10 Piedmont sites in North Carolina.

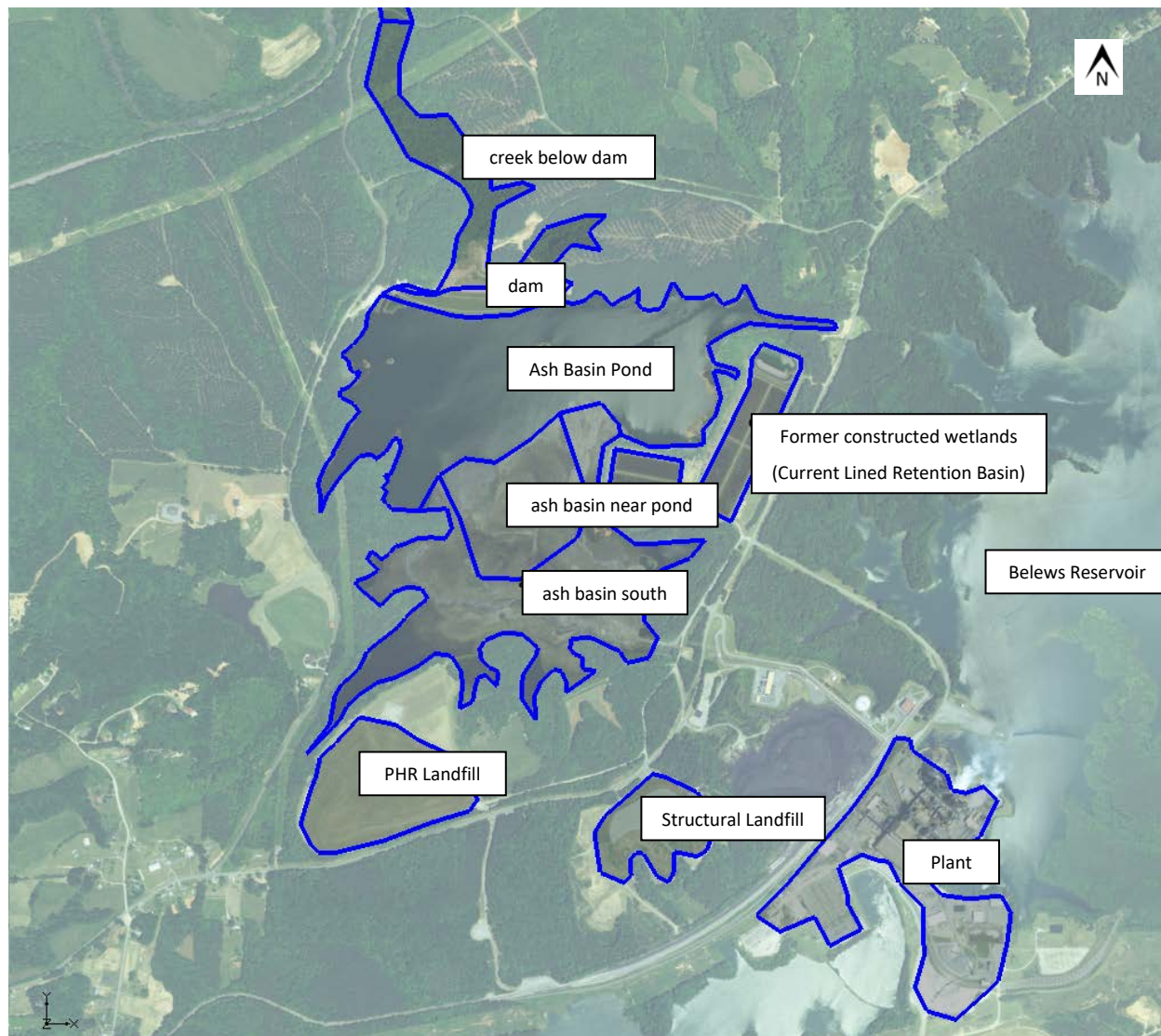


Figure 4-8. Distribution of recharge zones in the model. The background recharge rate is 8 inches/year. Blue lines represent different recharge zones.

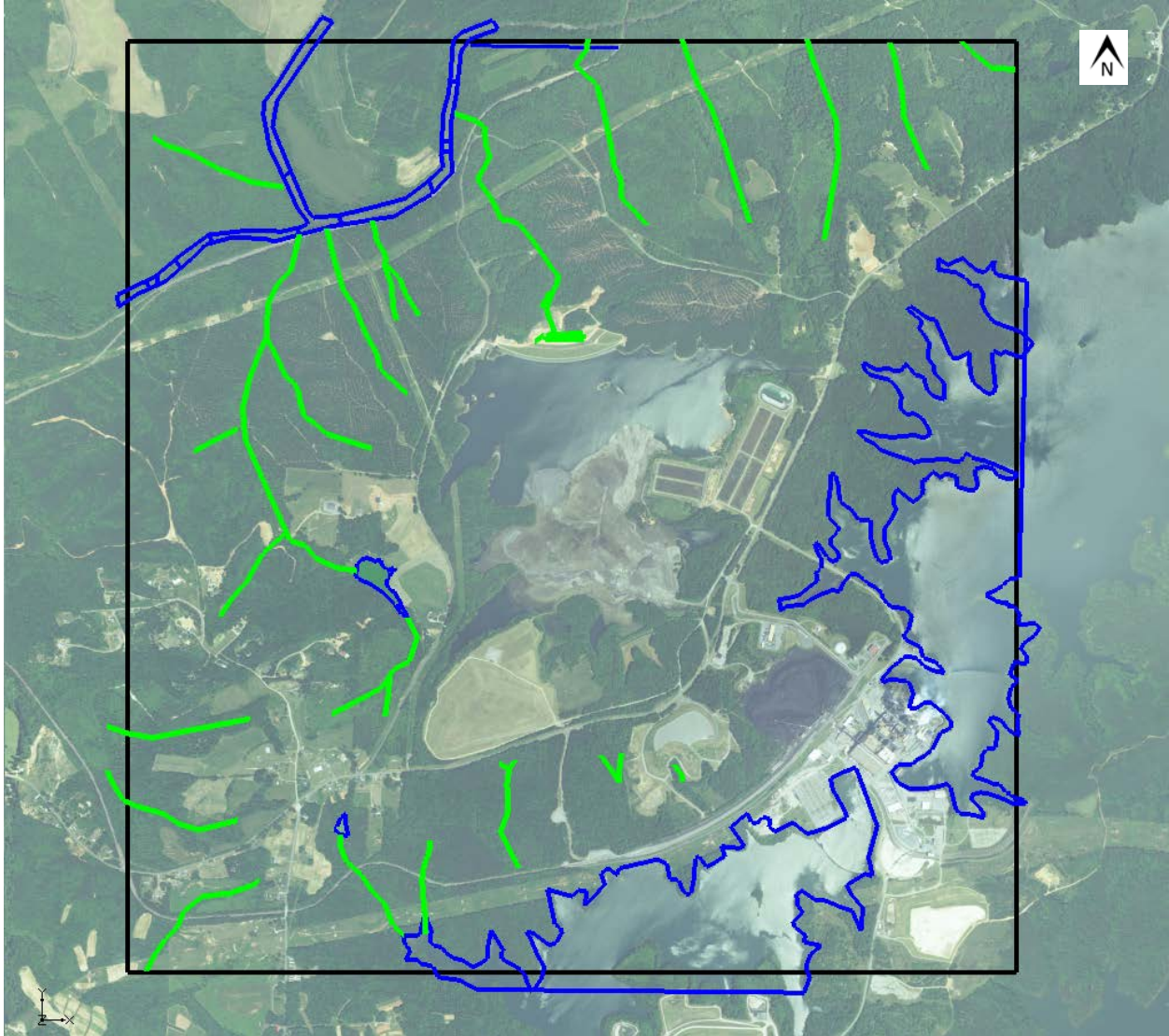


Figure 4-9. Surface water features included in the model outside of the ash basin area (the ash basin area is shown in Figure 4.10). The areas enclosed by dark blue lines are constant head zones in the uppermost active layer. The green lines represent drains, and the black line shows the model boundaries.

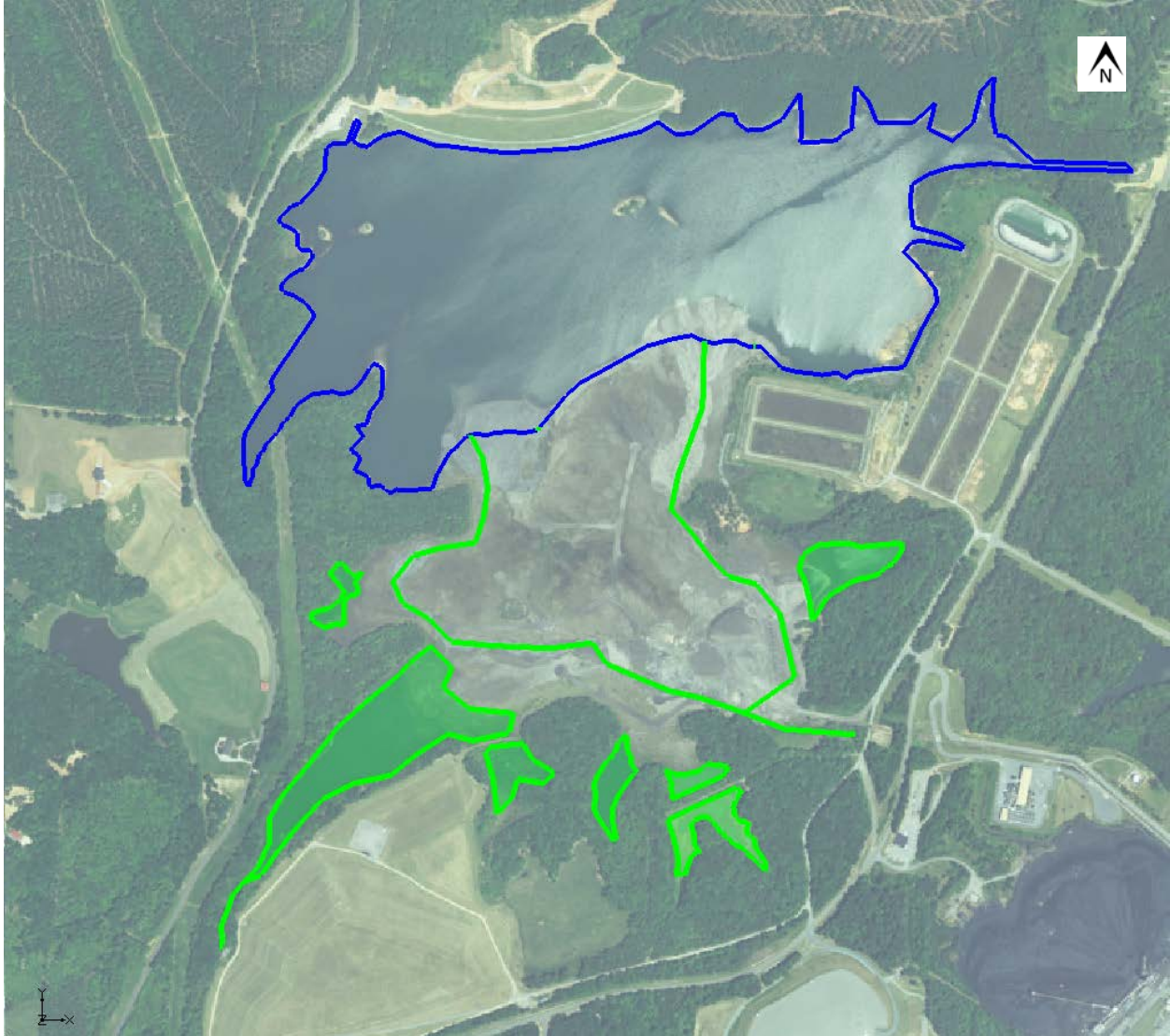


Figure 4-10. Surface water features included in the model in the ash basin area. The area enclosed by dark blue represents the ash basin pond, which is maintained at an elevation of 750 ft. The green lines and areas represent drains that are set to the approximate ground or water surface elevation.

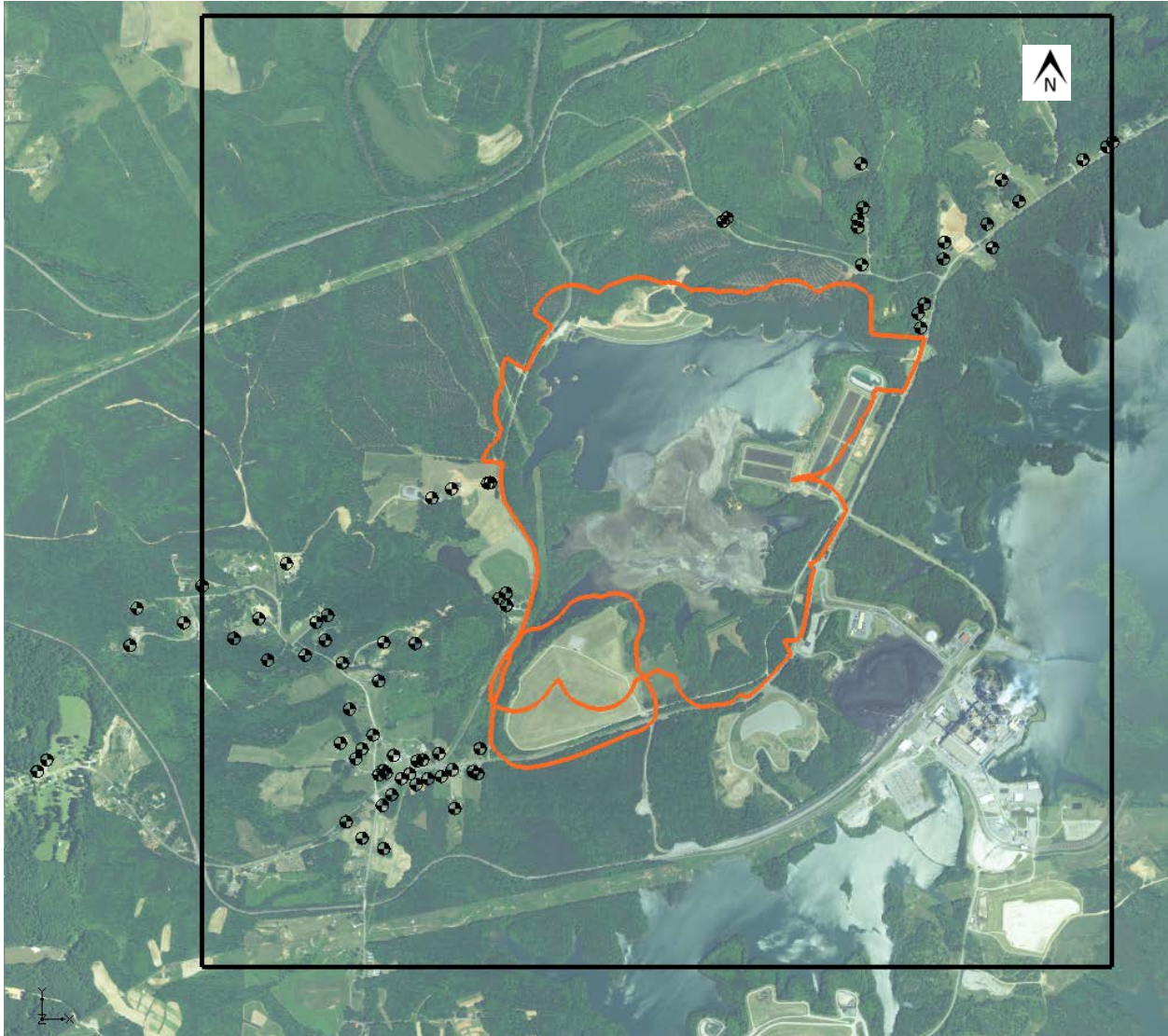


Figure 4-11. Location of water supply wells in the model area. Black symbols represent supply wells, the black square is the model domain, and the orange outline is the ash basin compliance boundary and the Pine Hall Road Landfill compliance boundary.



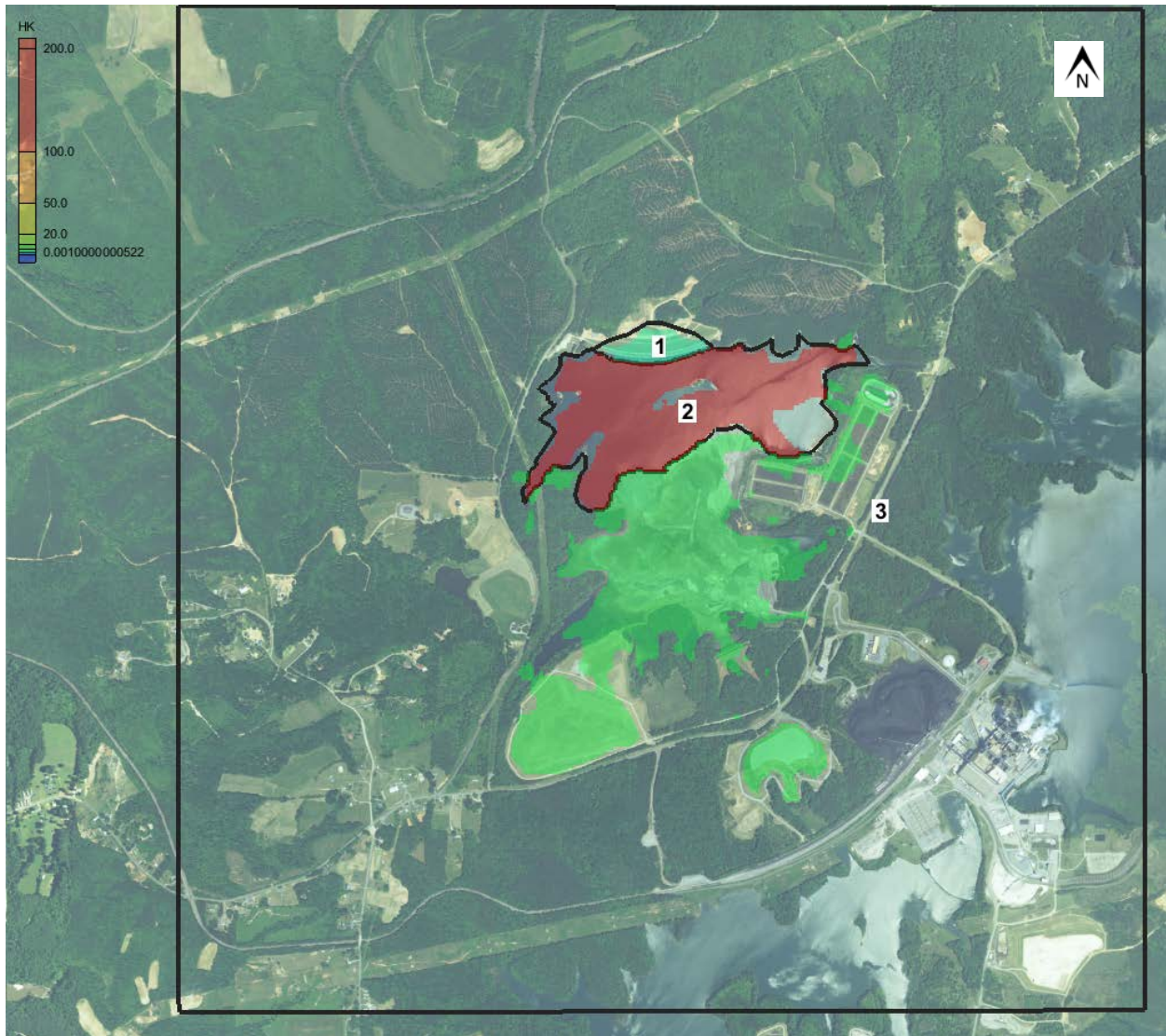


Figure 5-1. Zones used to define horizontal hydraulic conductivity and horizontal to vertical anisotropy in the ash (model layer 3 shown).

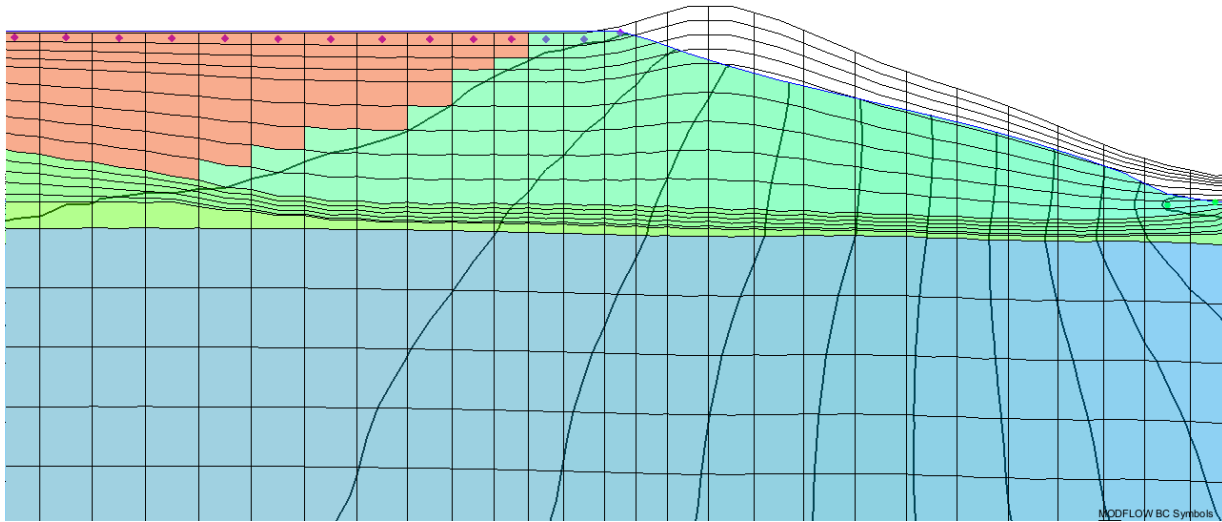


Figure 5-2. Cross-section through ash basin dam showing hydraulic conductivity (colors) and hydraulic heads (lines). The red area represents open water in the pond, which is assigned a conductivity of 200 ft/d. The light green area in the dam represents the dam fill which is assigned a value of 0.8 ft/d.

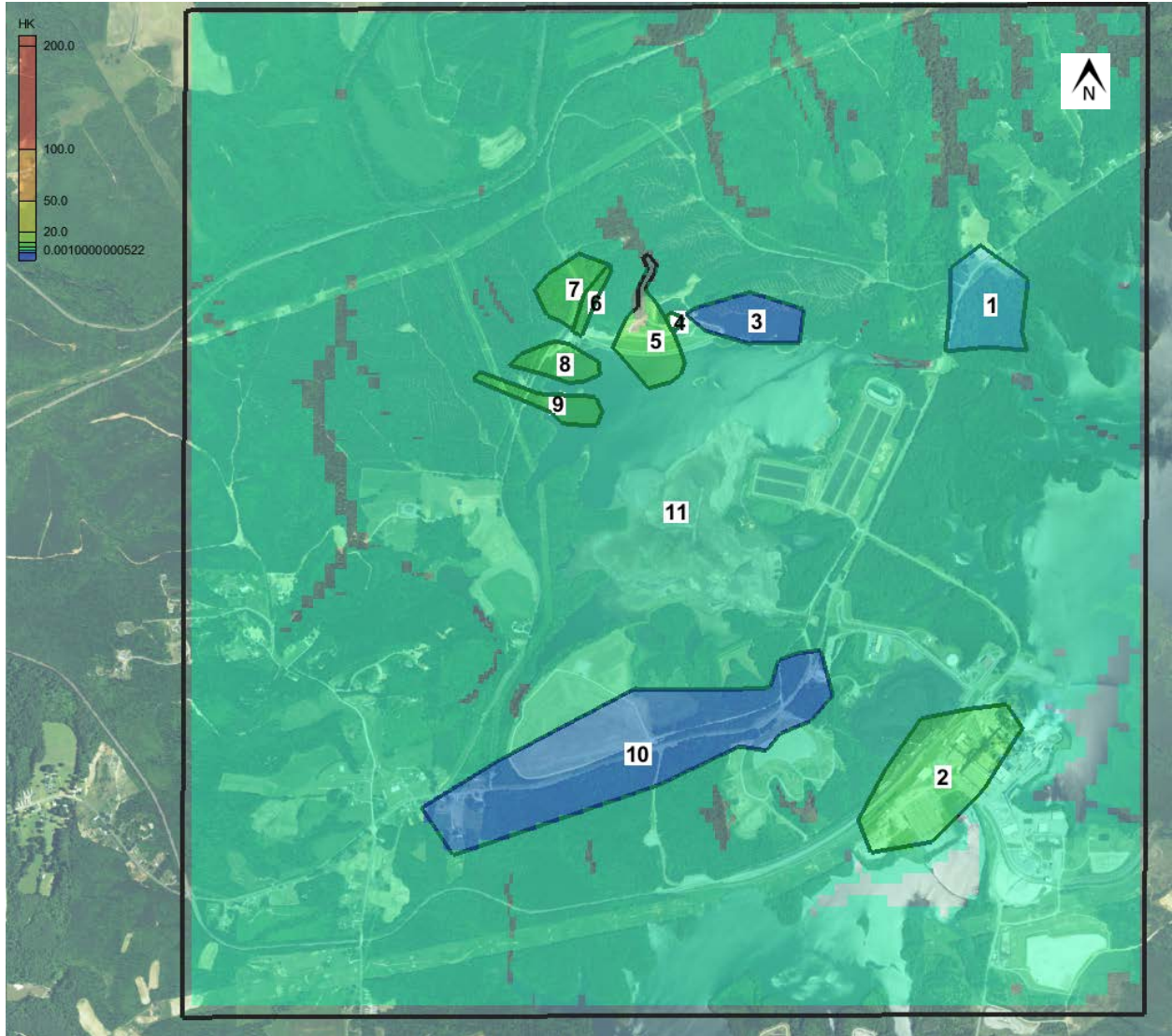


Figure 5-3. Zones used to define horizontal hydraulic conductivity and horizontal to vertical anisotropy in the saprolite, model layers 10-12.

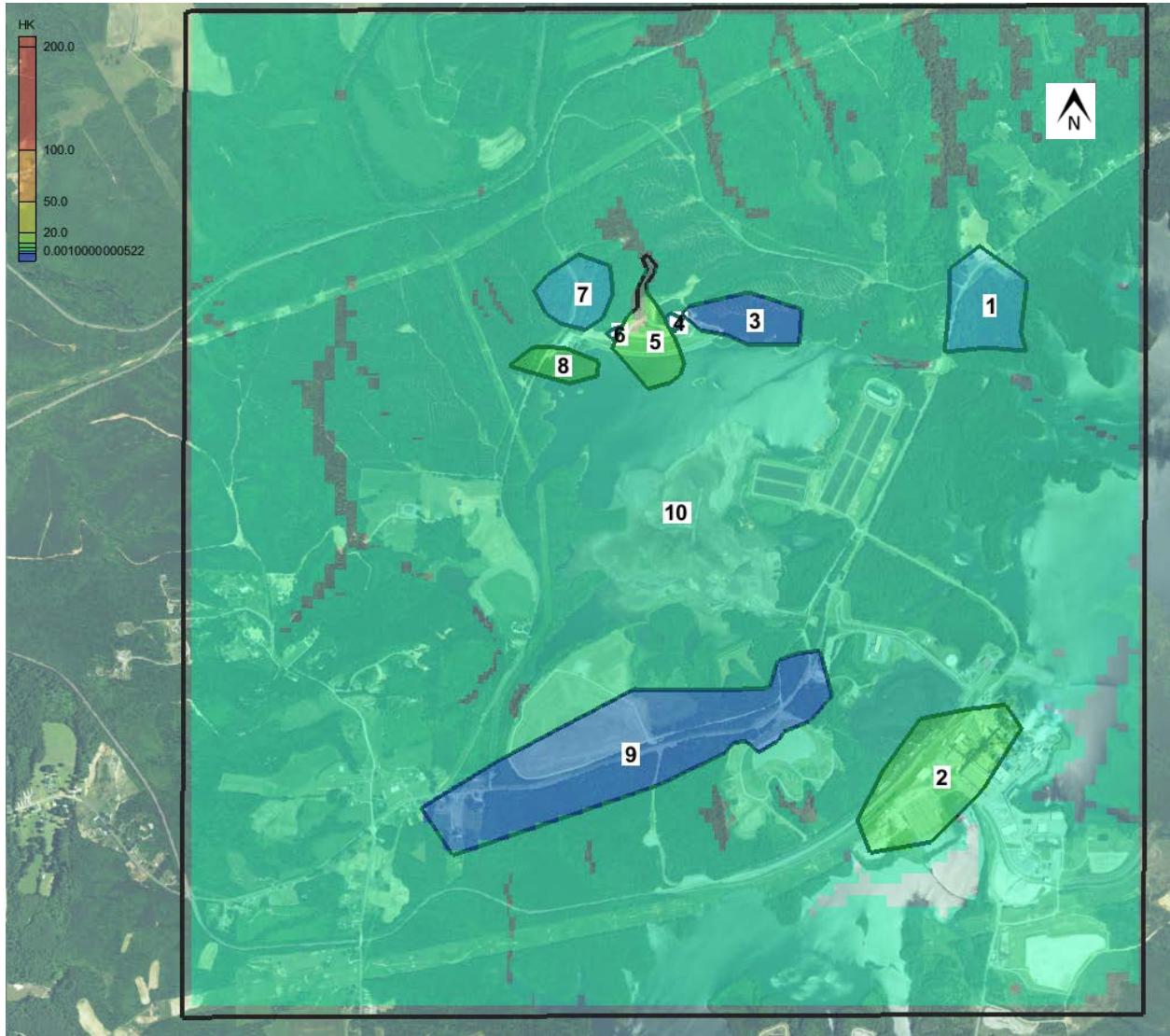


Figure 5-4. Zones used to define horizontal hydraulic conductivity and horizontal to vertical anisotropy in the saprolite, model layers 13-14.



Figure 5-5. Zones used to define horizontal hydraulic conductivity and horizontal to vertical anisotropy in the transition zone, model layer 15.

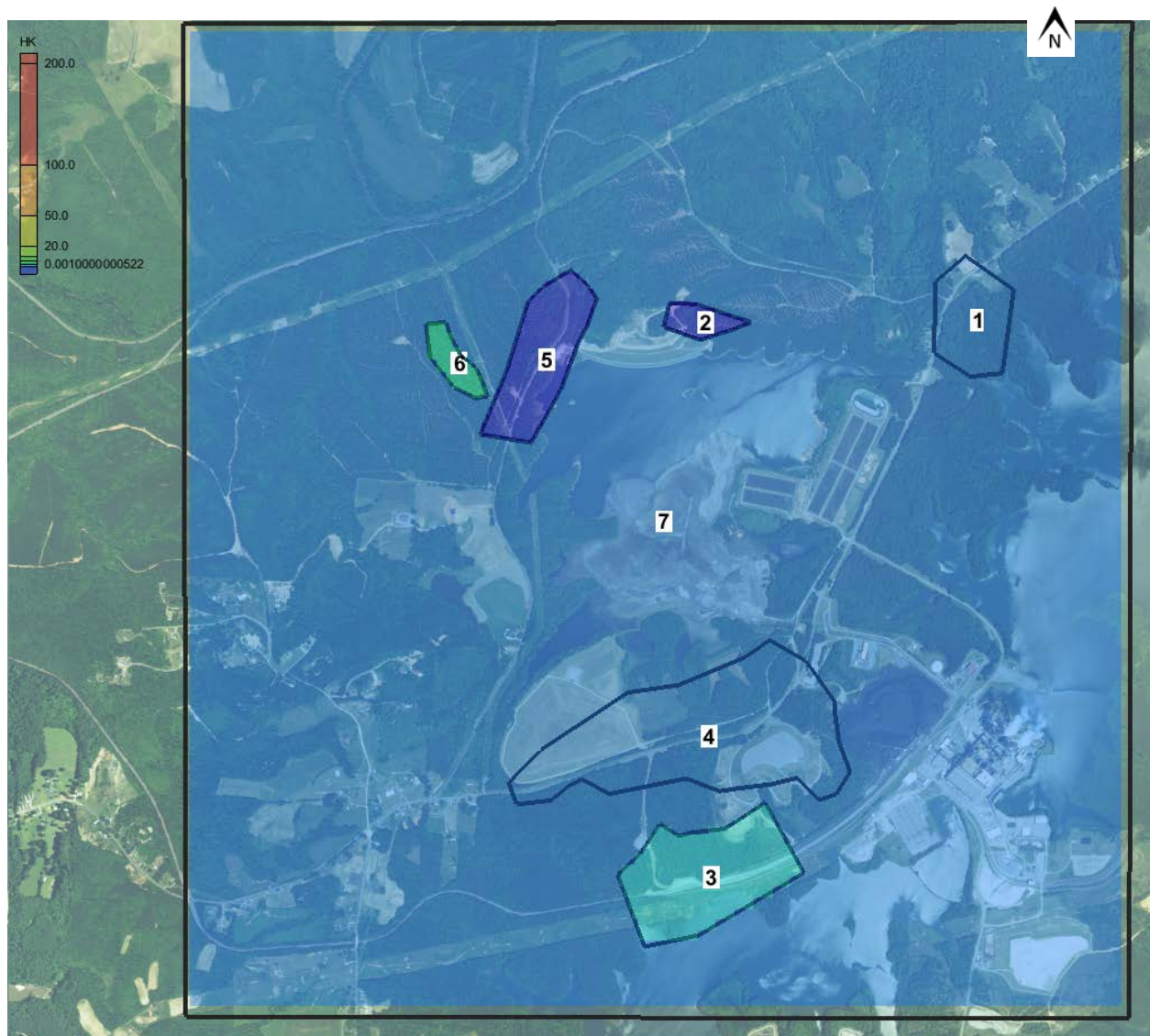


Figure 5-6. Zones used to define horizontal hydraulic conductivity and horizontal to vertical anisotropy in the fractured bedrock, model layers 16-20.

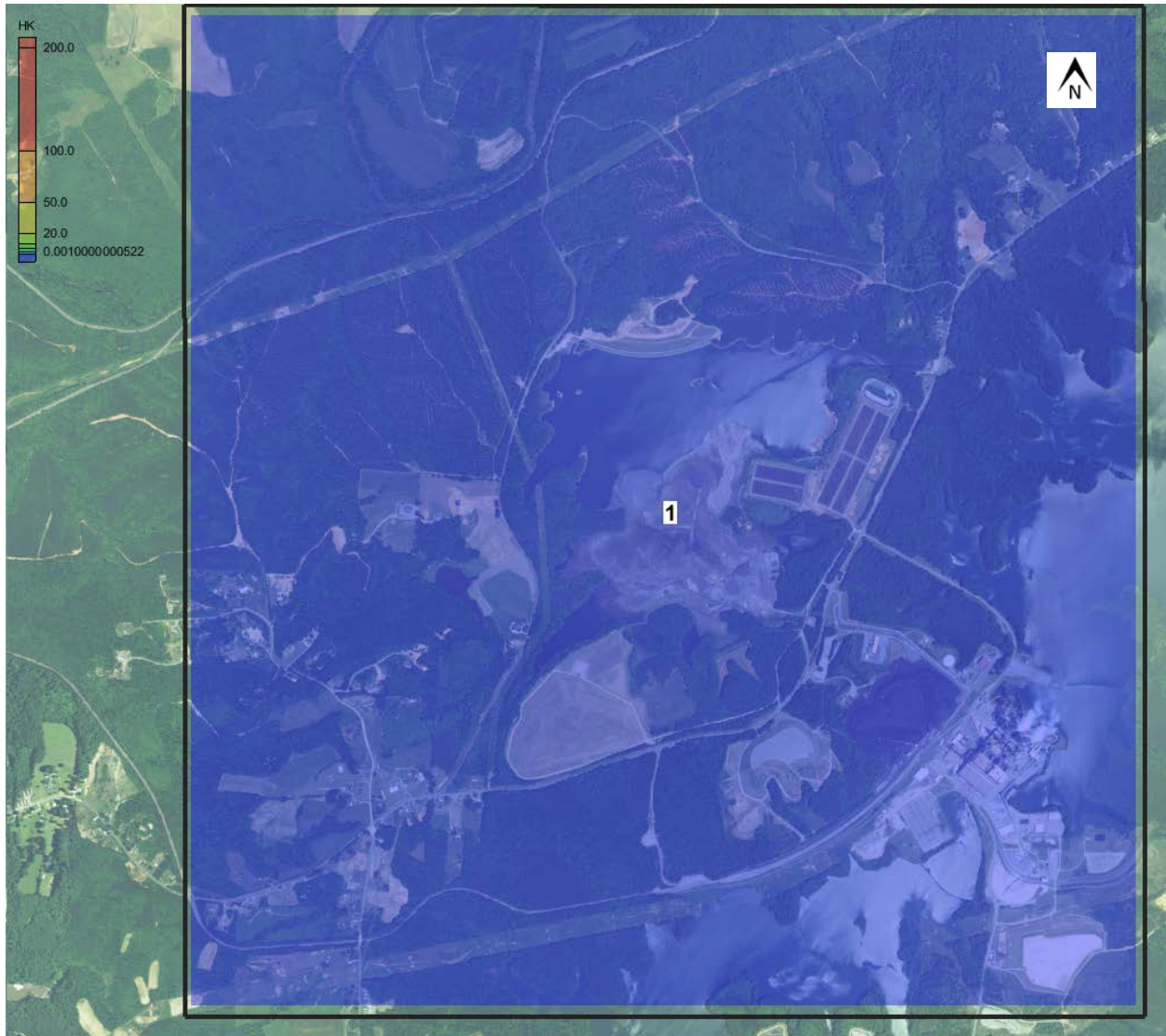


Figure 5-7. Zones used to define horizontal hydraulic conductivity and horizontal to vertical anisotropy in the deep bedrock, model layers 21-27.

# Computed vs. Observed Values Head

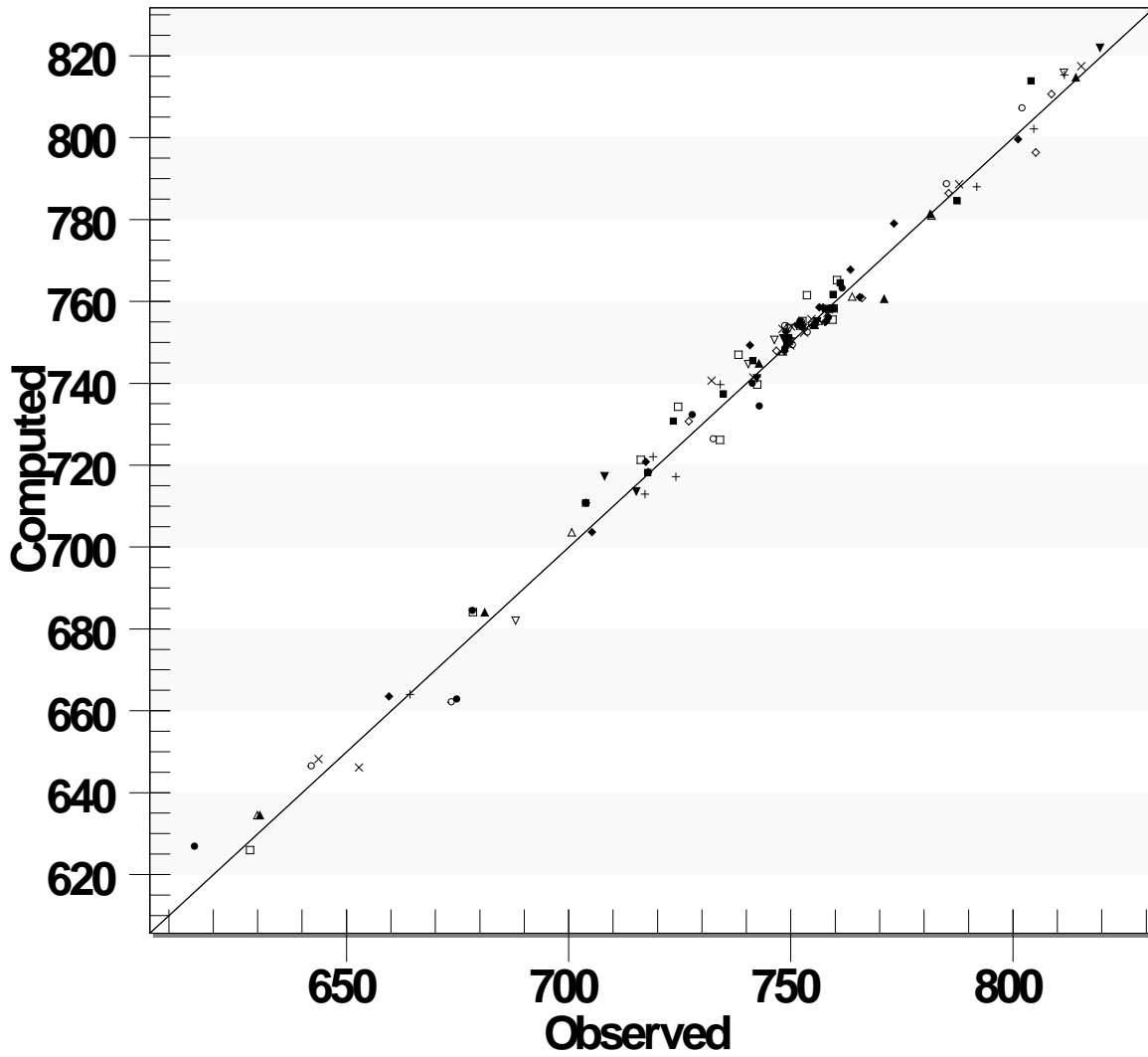


Figure 5-8. Comparison of observed and computed heads from the calibrated steady state flow model.



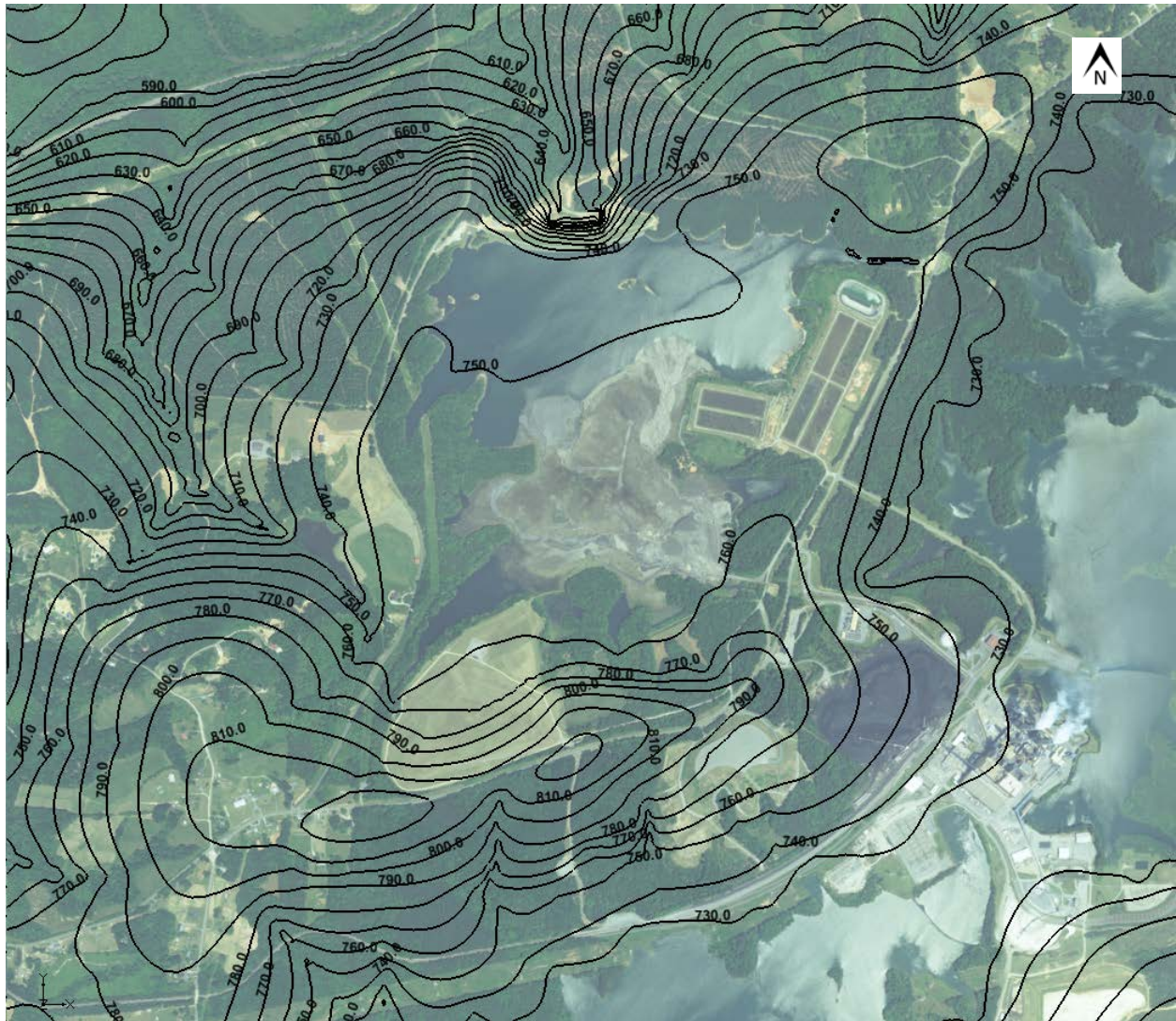


Figure 5-9. Simulated heads in the transition zone (model layer 15).

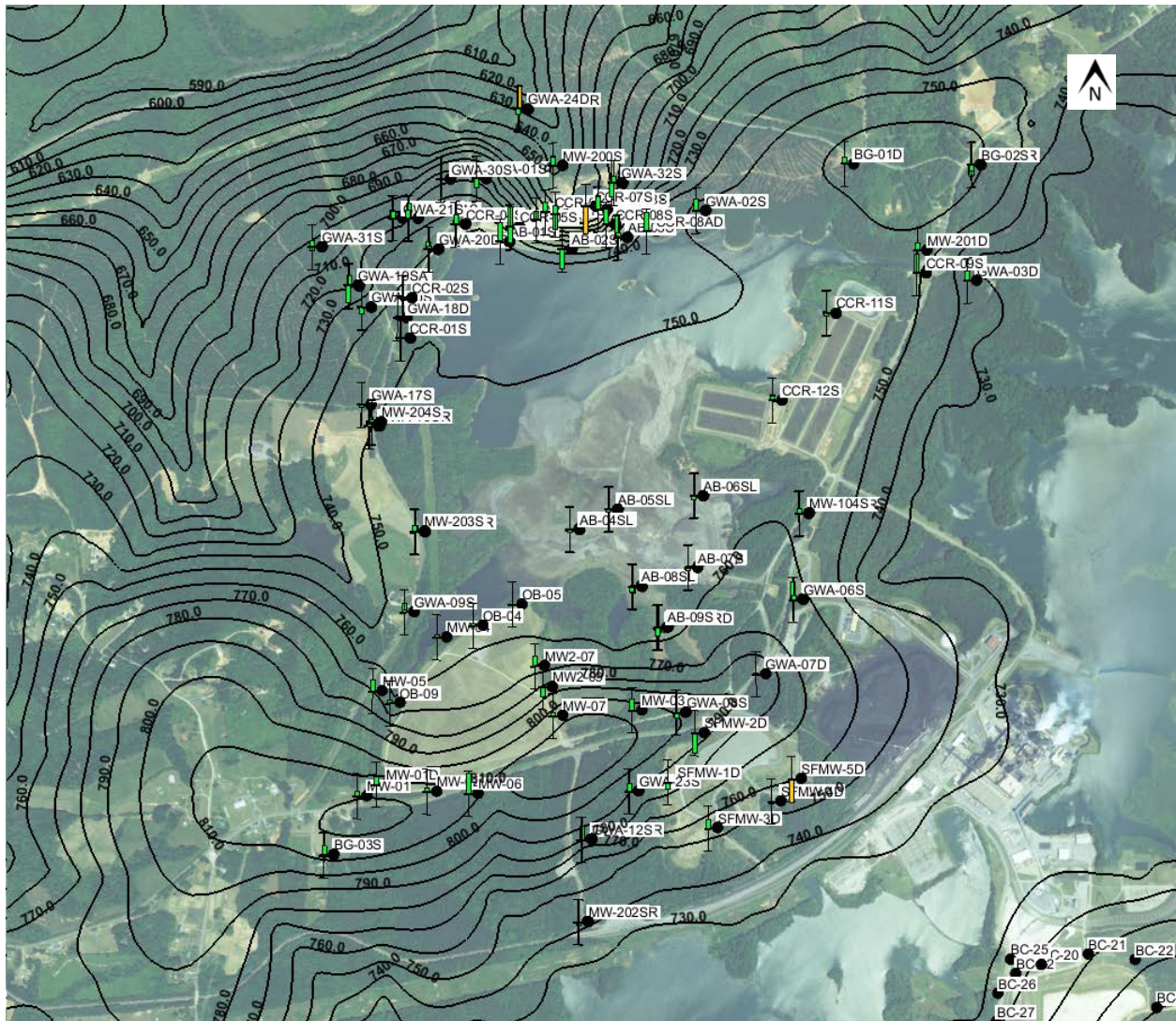


Figure 5-10. Simulated heads in the second fractured bedrock model layer (model layer 17).

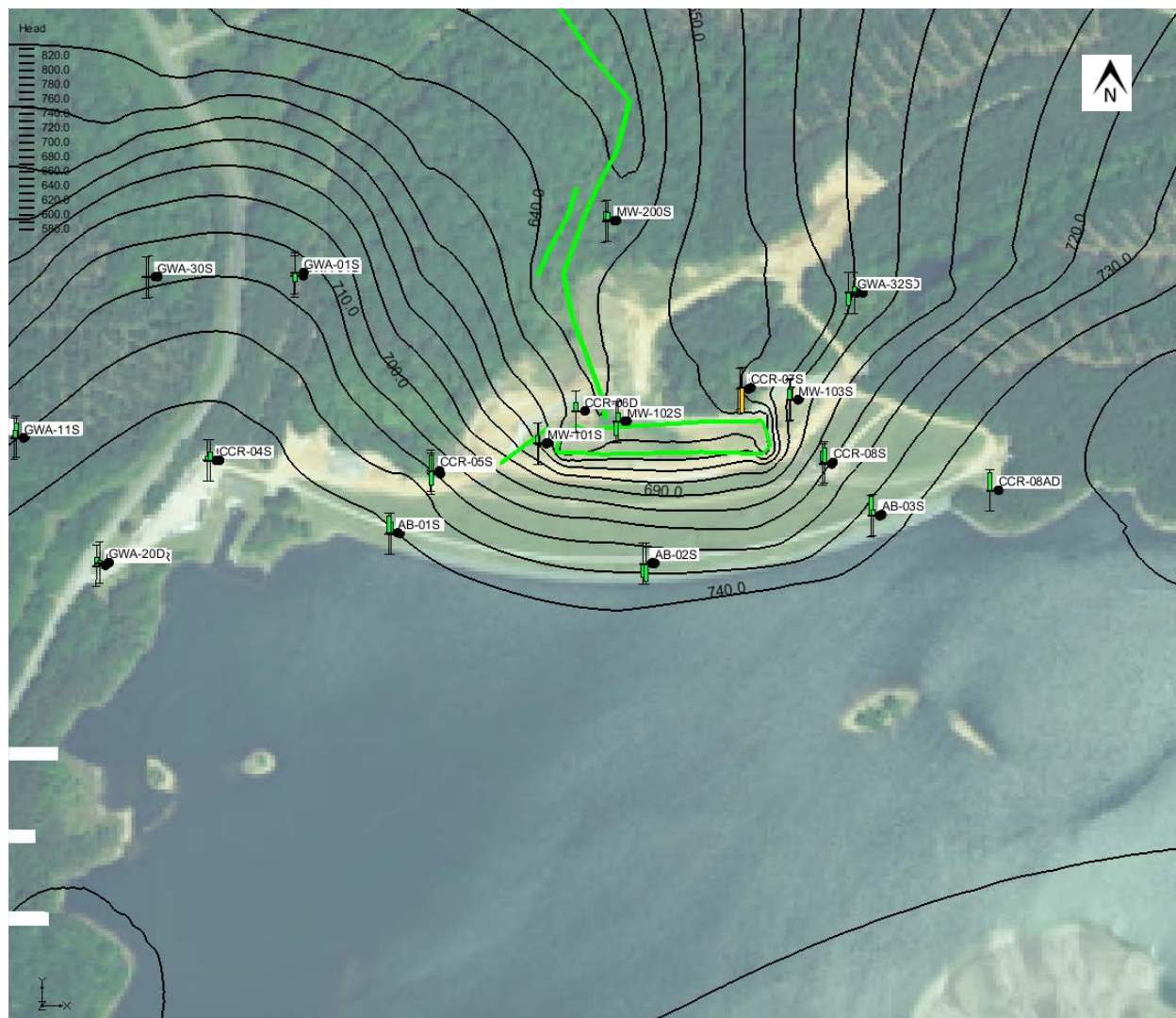


Figure 5-11. Close-up view of simulated hydraulic heads near the ash basin dam. The model drains (green lines) collect 185 gpm, which compares favorably with the measured value at S-11.

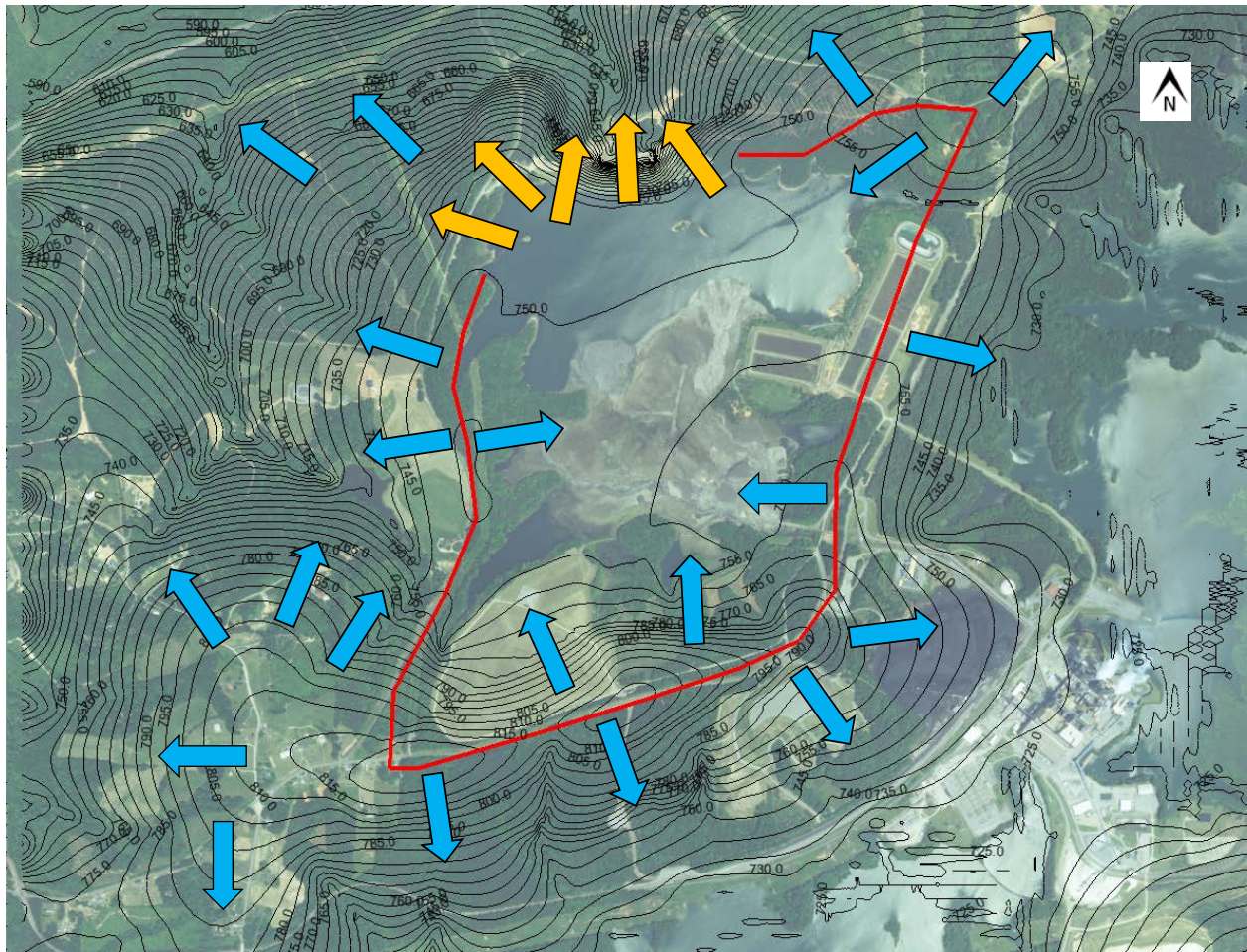


Figure 5-12. Groundwater divide and flow directions under current conditions at the BCSS. The groundwater divide is shown as the red line, and the arrows indicate groundwater flow directions. The yellow arrows show locations and direction of COI transport away from the ash basin.

**Flow through/immediately under dam -185 gpm**

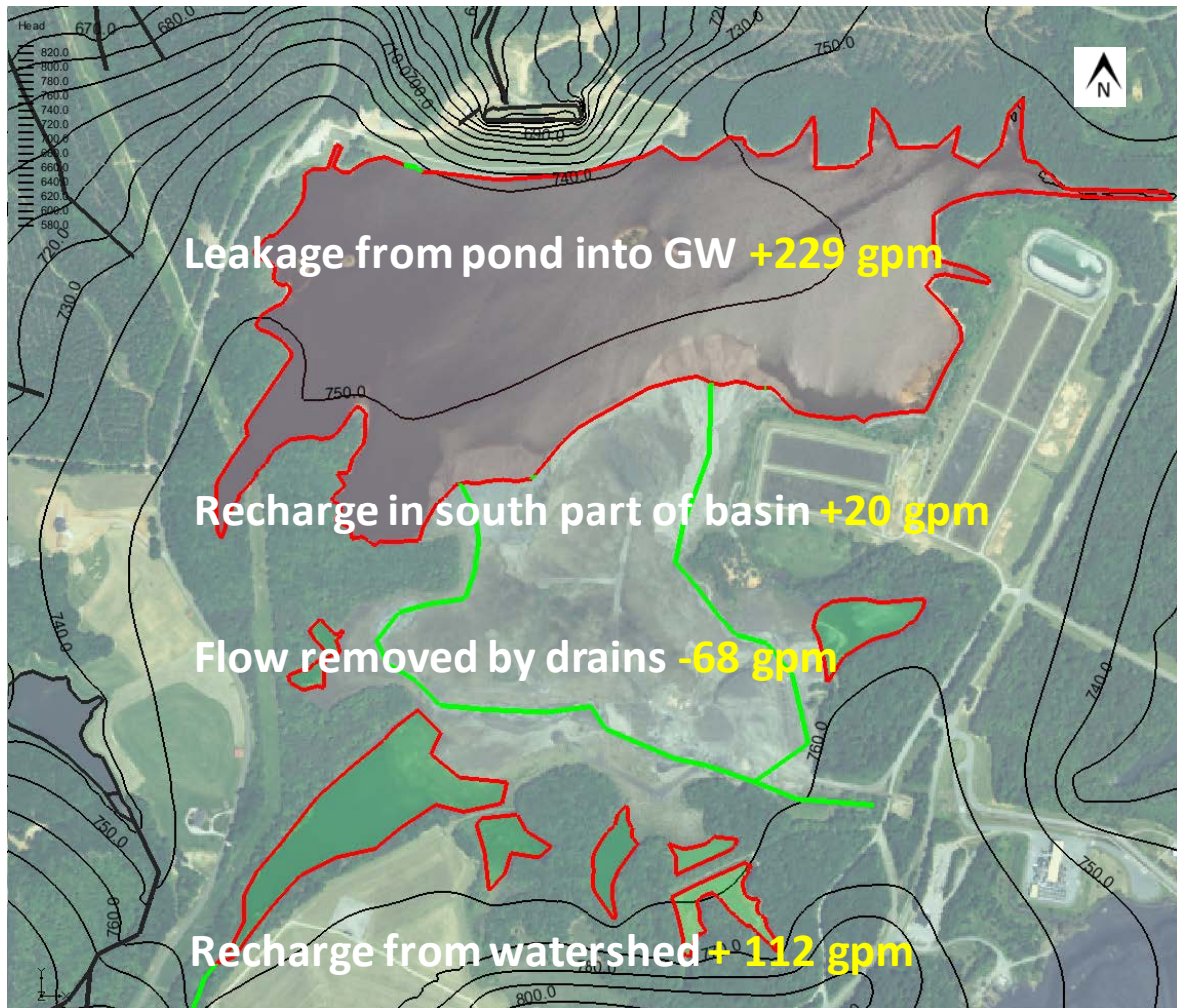


Figure 5-13. Approximate groundwater budget under current conditions in the ash basin area.

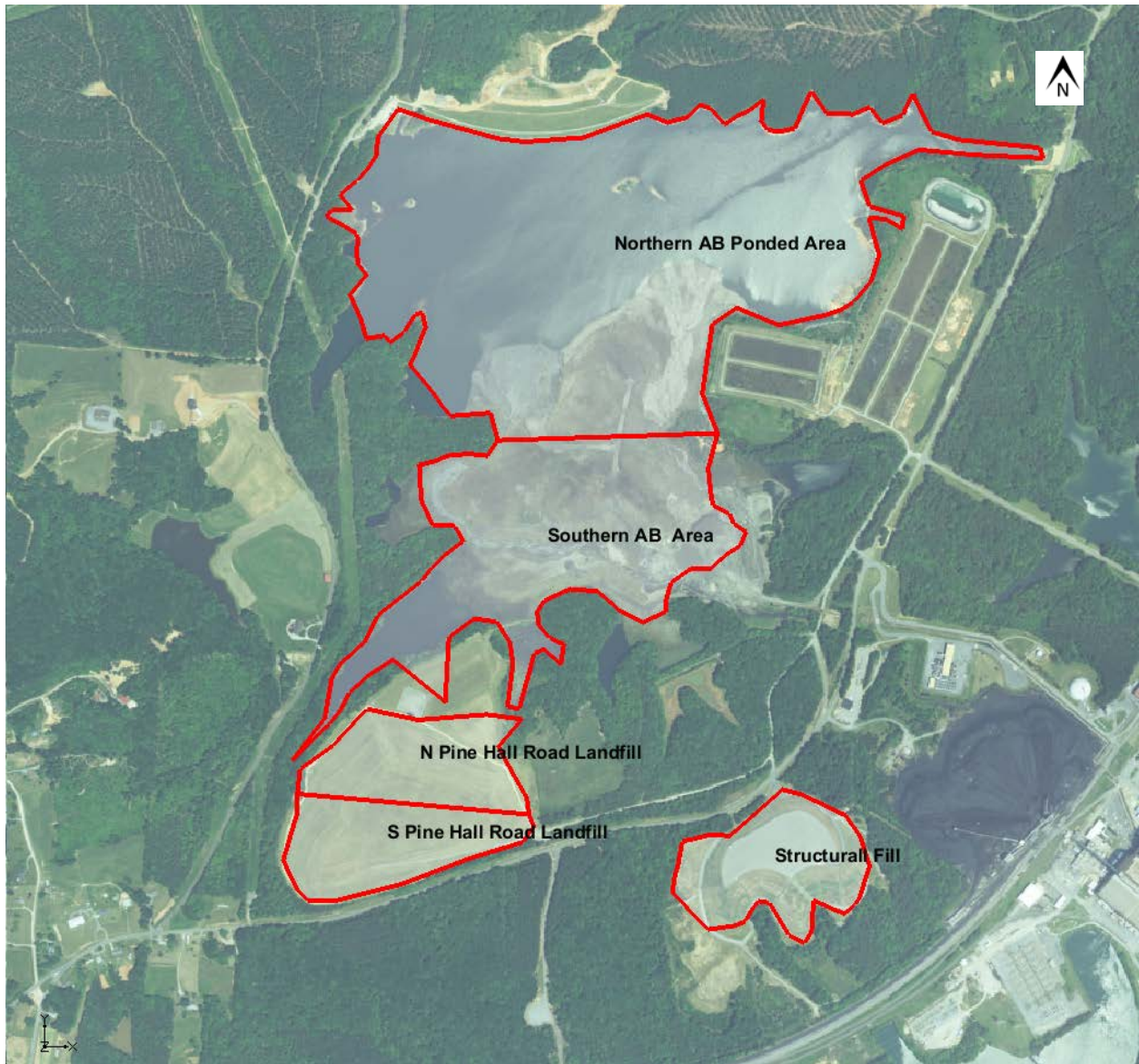


Figure 5-14. COI source zones for the historical transport model.

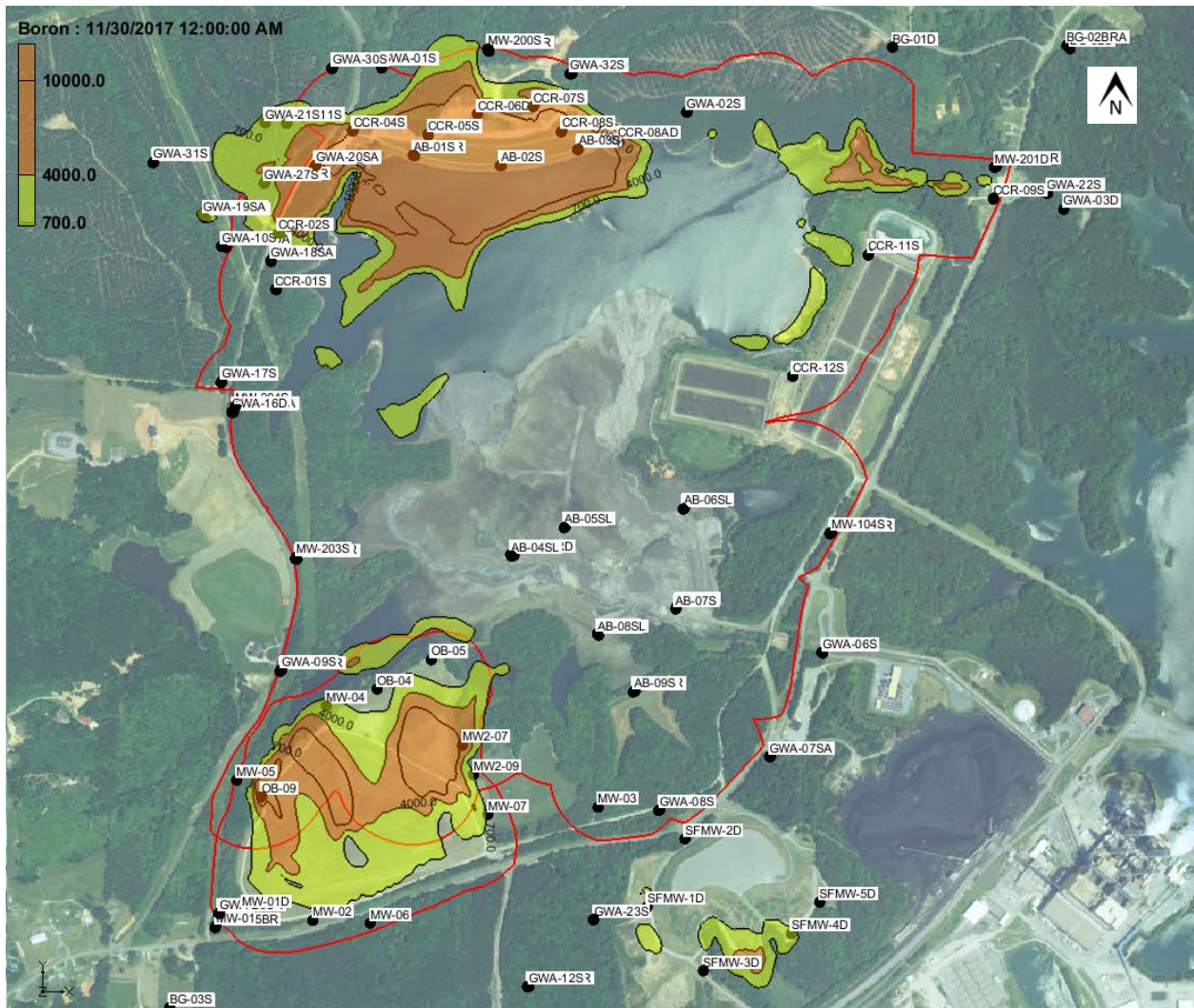


Figure 5-15a. Simulated December 2017 boron concentrations ( $\mu\text{g/L}$ ) in the transition zone (layer 15). The larger red outline is the ash basin compliance boundary and the smaller red outline is Pine Hall Road Landfill compliance boundary.

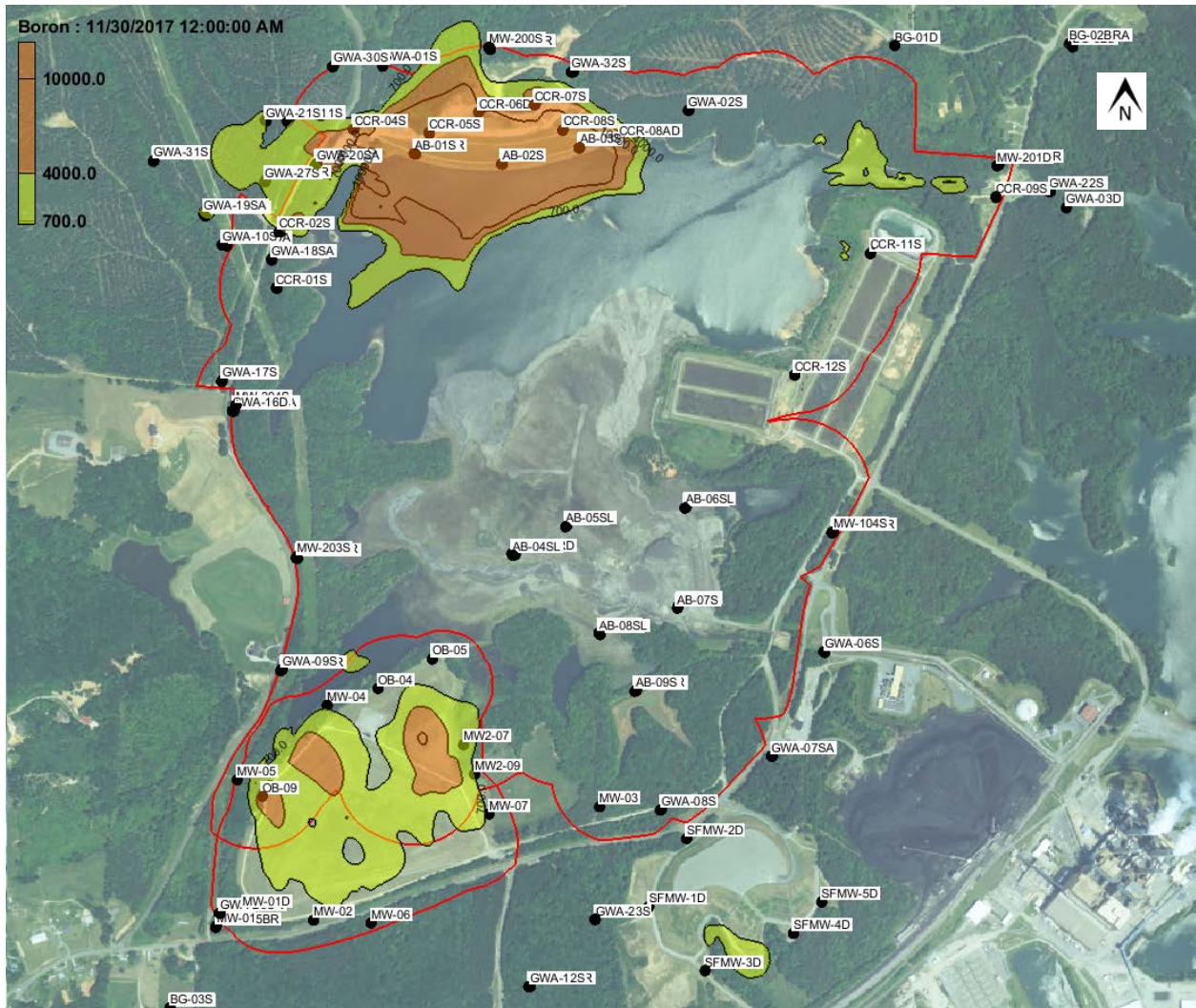


Figure 5-15b. Simulated December 2017 boron concentrations ( $\mu\text{g/L}$ ) in the upper bedrock (layer 16). The larger red outline is the ash basin compliance boundary and the smaller red outline is Pine Hall Road Landfill compliance boundary.





Figure 6-1. Location of current accelerated remediation wells. The red line is the compliance boundary and the yellow circles are the 10 interim action groundwater extraction wells. The red outline is the compliance boundary.

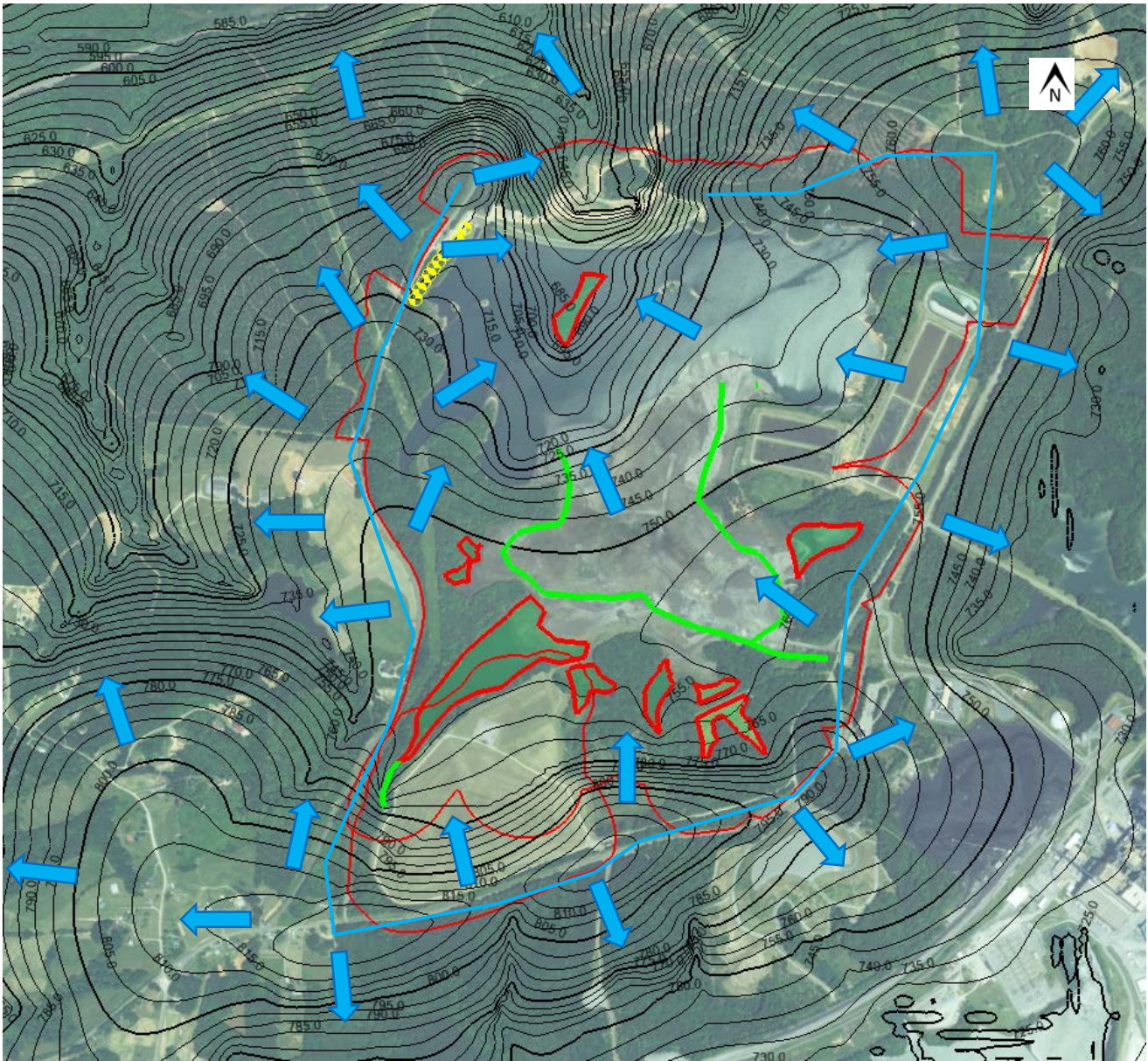


Figure 6-2. Simulated hydraulic heads in the transition zone after ash basin pond drainage. Drains are represented as green lines and green polygons with a thick red outline. The larger thin red outline is the ash basin compliance boundary and the smaller thin red outline is Pine Hall Road Landfill compliance boundary. Approximate groundwater divide in light blue and approximate flow directions as light blue arrows.

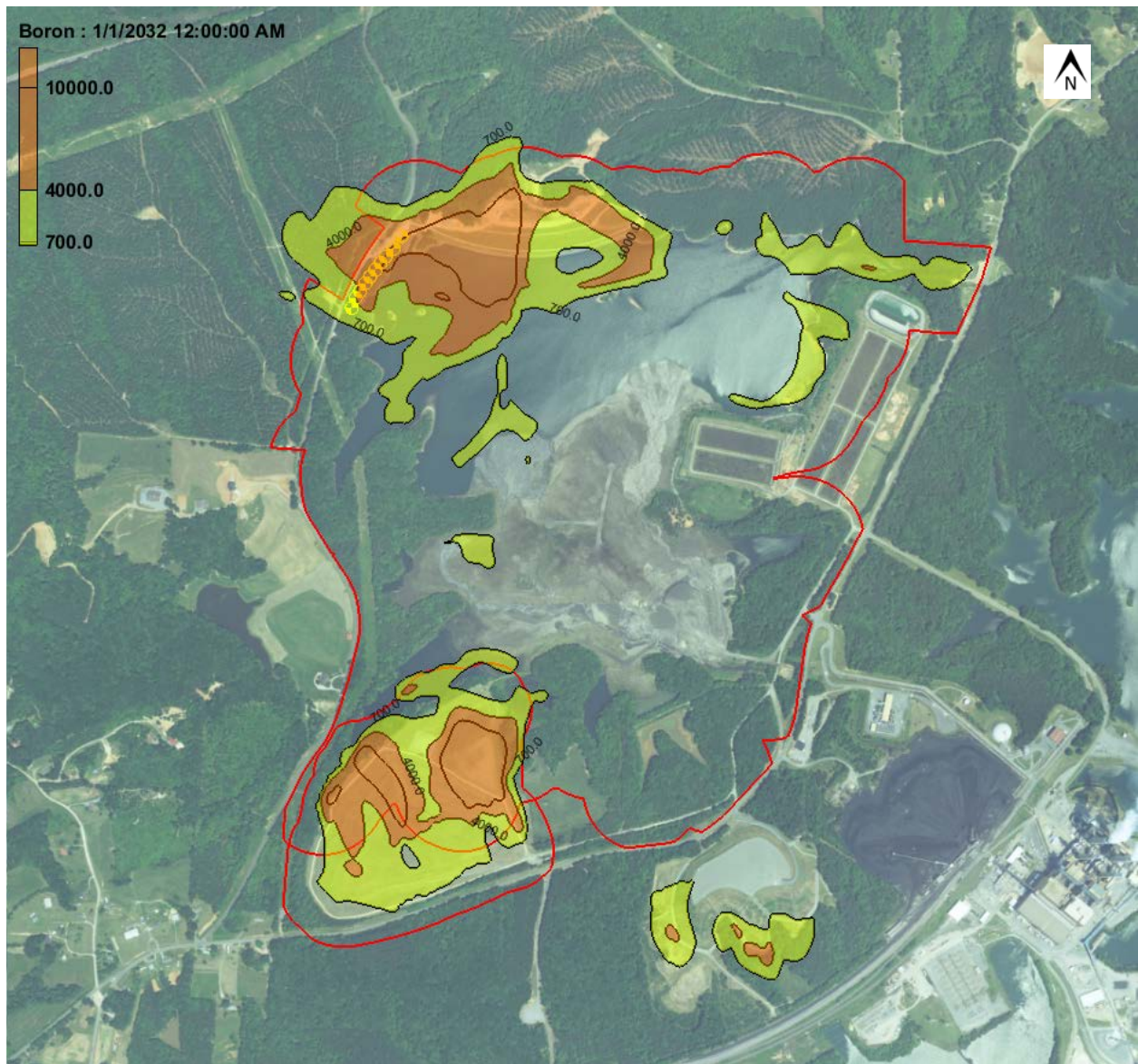


Figure 6-3. Simulated boron concentrations in the transition zone in 2032 for a simulation where the ash basin pond has been decanted, and 10 interim action groundwater extraction wells are operating. The larger red outline is the ash basin compliance boundary and the smaller red outline is Pine Hall Road Landfill compliance boundary.

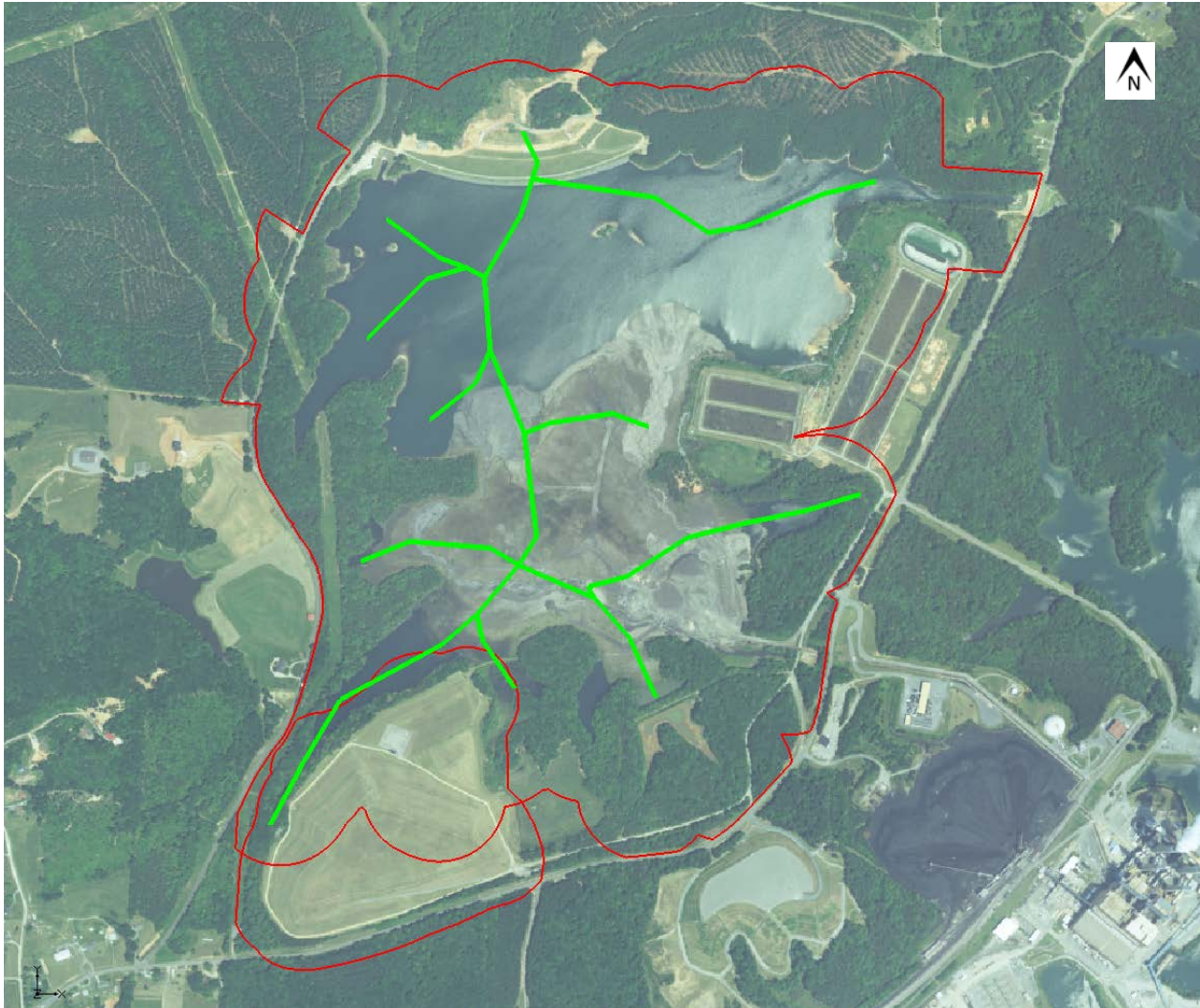


Figure 6-4. Drain network used in excavation simulations to represent springs and streams that may form. The elevations are set to the top of the saprolite surface, which approximately corresponds to the original ground surface. Drains are represented as green lines. The larger red outline is the ash basin compliance boundary and the smaller red outline is Pine Hall Road Landfill compliance boundary.

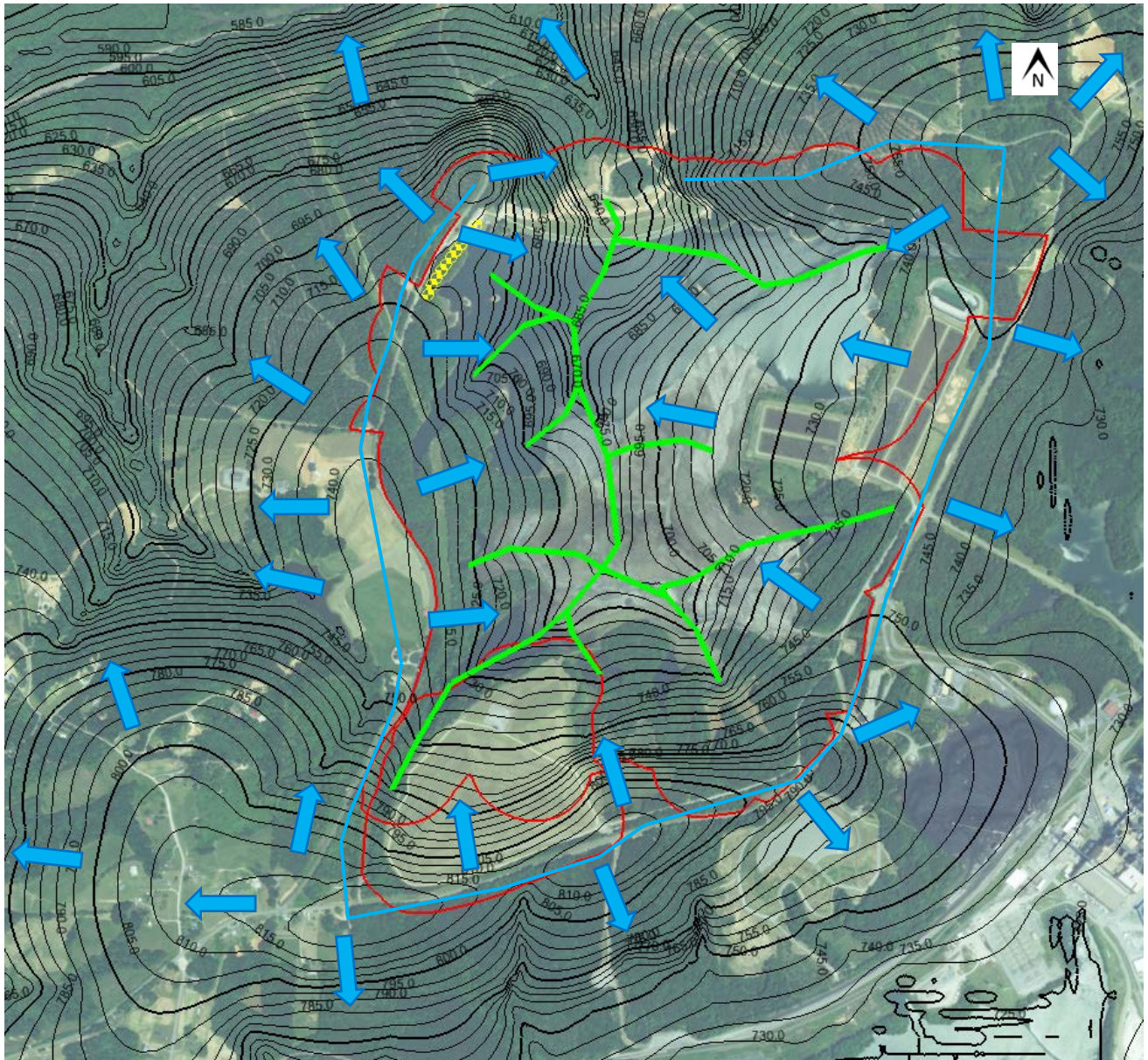


Figure 6-5. Simulated hydraulic heads for excavation scenario with 10 interim action groundwater extraction wells. The larger red outline is the ash basin compliance boundary and the smaller red outline is Pine Hall Road Landfill compliance boundary. Approximate groundwater divide in light blue and approximate flow directions as light blue arrows.

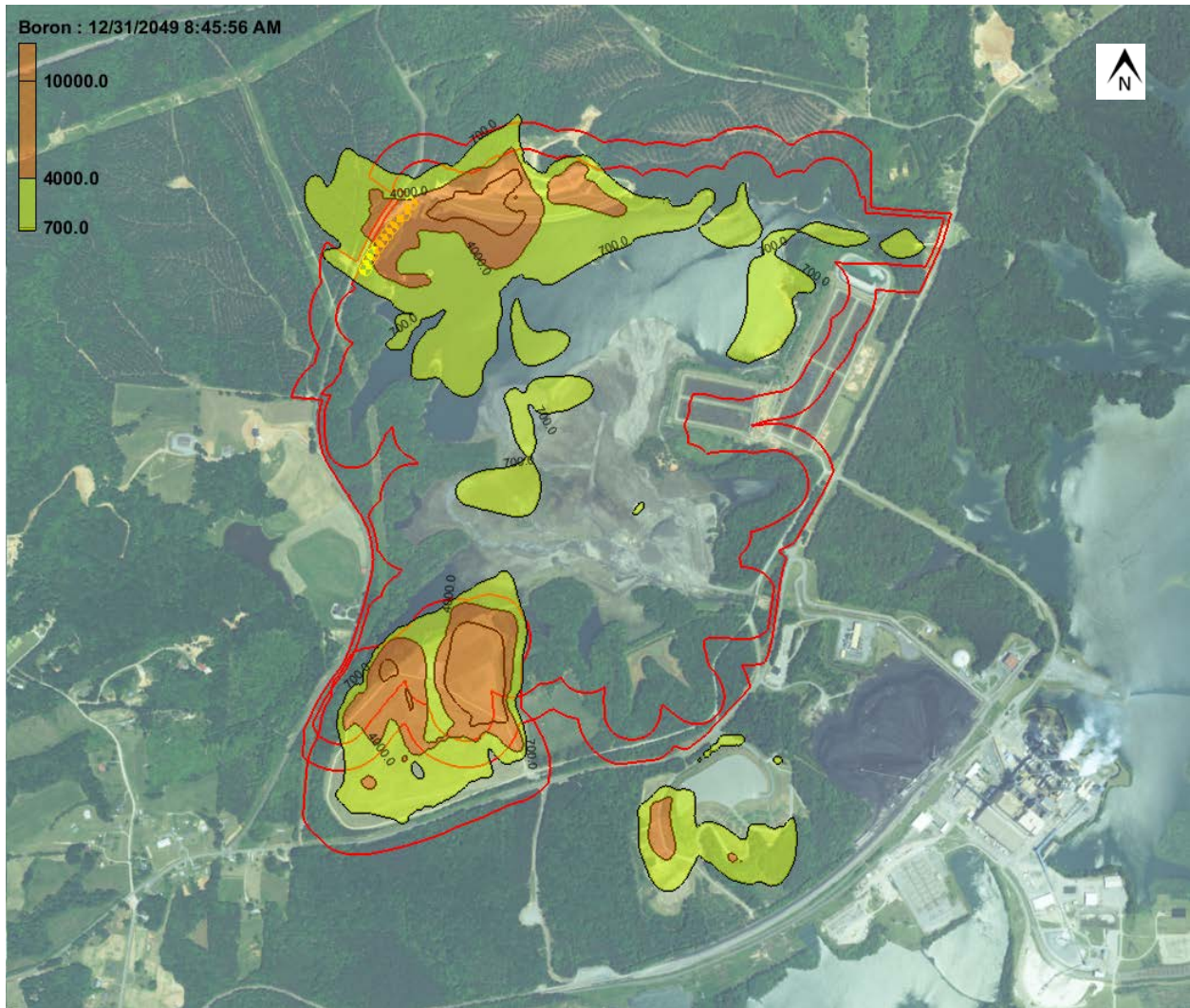


Figure 6-6a. Simulated boron concentrations in the transition zone (layer 15) in 2050 for the excavation scenario with 10 interim action groundwater extraction wells. The outer red line is the current compliance boundary, while the inner red line is the new compliance boundary following excavation.

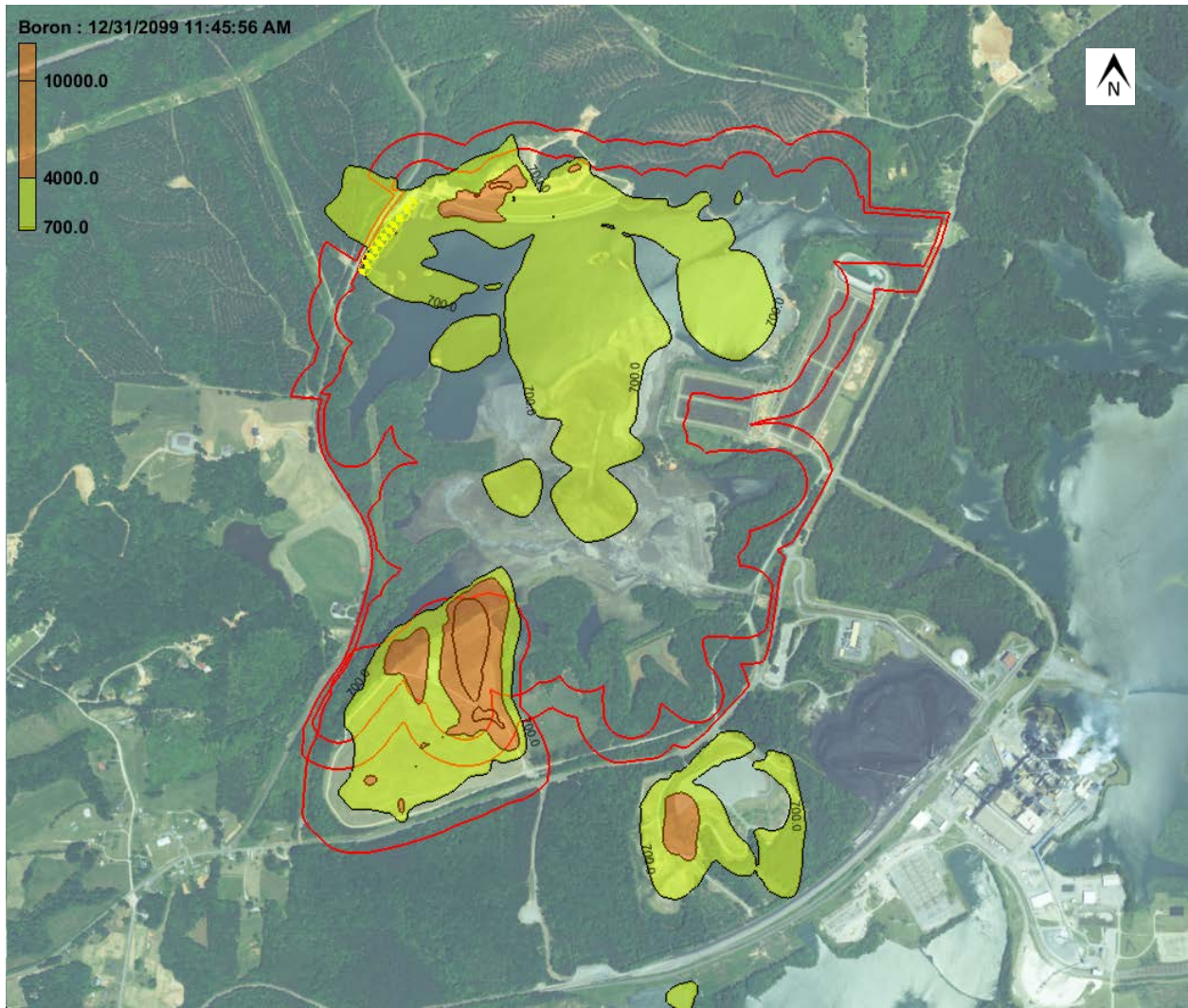


Figure 6-6b. Simulated boron concentrations in the transition zone (layer 15) in 2100 for the excavation scenario with 10 interim action groundwater extraction wells. The outer red line is the current compliance boundary, while the inner red line is the new compliance boundary following excavation.

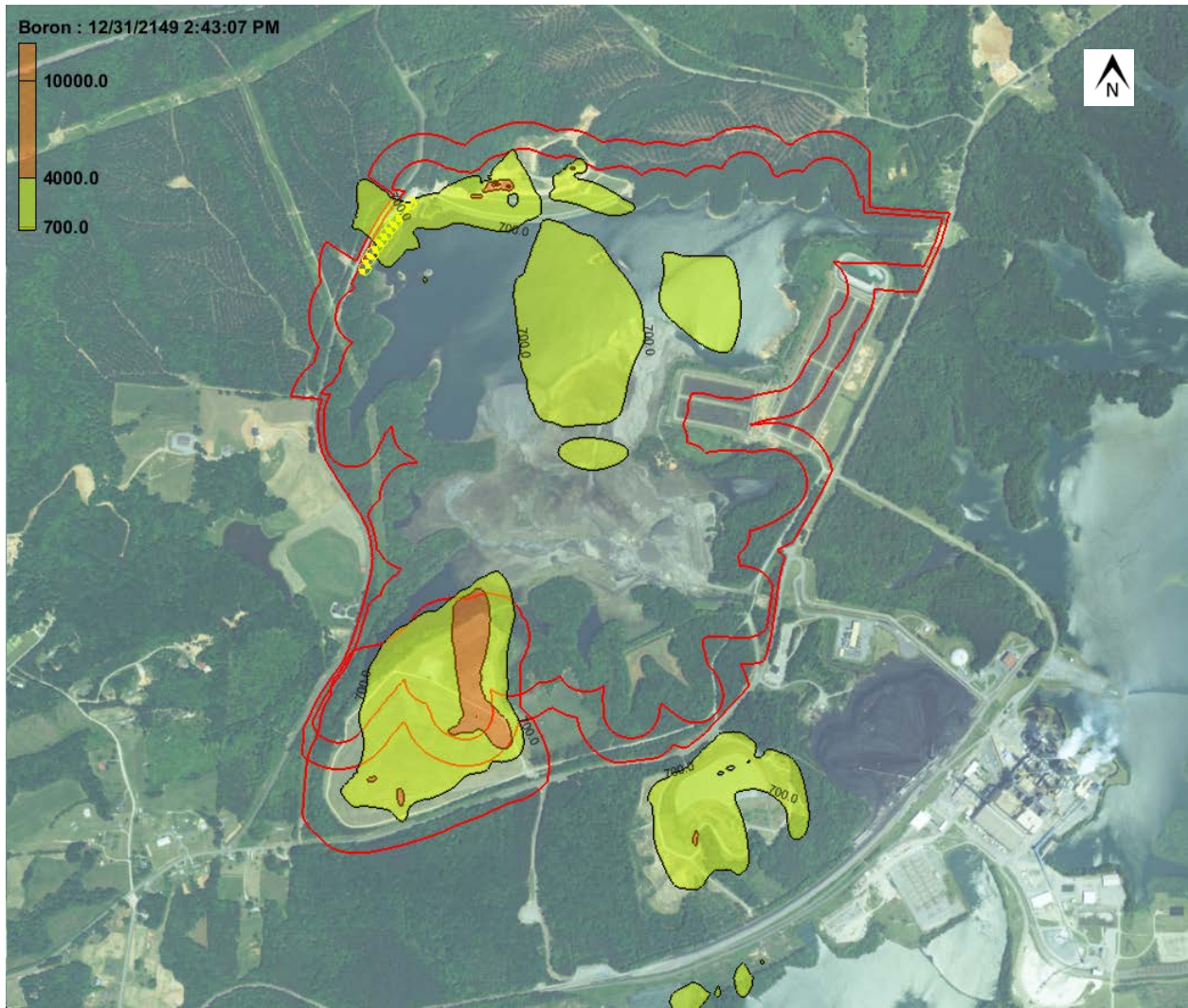


Figure 6-6c. Simulated boron concentrations in the transition zone (layer 15) in 2150 for the excavation scenario with 10 interim action groundwater extraction wells. The outer red line is the current compliance boundary, while the inner red line is the new compliance boundary following excavation.



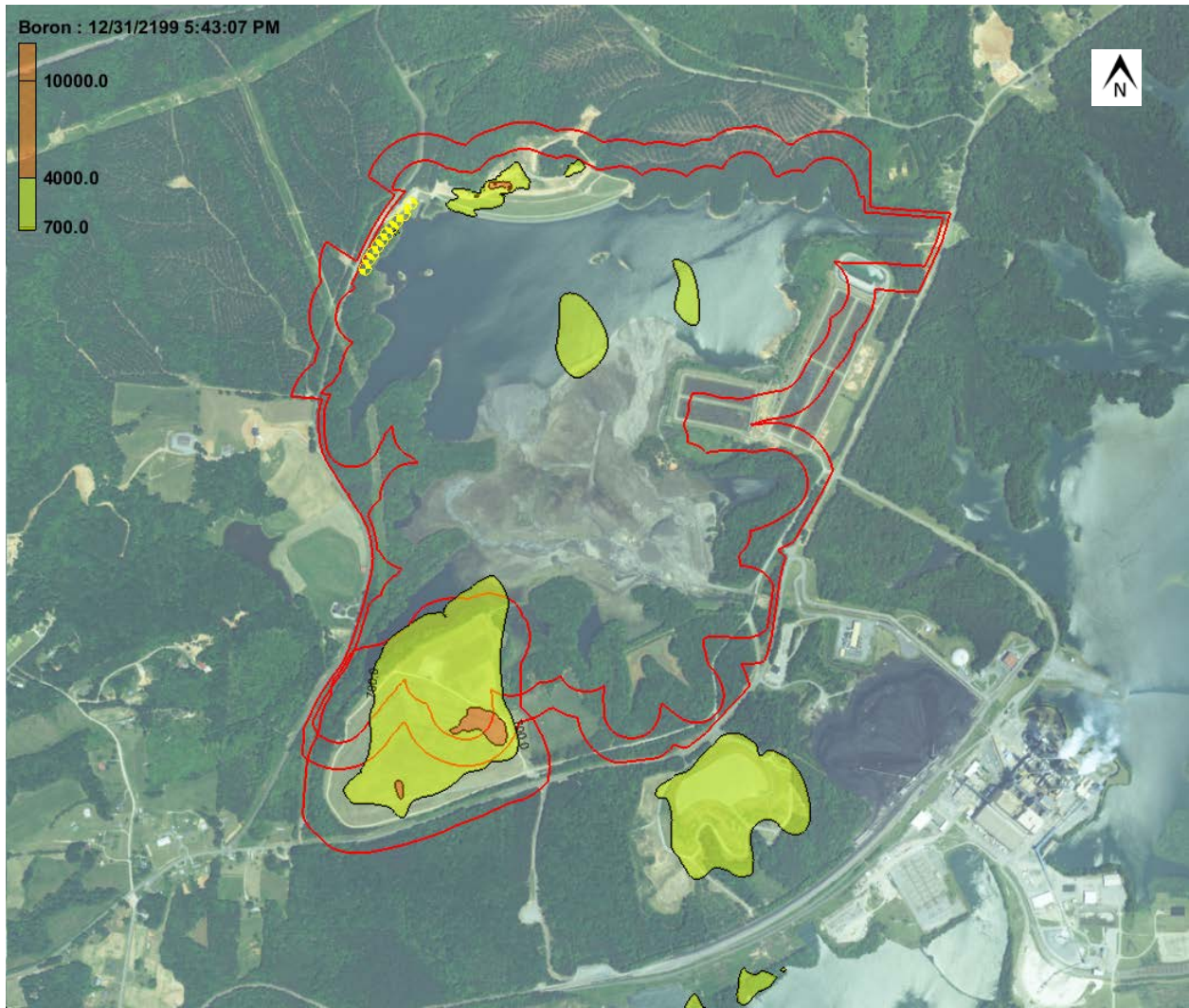


Figure 6-6d. Simulated boron concentrations in the transition zone (layer 15) in 2200 for the excavation scenario with 10 interim action groundwater extraction wells. The outer red line is the current compliance boundary, while the inner red line is the new compliance boundary following excavation.

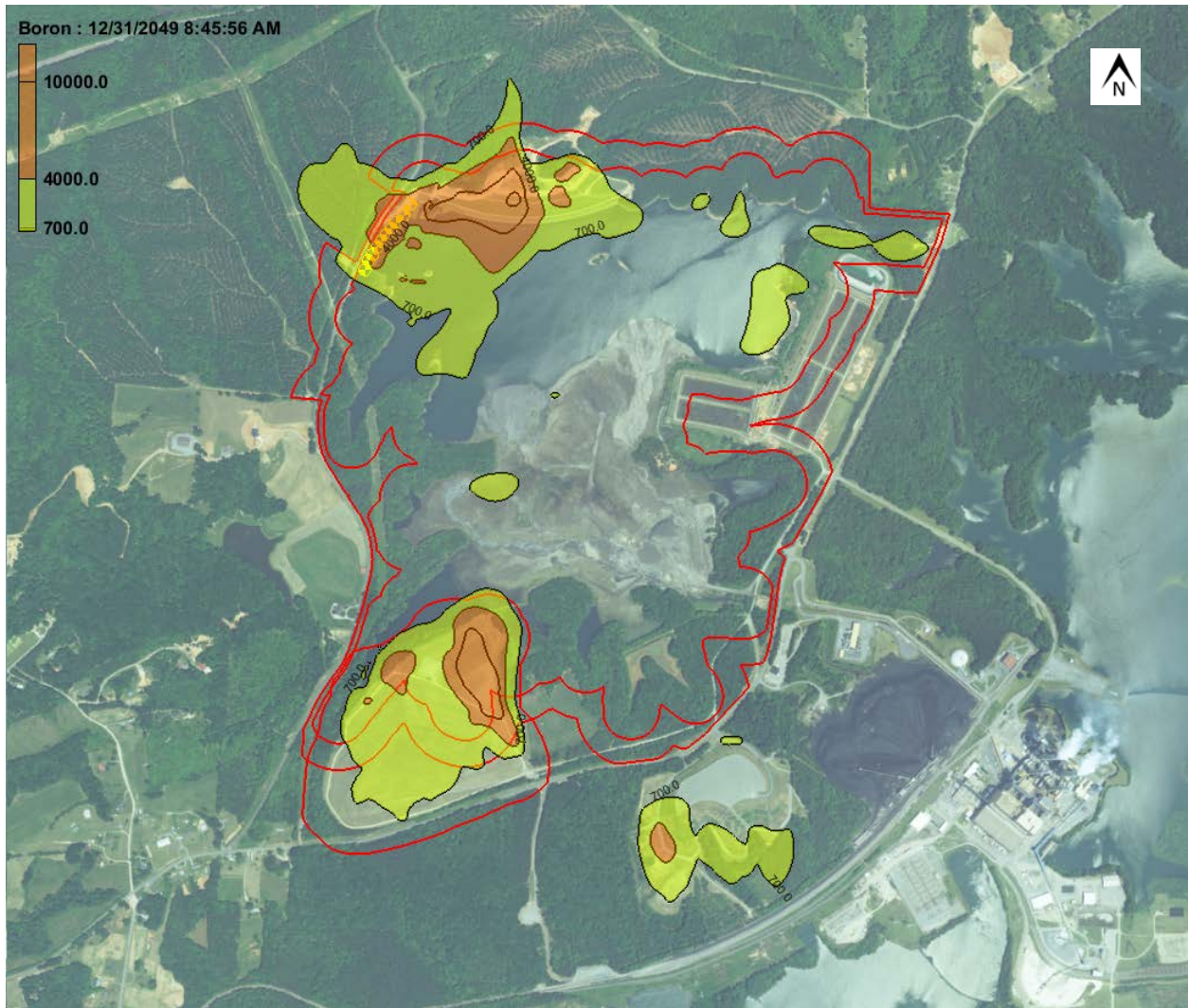


Figure 6-7a. Simulated boron concentrations in the upper bedrock (layer 16) in 2050 for the excavation scenario with 10 interim action groundwater extraction wells. The outer red line is the current compliance boundary, while the inner red line is the new compliance boundary following excavation.

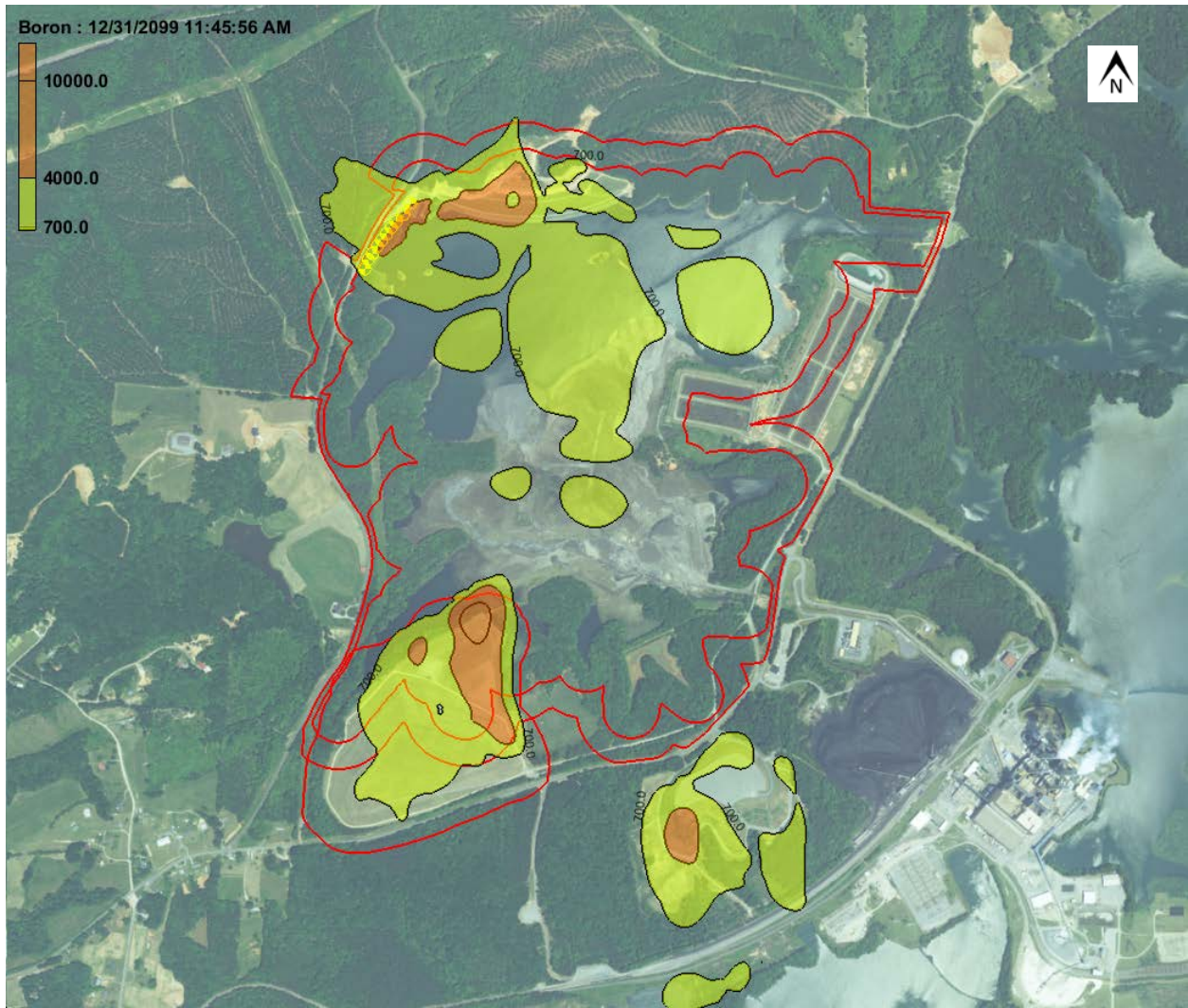


Figure 6-7b. Simulated boron concentrations in the upper bedrock (layer 16) in 2100 for the excavation scenario with 10 interim action groundwater extraction wells. The outer red line is the current compliance boundary, while the inner red line is the new compliance boundary following excavation.

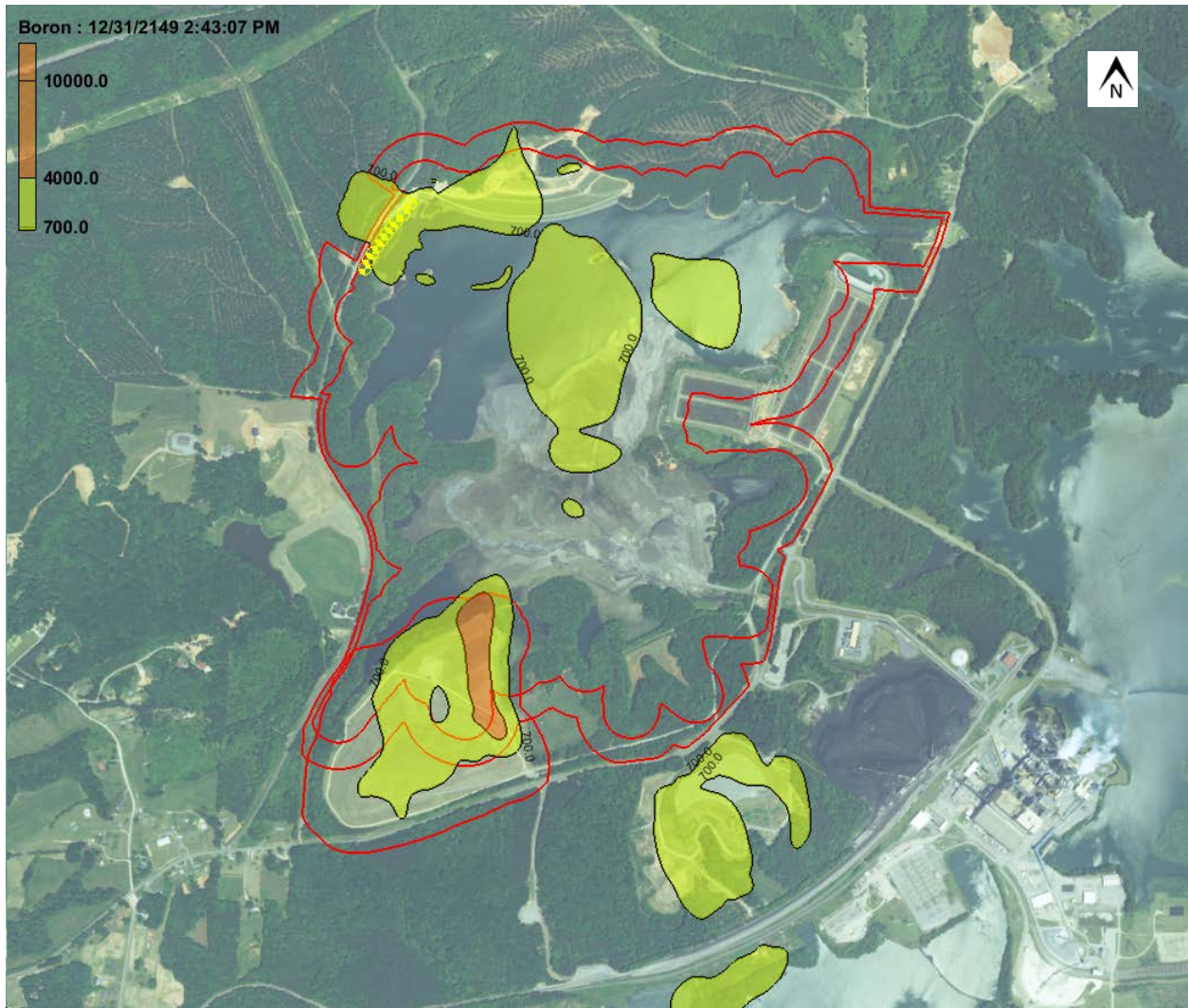


Figure 6-7c. Simulated boron concentrations in the upper bedrock (layer 16) in 2150 for the excavation scenario with 10 interim action groundwater extraction wells. The outer red line is the current compliance boundary, while the inner red line is the new compliance boundary following excavation.

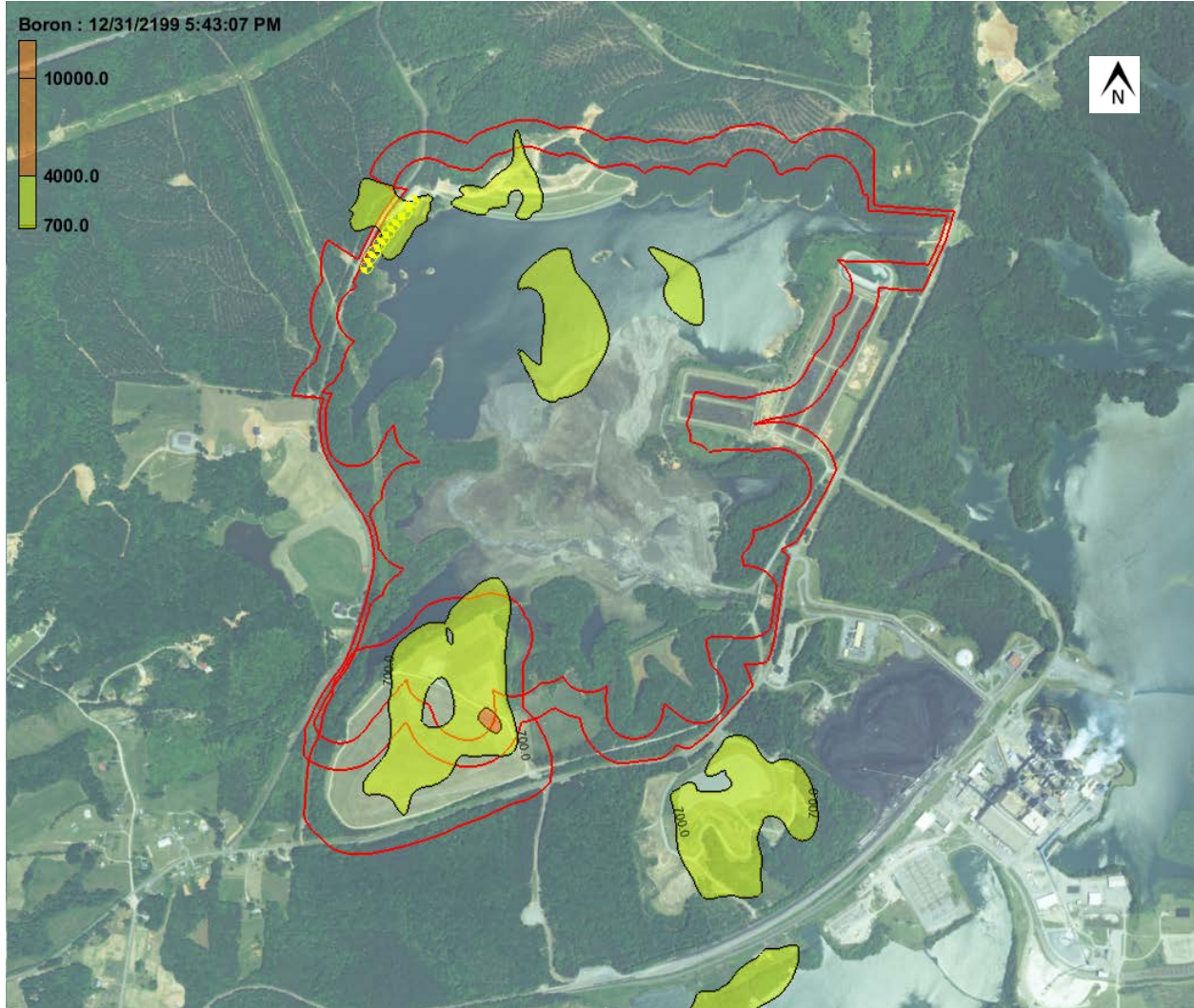


Figure 6-7d. Simulated boron concentrations in the upper bedrock (layer 16) in 2200 for the excavation scenario with 10 interim action groundwater extraction wells. The outer red line is the current compliance boundary, while the inner red line is the new compliance boundary following excavation.



Figure 6-8. Locations for boron time-series plots. The outer red line is the current compliance boundary, while the inner red line is the new compliance boundary following excavation.

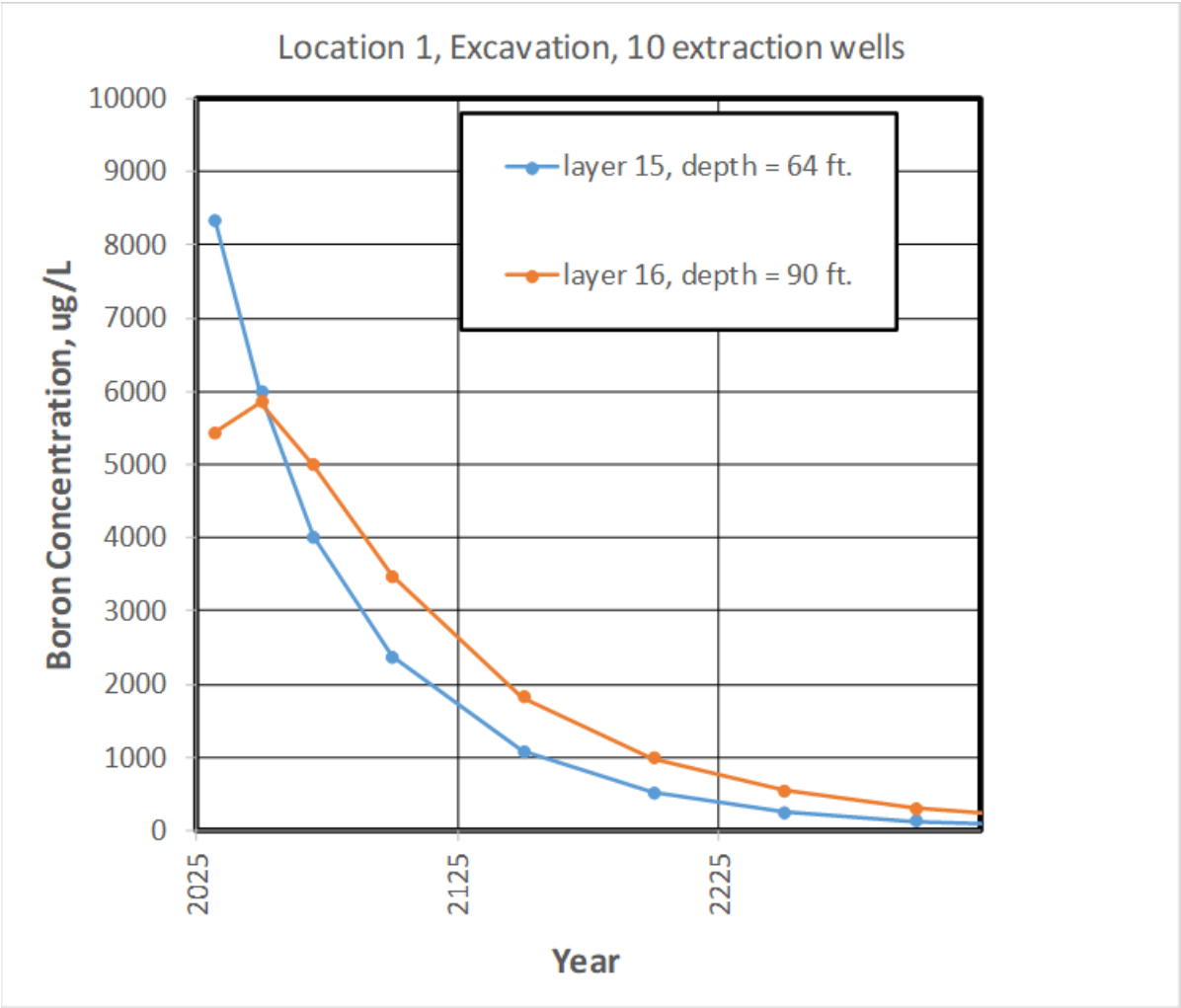


Figure 6-9. Predicted boron concentrations at location 1 along Middleton Loop Road for the excavation scenario with 10 interim action groundwater extraction wells.

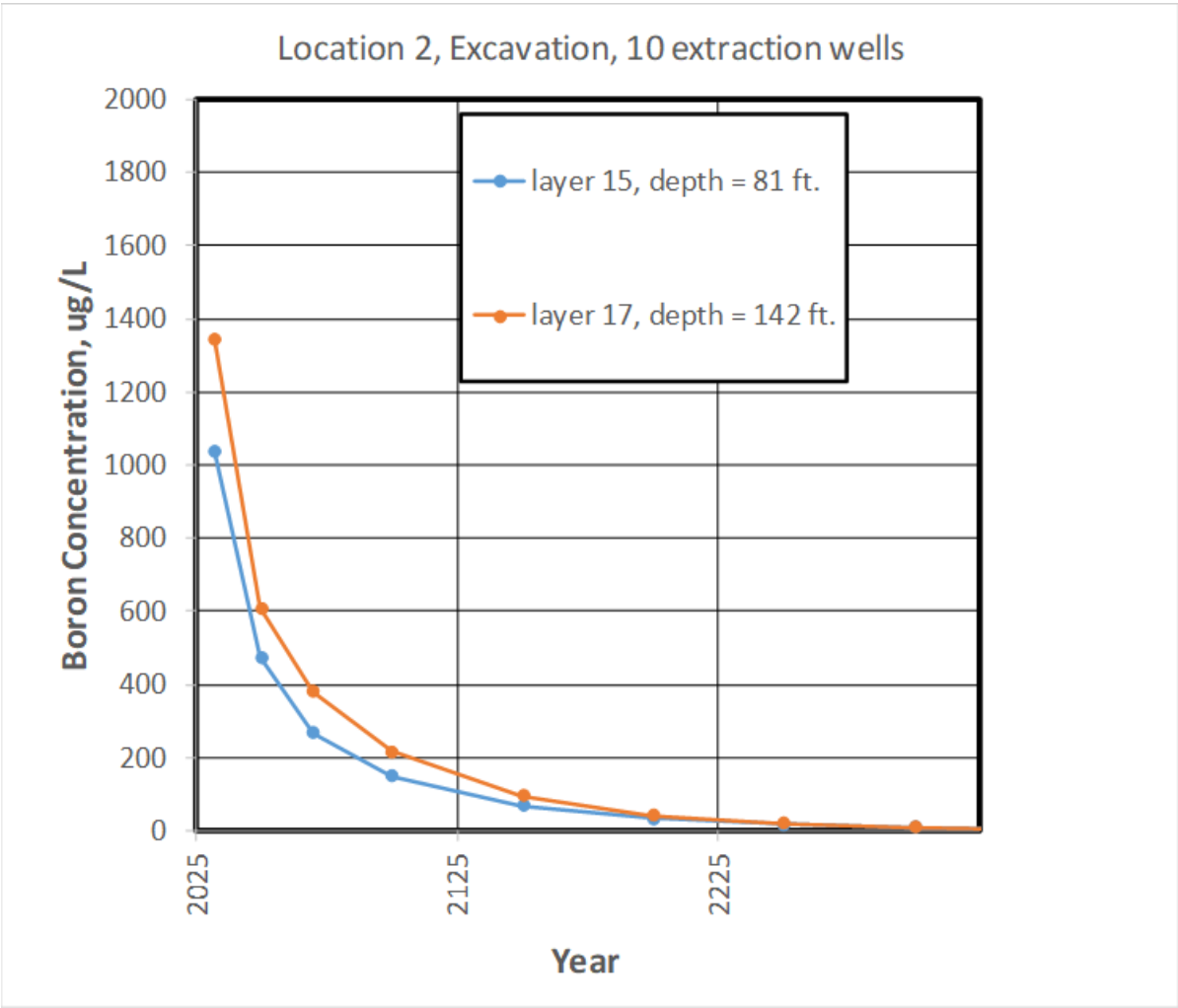


Figure 6-10. Predicted boron concentrations at location 2 below the ash basin dam for the excavation scenario with 10 interim action groundwater extraction wells.



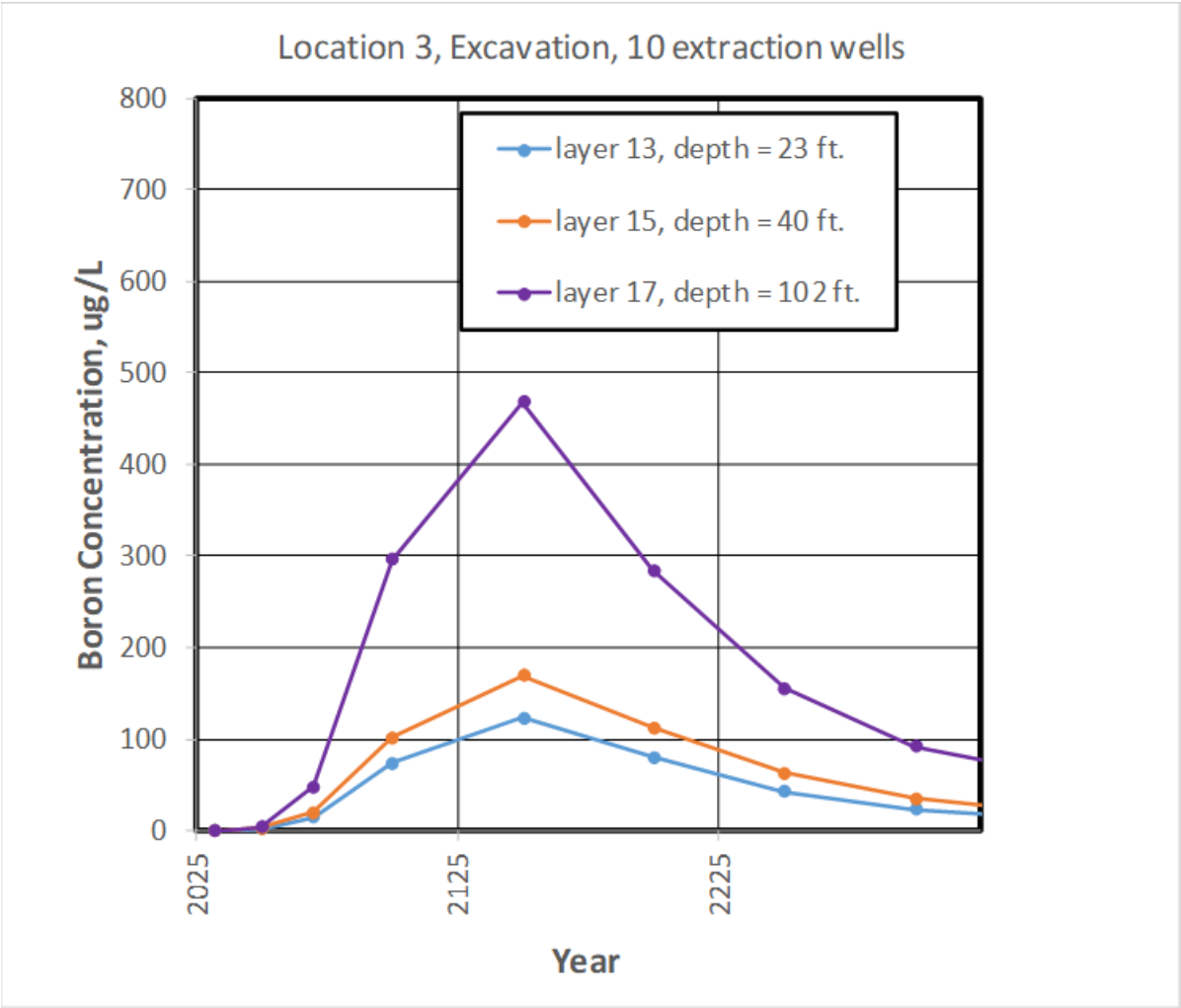


Figure 6-11. Predicted boron concentrations at location 3 near the Dan River for the excavation scenario with 10 interim action groundwater extraction wells.

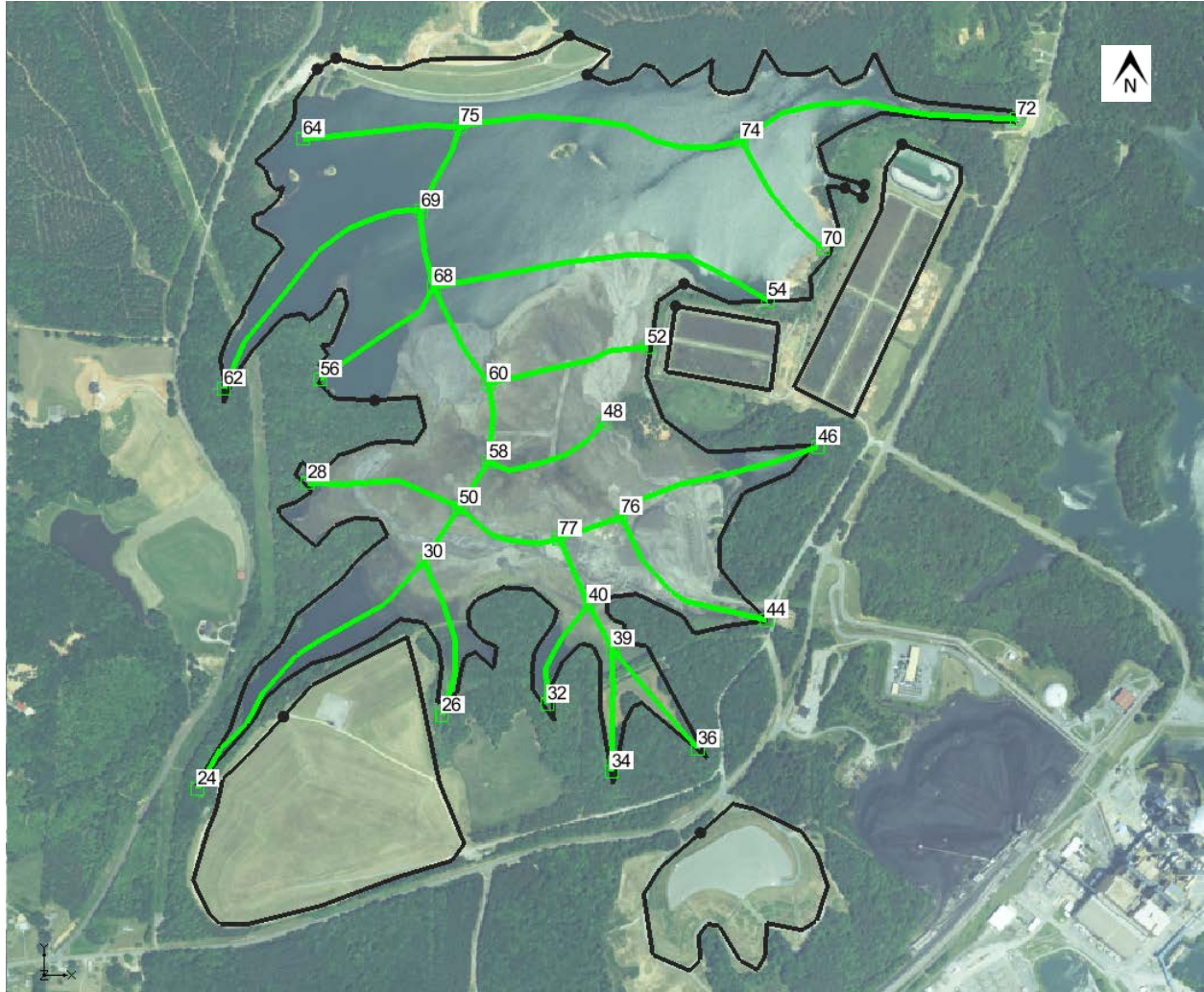


Figure 6-12. Proposed ash basin underdrain system for the final cover simulations. The numbered locations are nodes where the drain elevation was specified using the draft design from AECOM.

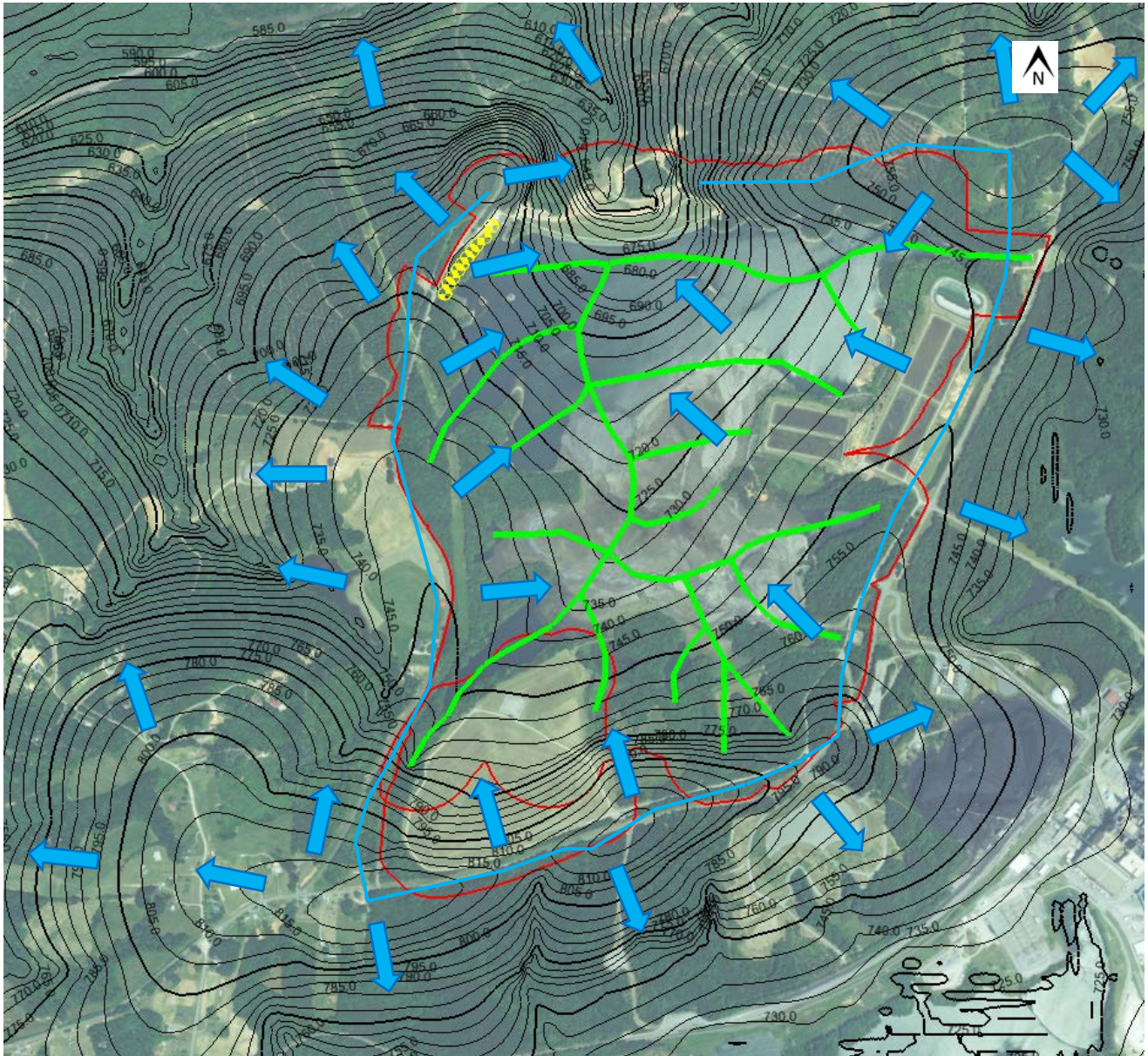


Figure 6-13. Simulated hydraulic heads for the final cover scenario with 10 interim action groundwater extraction wells. The larger red outline is the ash basin compliance boundary and the smaller red outline is Pine Hall Road Landfill compliance boundary. Approximate groundwater divide in light blue and approximate flow directions as light blue arrows.

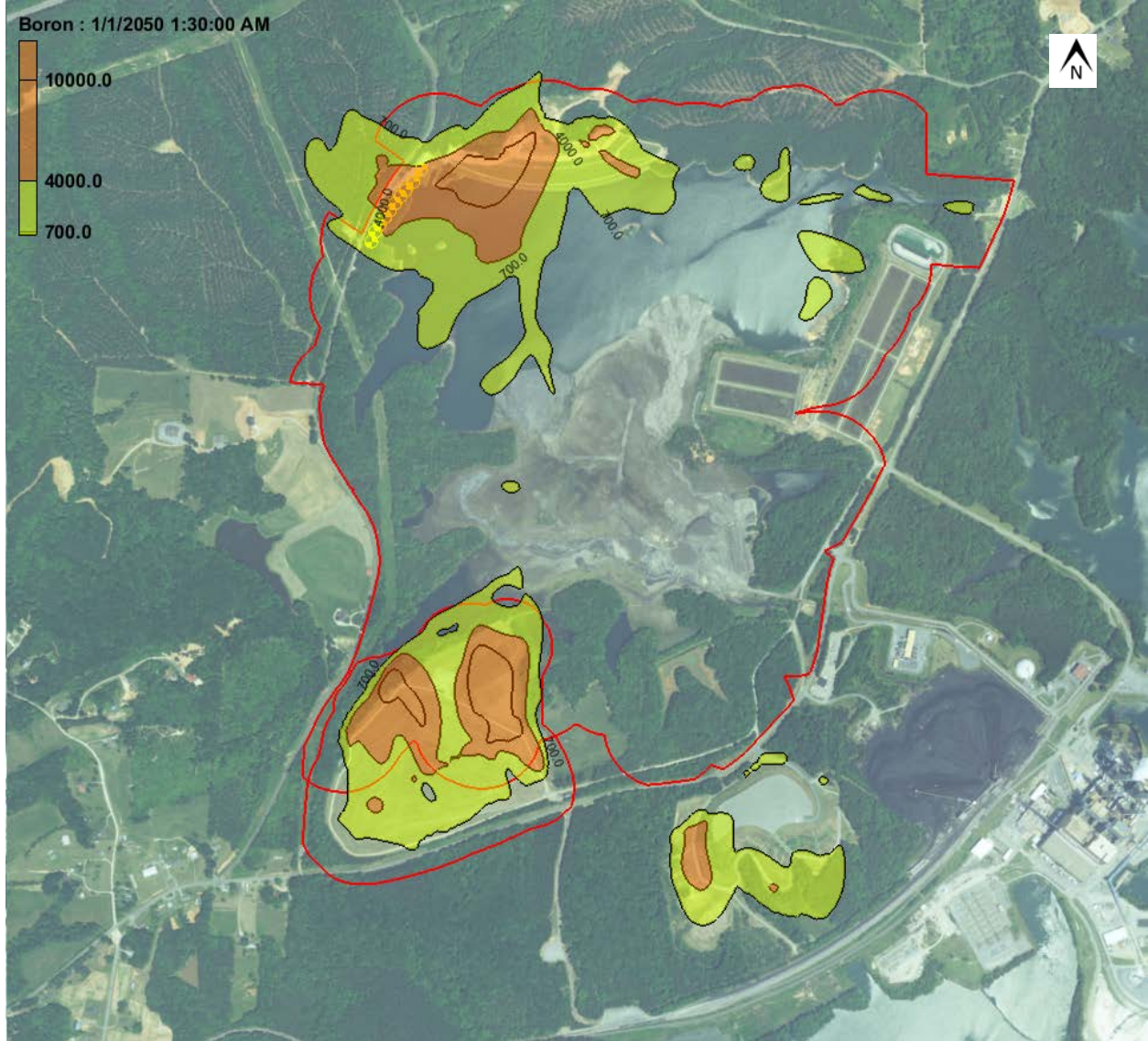


Figure 6-14a. Simulated boron concentrations in the transition zone (layer 15) in 2050 for the final cover scenario with 10 interim action groundwater extraction wells. The larger red outline is the ash basin compliance boundary and the smaller red outline is Pine Hall Road Landfill compliance boundary.

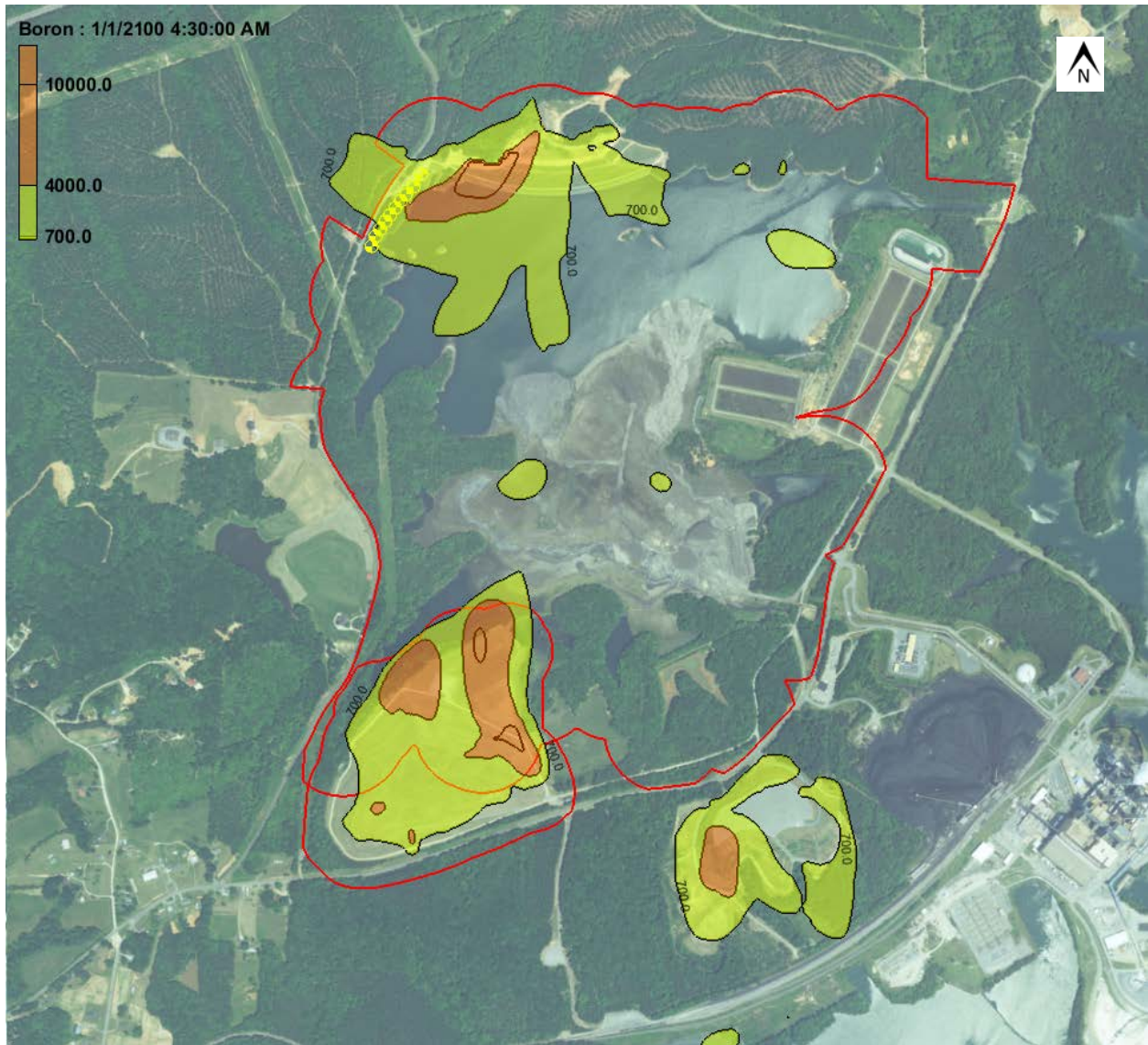


Figure 6-14b. Simulated boron concentrations in the transition zone (layer 15) in 2100 for the final cover scenario with 10 interim action groundwater extraction wells. The larger red outline is the ash basin compliance boundary and the smaller red outline is Pine Hall Road Landfill compliance boundary.

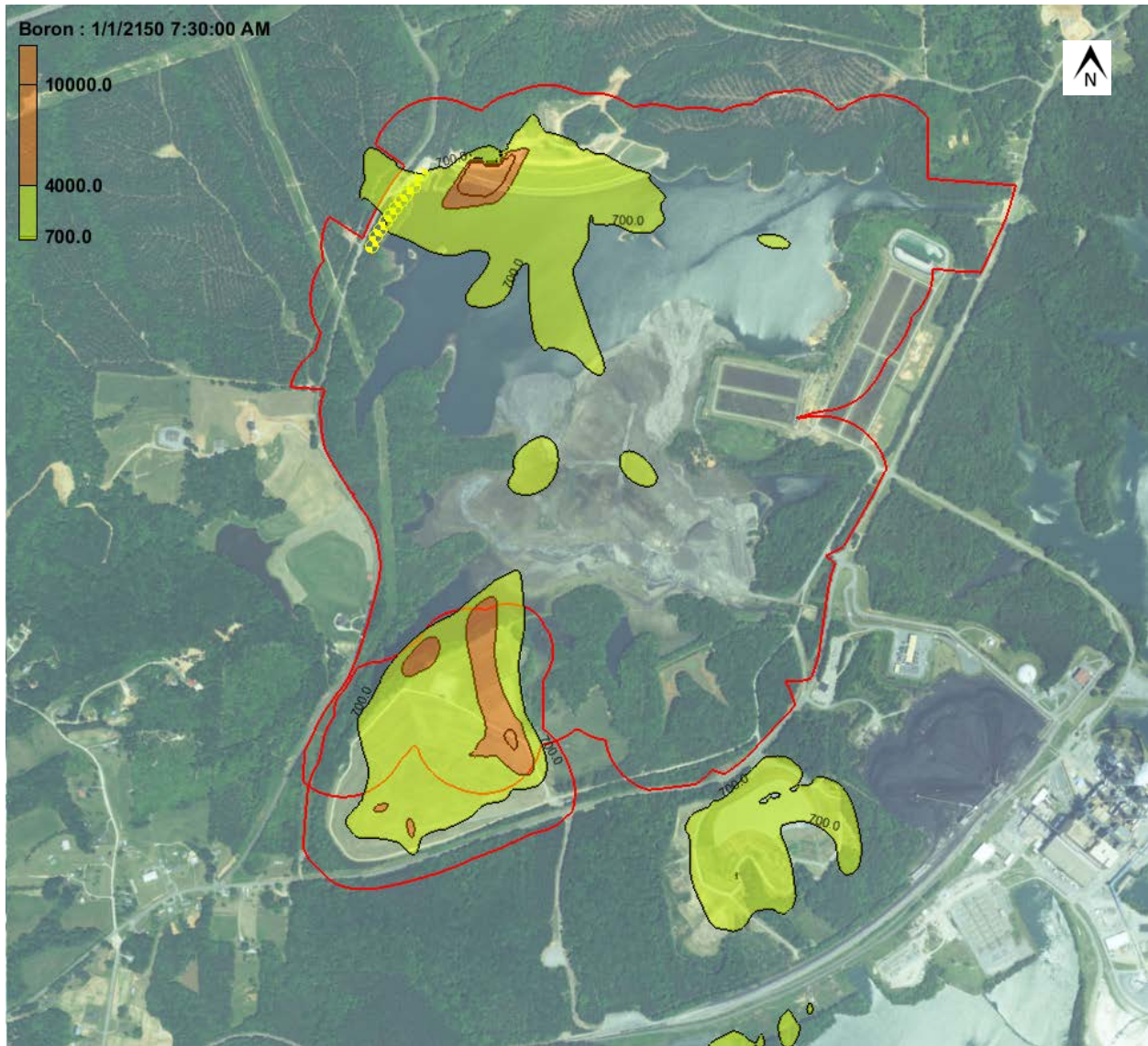


Figure 6-14c. Simulated boron concentrations in the transition zone (layer 15) in 2150 for the final cover scenario with 10 interim action groundwater extraction wells. The larger red outline is the ash basin compliance boundary and the smaller red outline is Pine Hall Road Landfill compliance boundary.

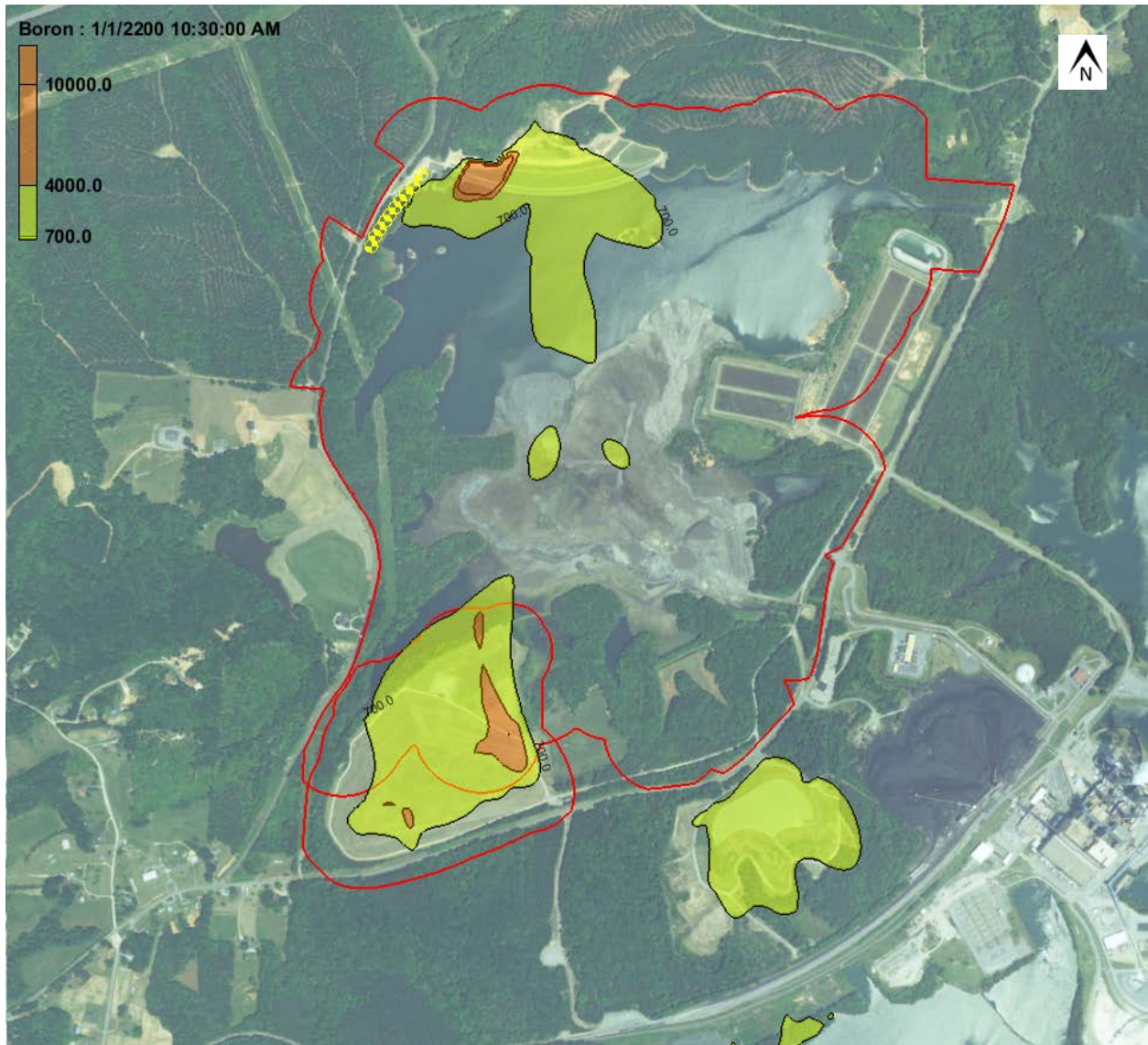


Figure 6-14d. Simulated boron concentrations in the transition zone (layer 15) in 2200 for the final cover scenario with 10 interim action groundwater extraction wells. The larger red outline is the ash basin compliance boundary and the smaller red outline is Pine Hall Road Landfill compliance boundary.

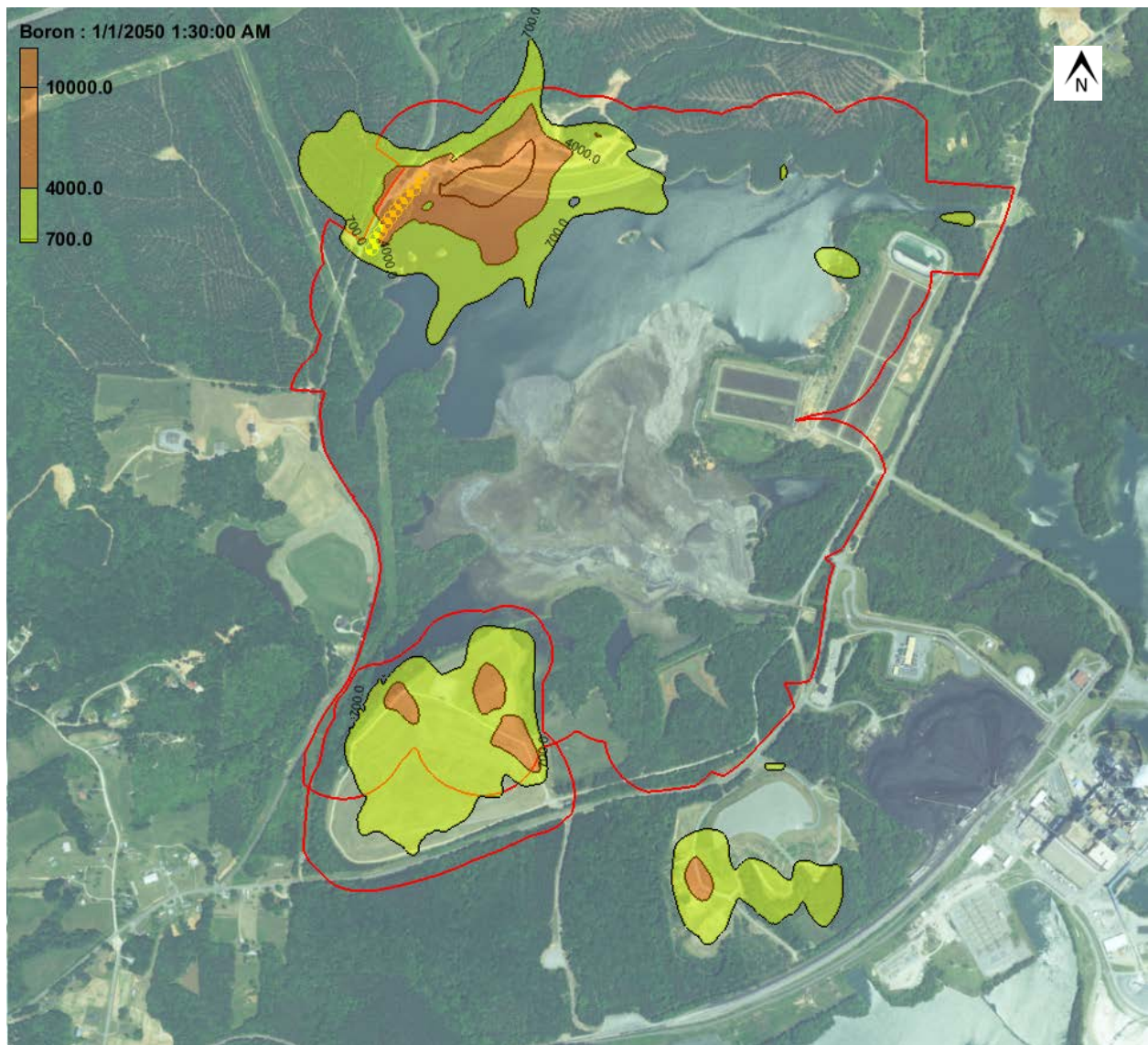


Figure 6-15a. Simulated boron concentrations in the upper bedrock (layer 16) in 2050 for the final cover scenario with 10 interim action groundwater extraction wells. The larger red outline is the ash basin compliance boundary and the smaller red outline is Pine Hall Road Landfill compliance boundary.



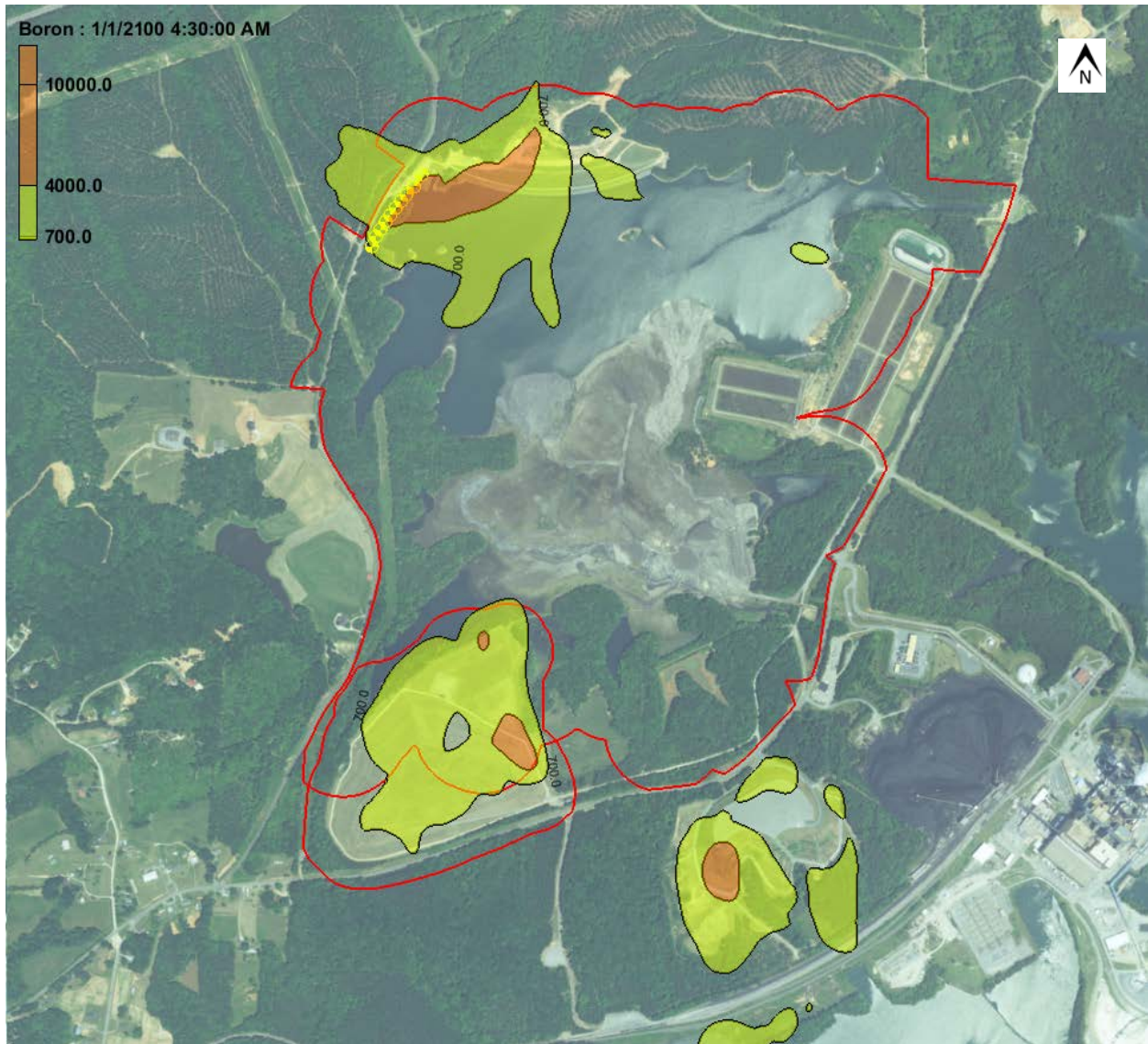


Figure 6-15b. Simulated boron concentrations in the upper bedrock (layer 16) in 2100 for the final cover scenario with 10 interim action groundwater extraction wells. The larger red outline is the ash basin compliance boundary and the smaller red outline is Pine Hall Road Landfill compliance boundary.

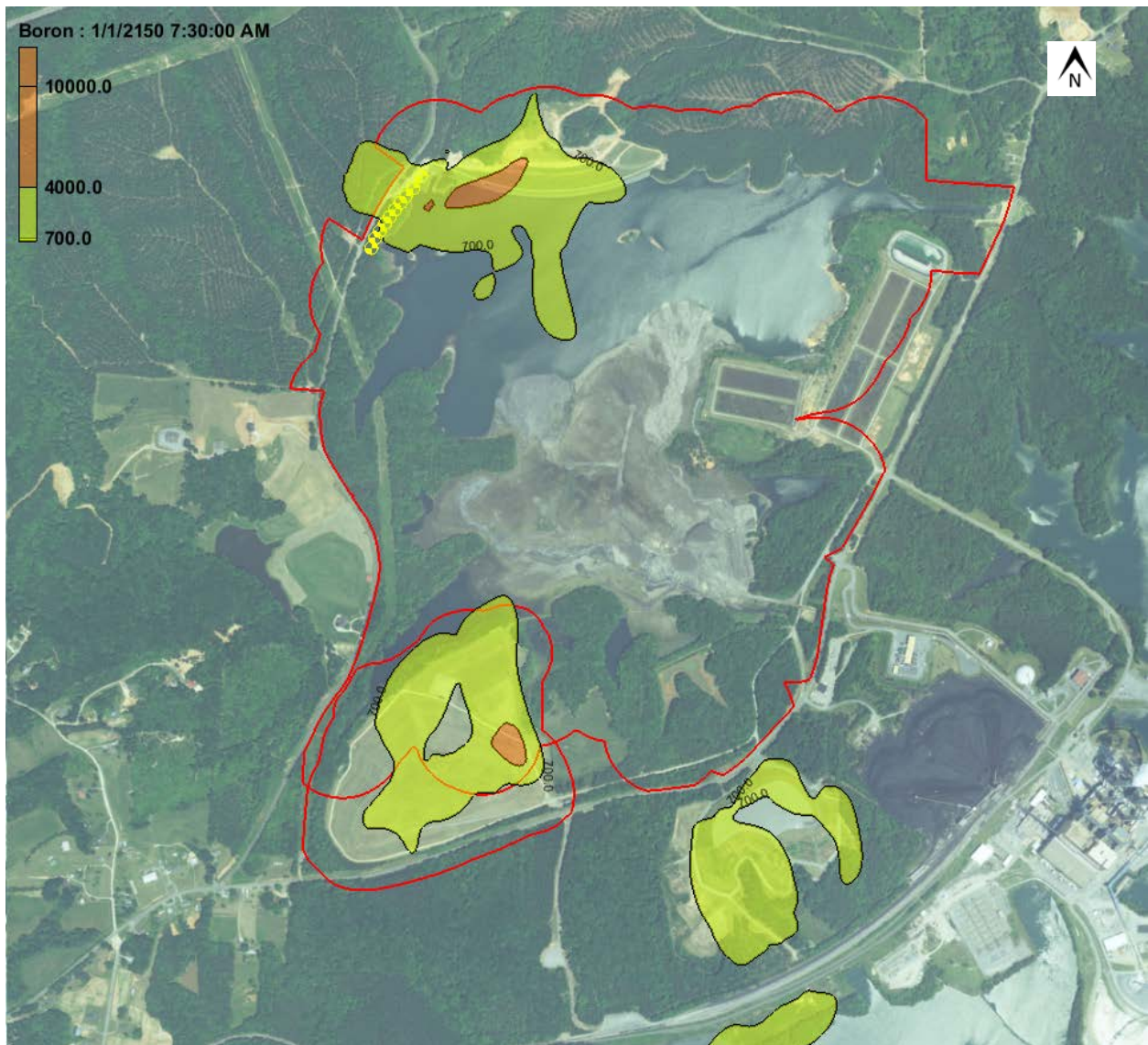


Figure 6-15c. Simulated boron concentrations in the upper bedrock (layer 16) in 2150 for the final cover scenario with 10 interim action groundwater extraction wells. The larger red outline is the ash basin compliance boundary and the smaller red outline is Pine Hall Road Landfill compliance boundary.

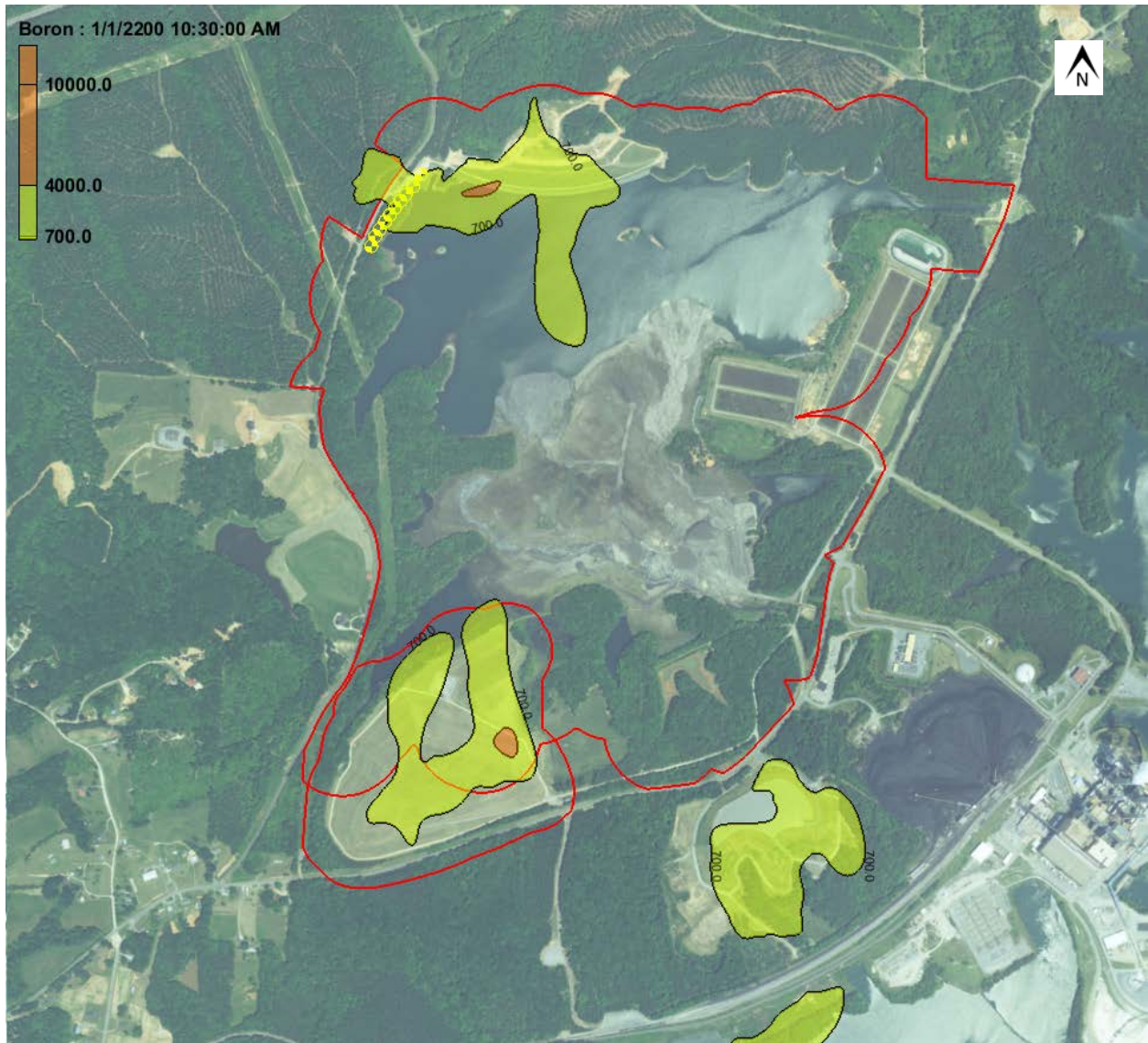


Figure 6-15d. Simulated boron concentrations in the upper bedrock (layer 16) in 2200 for the final cover scenario with 10 interim action groundwater extraction wells. The larger red outline is the ash basin compliance boundary and the smaller red outline is Pine Hall Road Landfill compliance boundary.

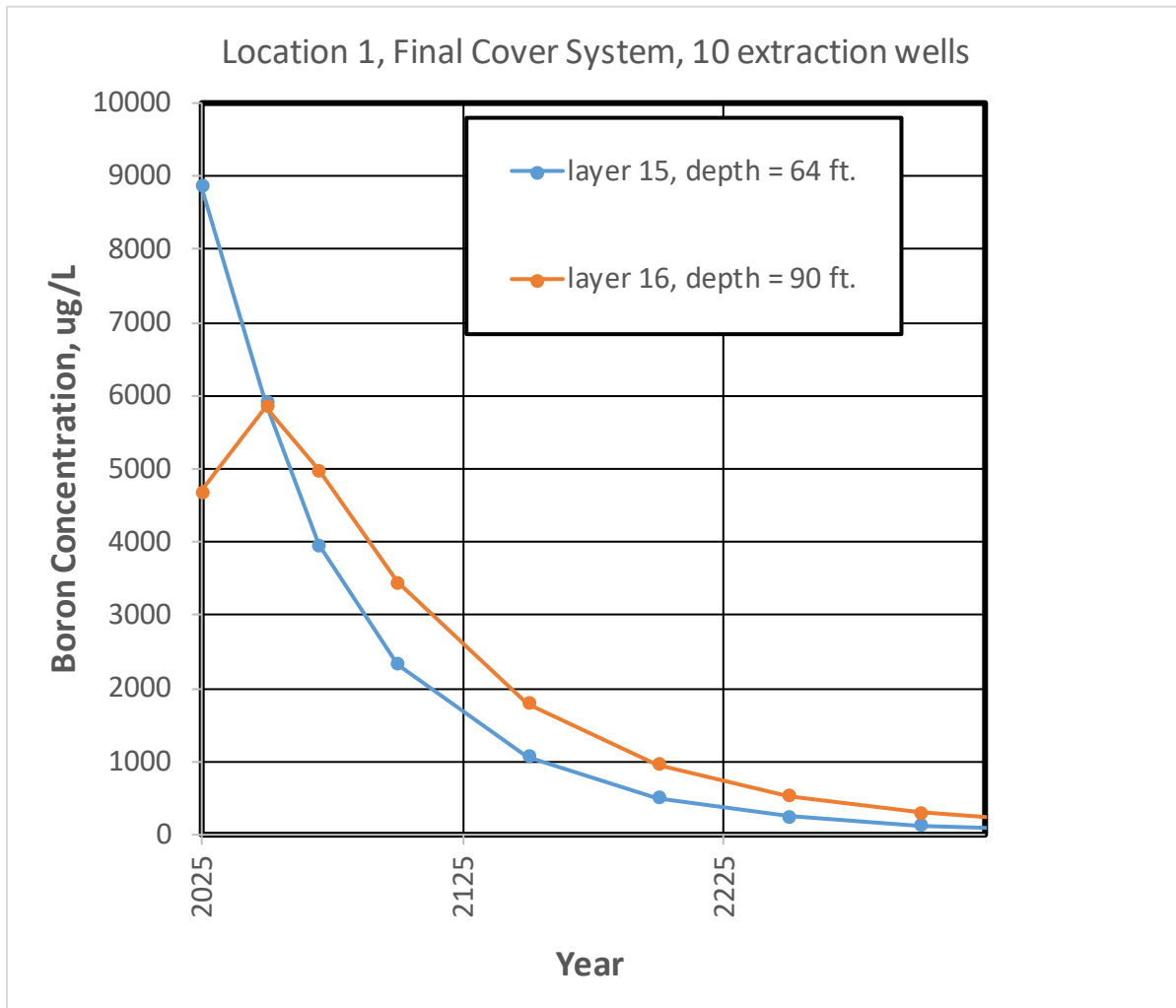


Figure 6-16. Predicted boron concentrations at location 1 along Middleton Loop Road for the final cover scenario with 10 interim action groundwater extraction wells.

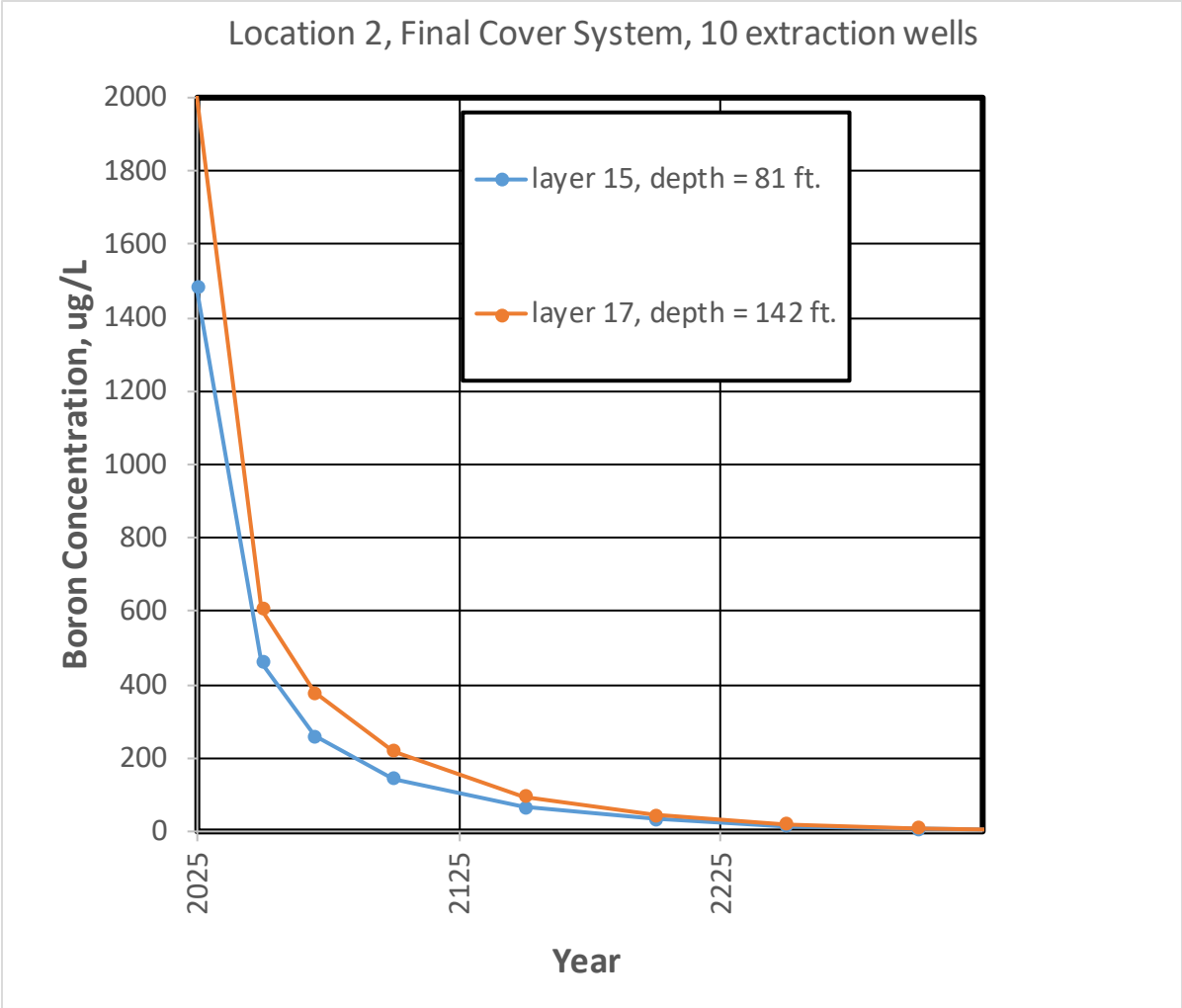


Figure 6-17. Predicted boron concentrations at location 2 below the ash basin dam for the final cover scenario with 10 interim action groundwater extraction wells.

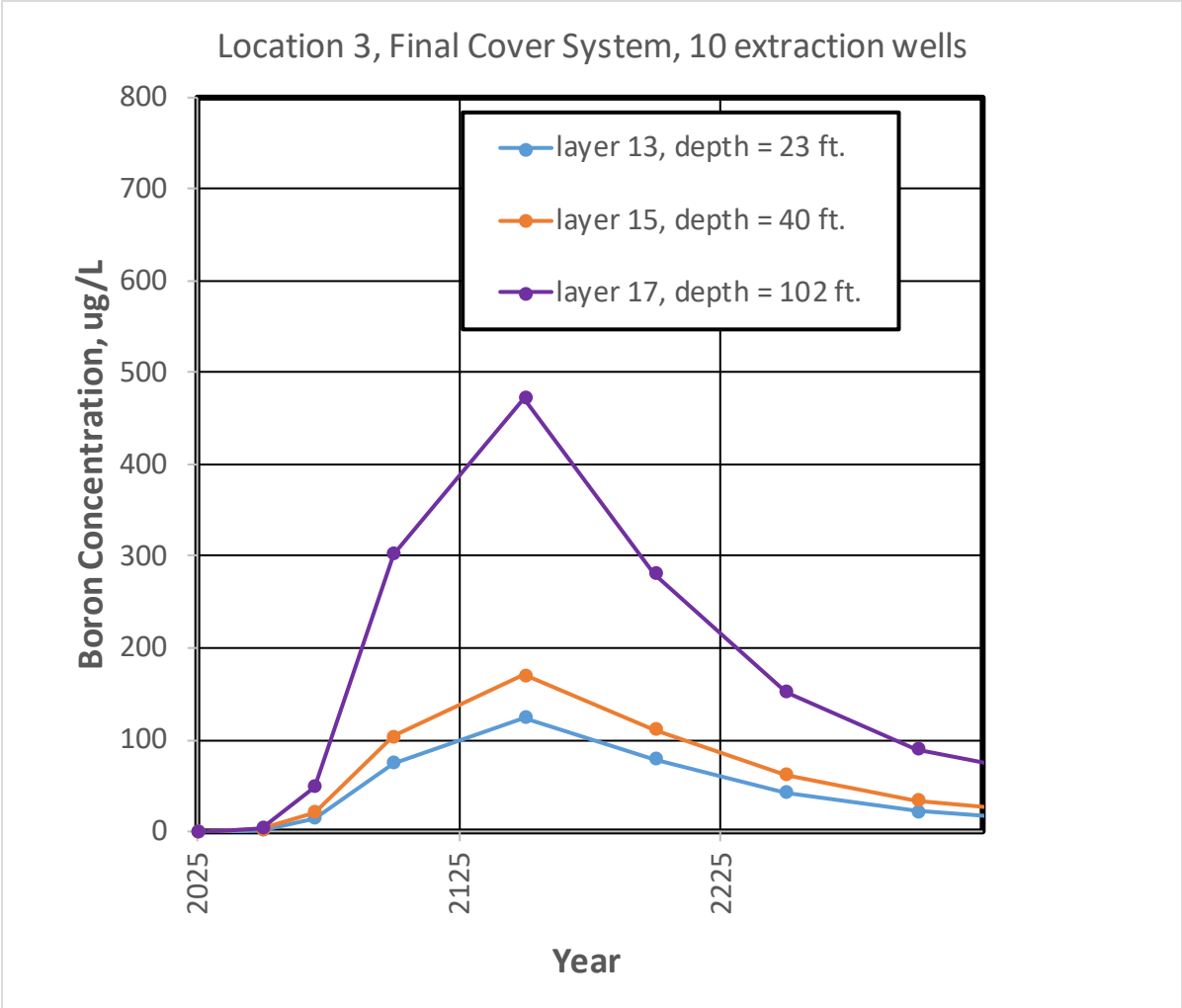


Figure 6-18. Predicted boron concentrations at location 3 near the Dan River for the final cover scenario with 10 interim action groundwater extraction wells.

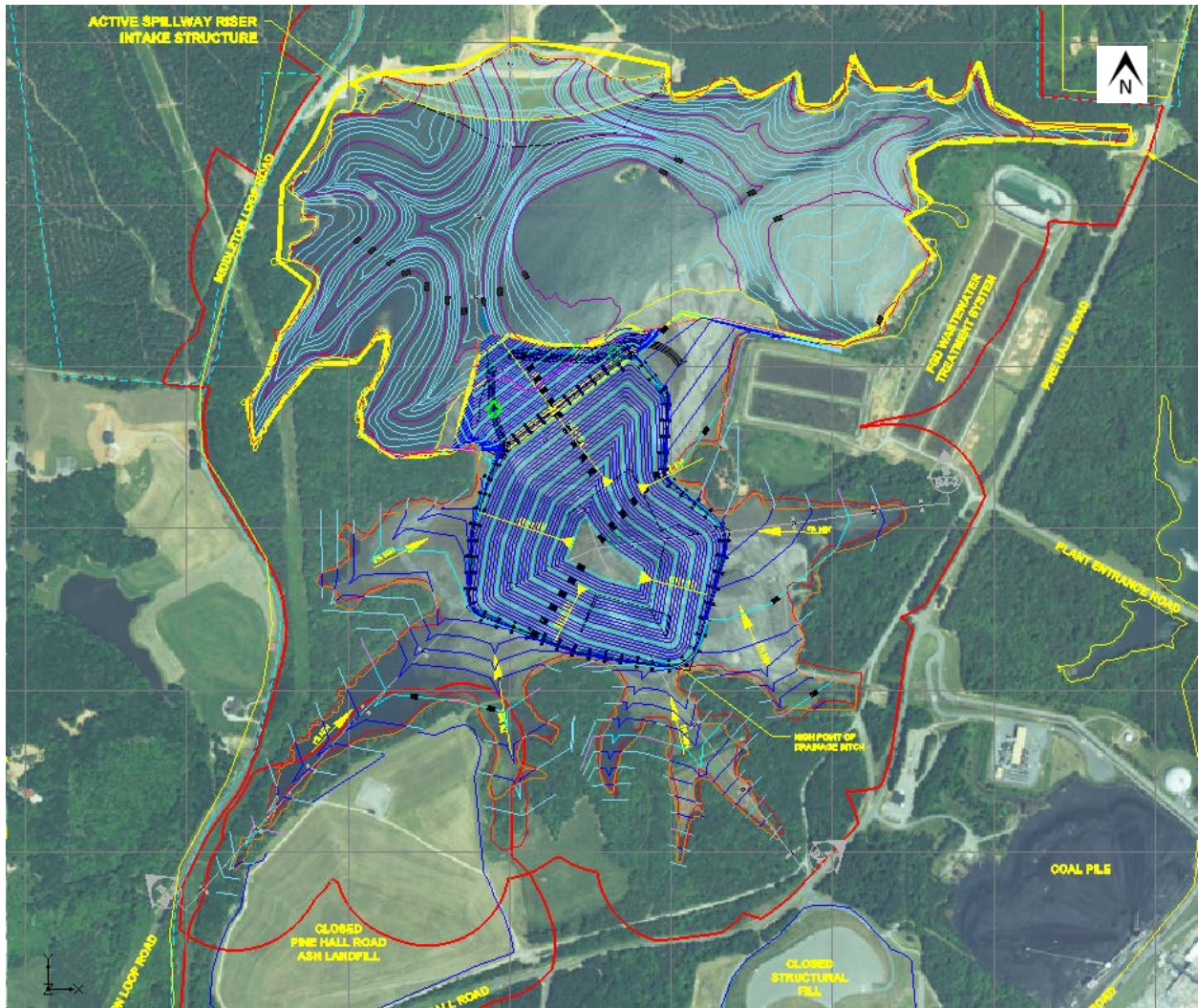


Figure 6-19. Hybrid closure design used in simulations. Depiction provided by AECOM.

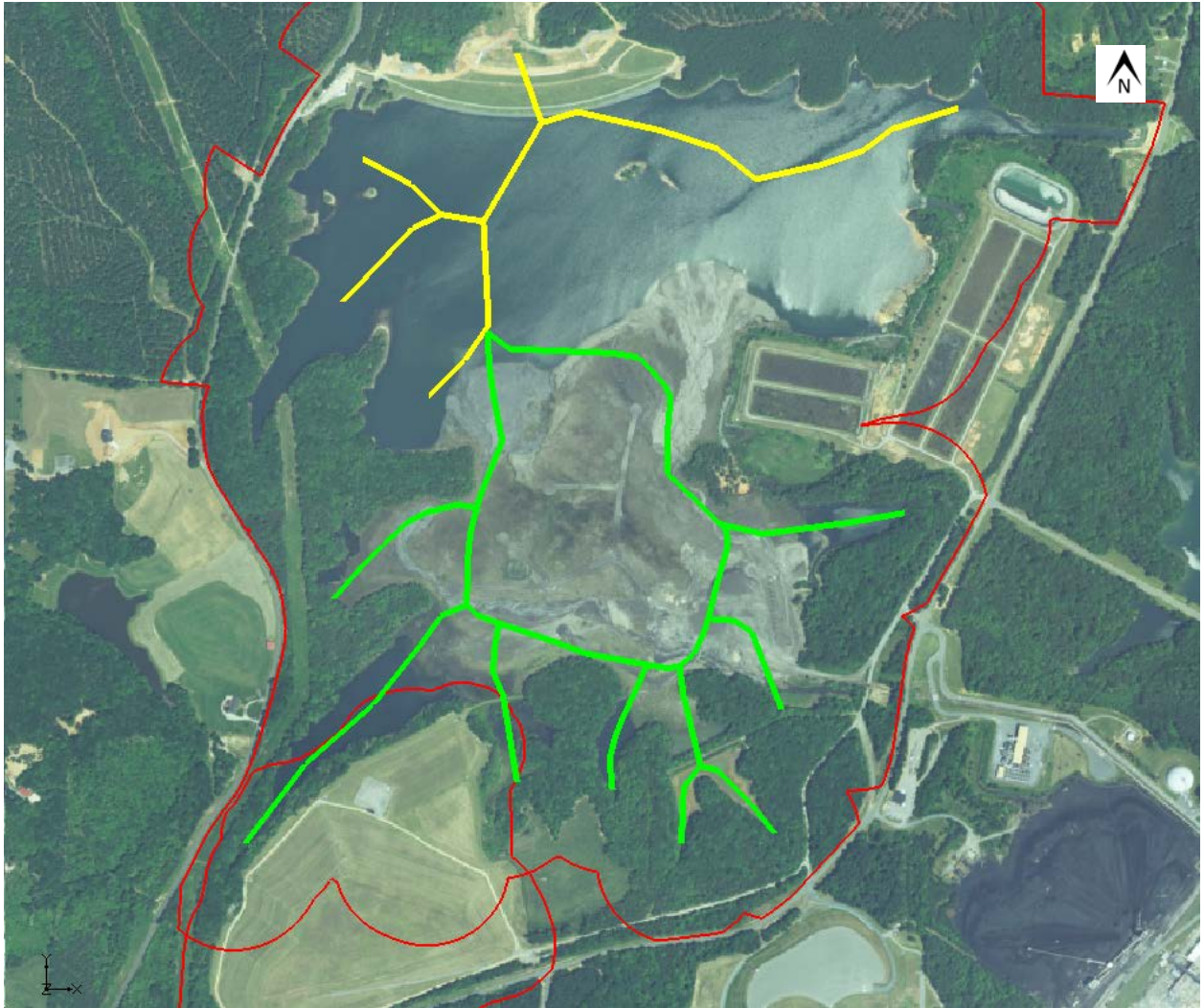


Figure 6-20. Drains used in the hybrid design simulation. Proposed ash basin underdrains (green lines) are present five feet beneath the cover system in the southern part of the basin. A drain network (yellow lines) is used in the excavated (northern) part of the basin to represent springs and streams that may form. The elevations are set to the top of the saprolite surface, which approximately corresponds to the original ground surface in this part of the basin.



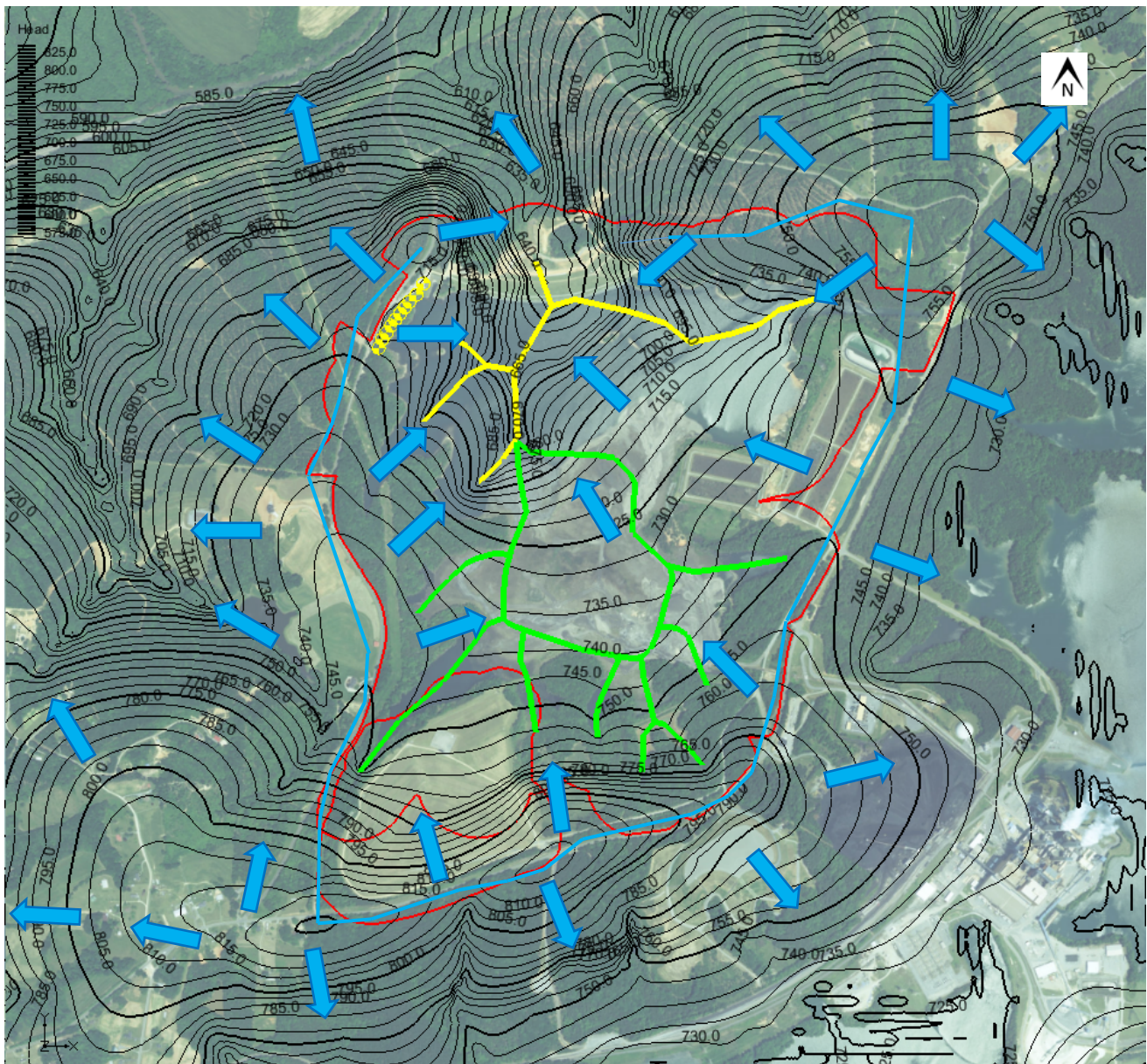


Figure 6-21. Simulated hydraulic heads for the hybrid scenario with 10 interim action groundwater extraction wells. The larger red outline is the ash basin compliance boundary and the smaller red outline is Pine Hall Road Landfill compliance boundary. Approximate groundwater divide in light blue and approximate flow directions as light blue arrows.

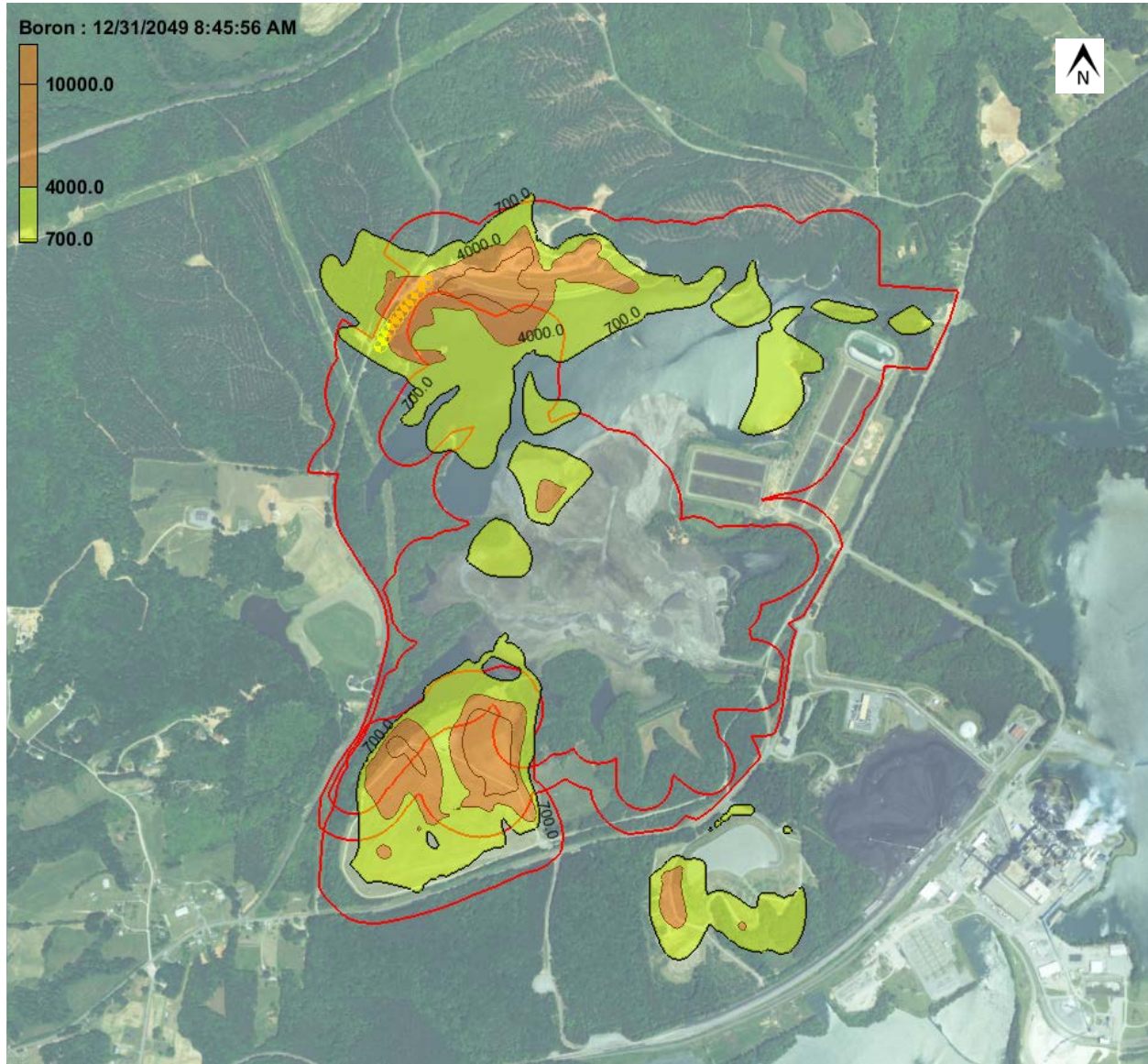


Figure 6-22a. Simulated boron concentrations in the transition zone (layer 15) in 2050 for the hybrid scenario with 10 interim action groundwater extraction wells. The outer red line is the current compliance boundary, and the inner red line is the new compliance boundary for the hybrid closure.

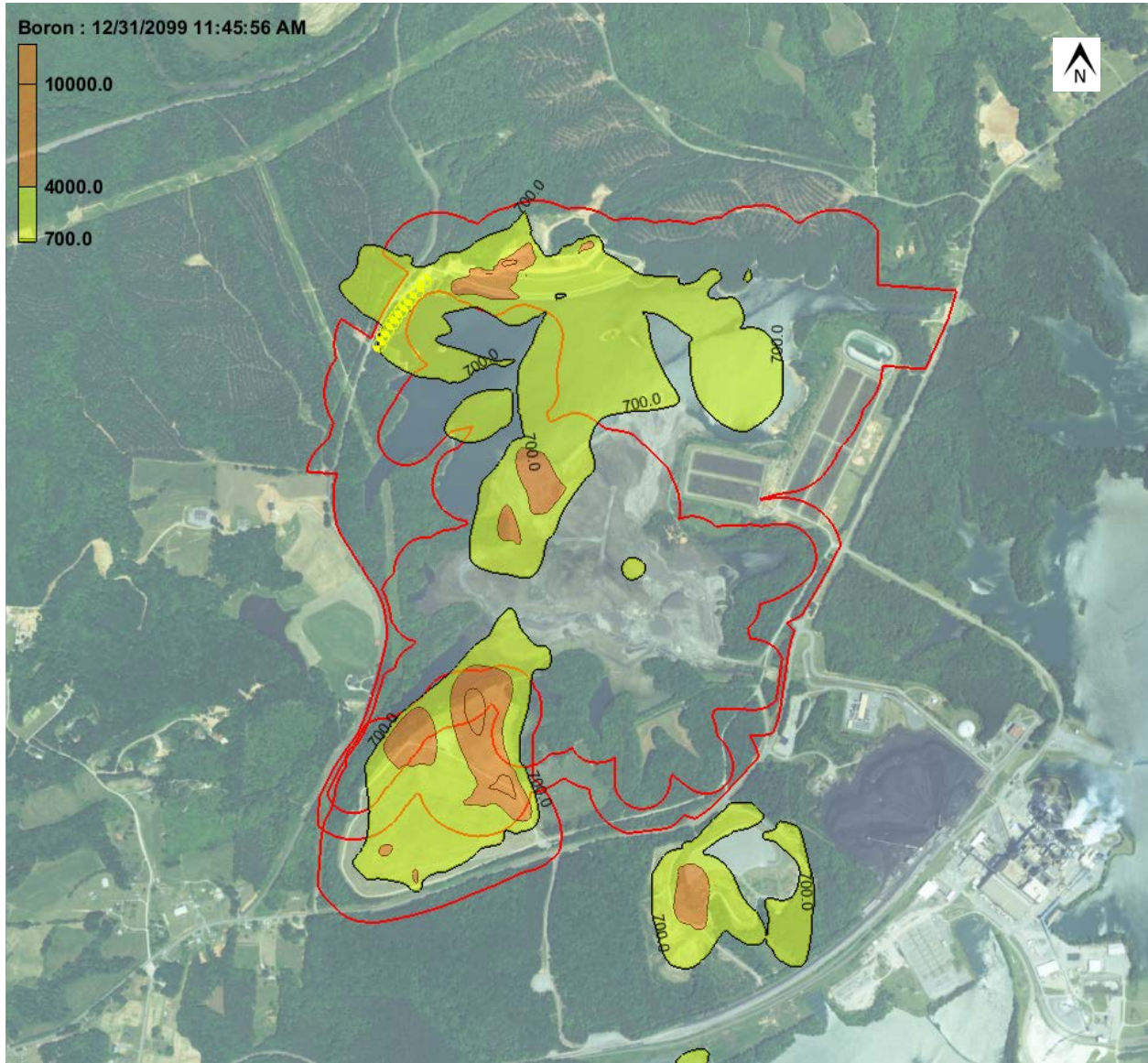


Figure 6-22b. Simulated boron concentrations in the transition zone (layer 15) in 2100 for the hybrid scenario with 10 interim action groundwater extraction wells. The outer red line is the current compliance boundary, and the inner red line is the new compliance boundary for the hybrid closure.

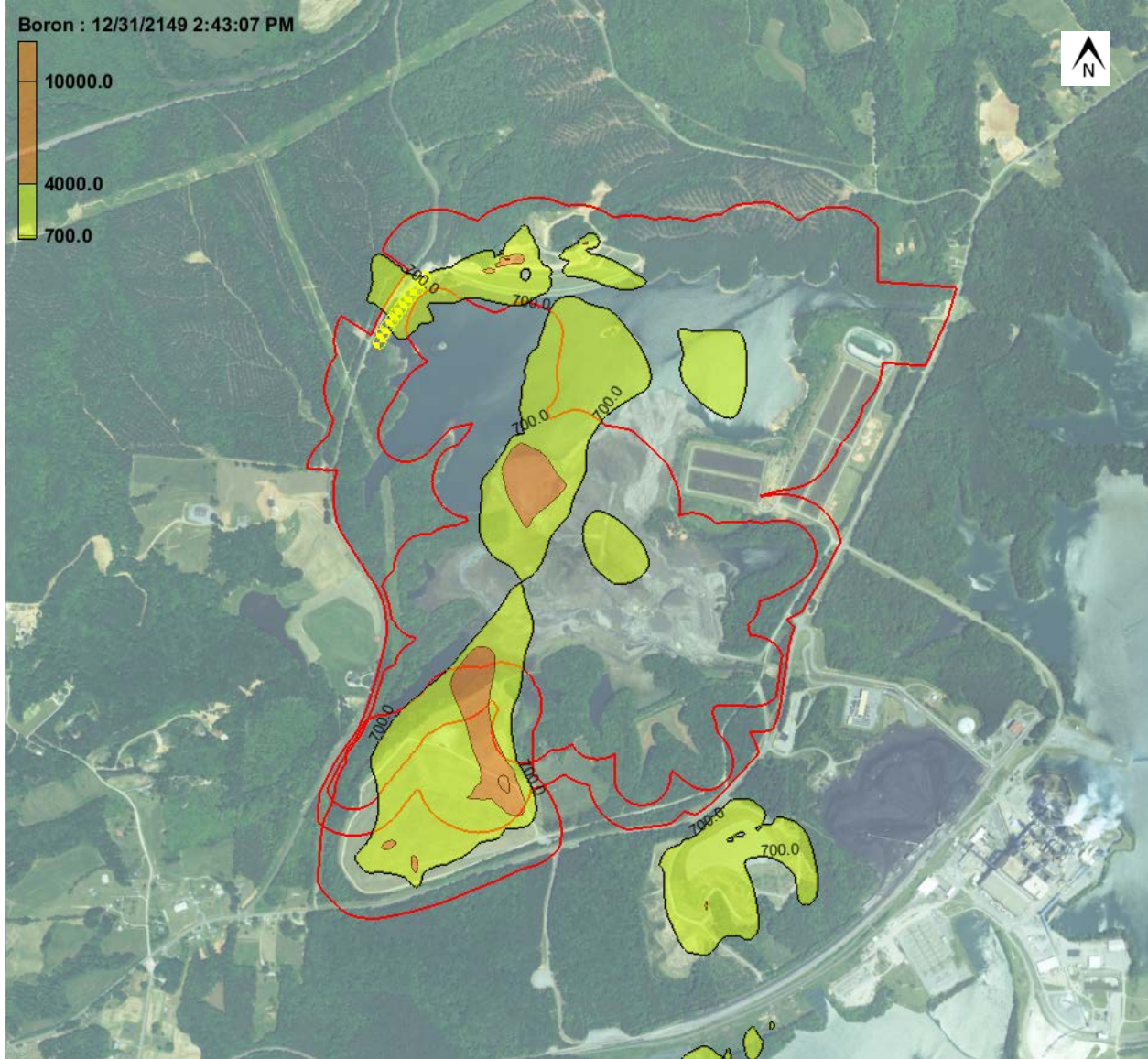


Figure 6-22c. Simulated boron concentrations in the transition zone (layer 15) in 2150 for the hybrid scenario with 10 interim action groundwater extraction wells. The outer red line is the current compliance boundary, and the inner red line is the new compliance boundary for the hybrid closure.

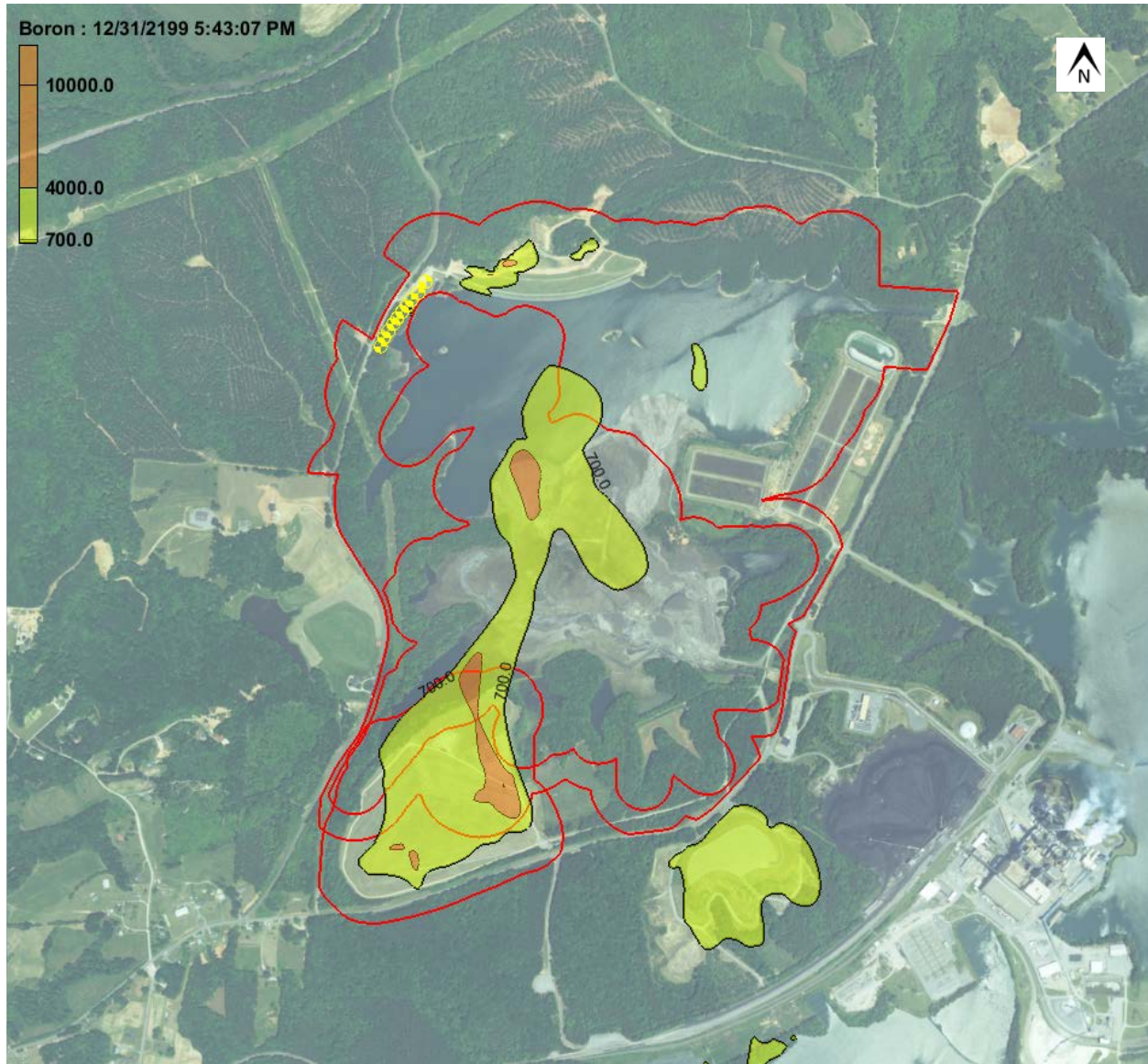


Figure 6-22d. Simulated boron concentrations in the transition zone (layer 15) in 2200 for the hybrid scenario with 10 interim action groundwater extraction wells. The outer red line is the current compliance boundary, and the inner red line is the new compliance boundary for the hybrid closure.

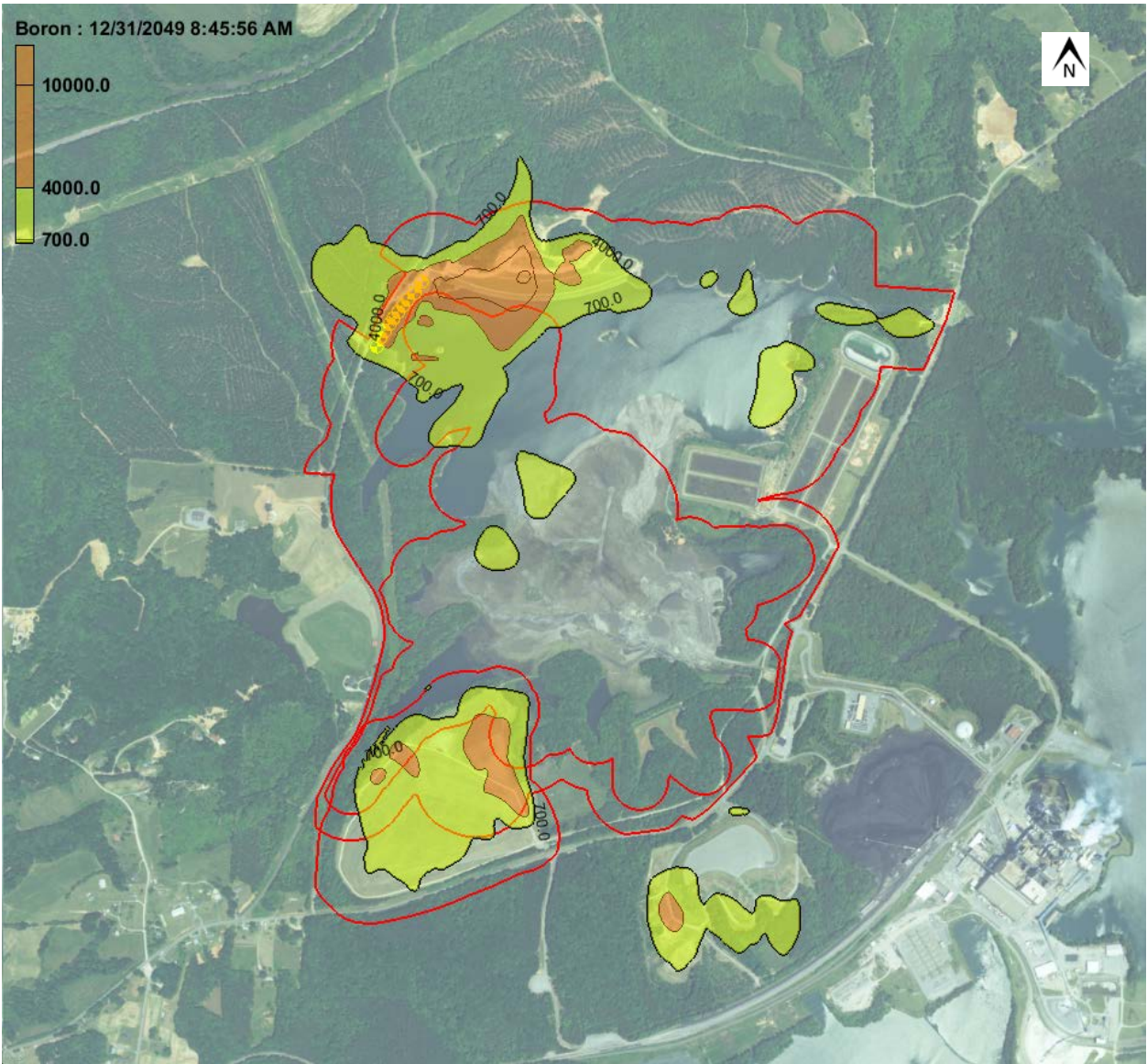


Figure 6-23a. Simulated boron concentrations in the upper bedrock (layer 16) in 2050 for the hybrid scenario with 10 interim action groundwater extraction wells. The outer red line is the current compliance boundary, and the inner red line is the new compliance boundary for the hybrid closure.

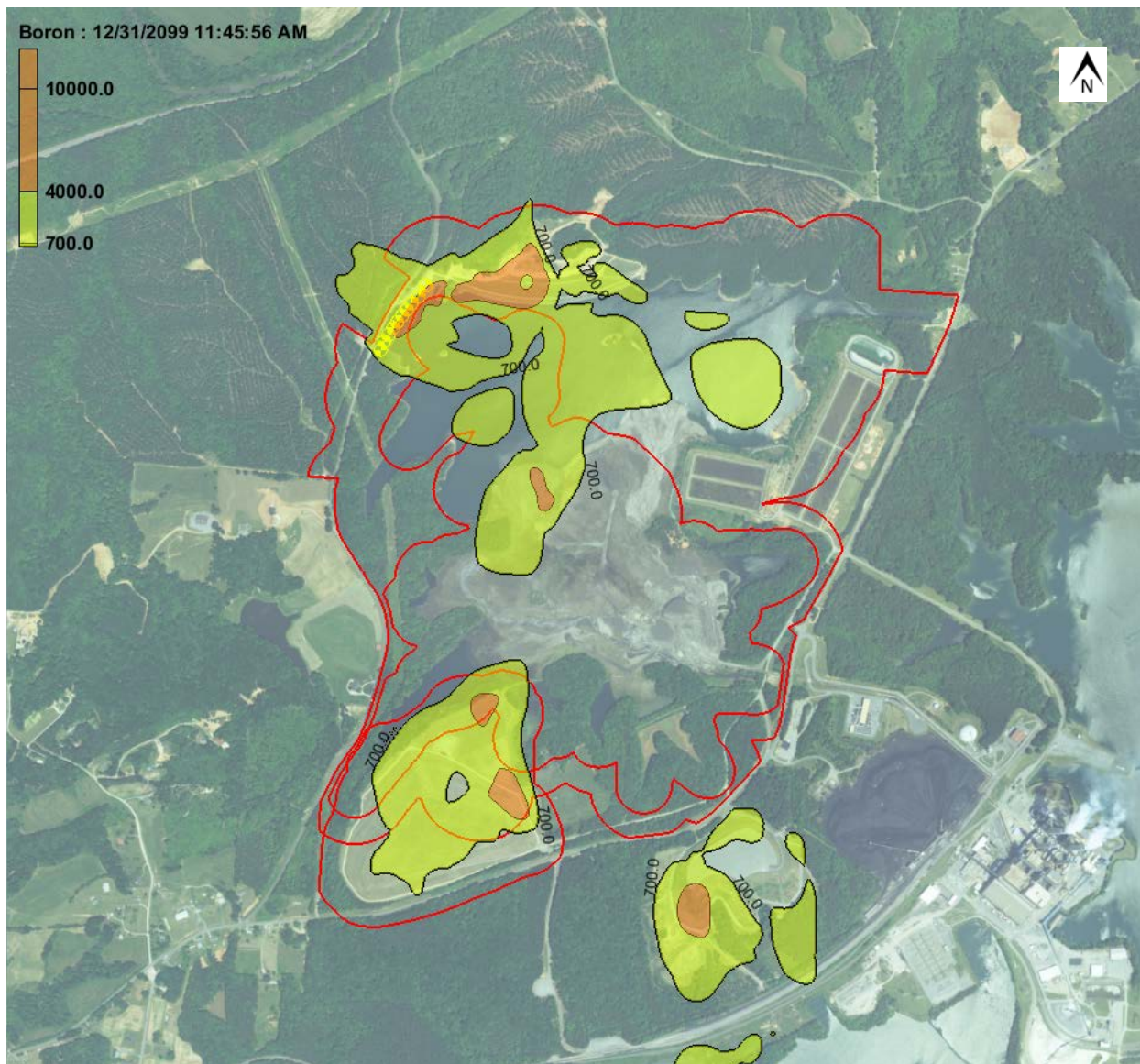


Figure 6-23b. Simulated boron concentrations in the upper bedrock (layer 16) in 2100 for the hybrid scenario with 10 interim action groundwater extraction wells. The outer red line is the current compliance boundary, and the inner red line is the new compliance boundary for the hybrid closure.

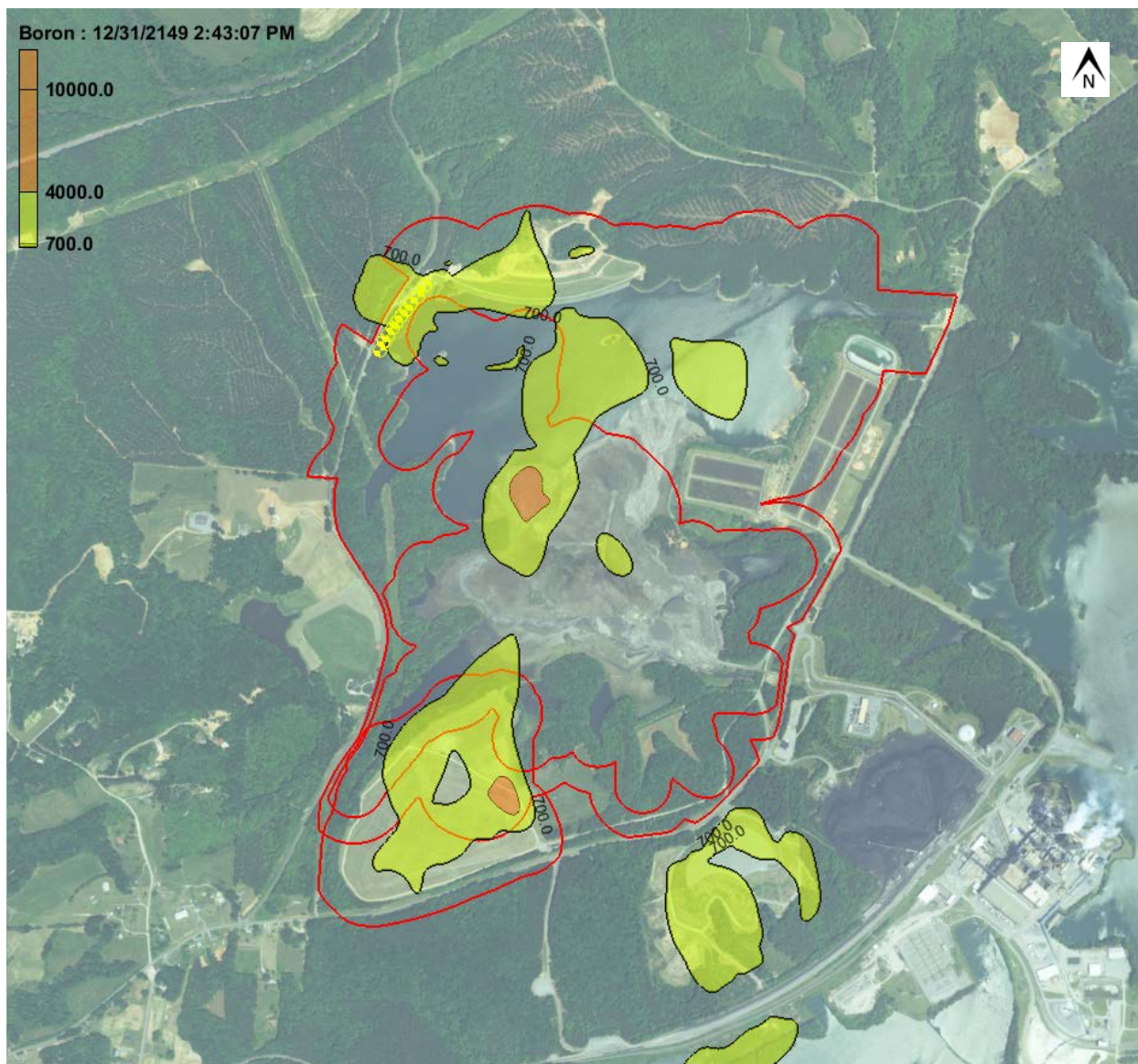


Figure 6-23c. Simulated boron concentrations in the upper bedrock (layer 16) in 2150 for the hybrid scenario with 10 interim action groundwater extraction wells. The outer red line is the current compliance boundary, and the inner red line is the new compliance boundary for the hybrid closure.



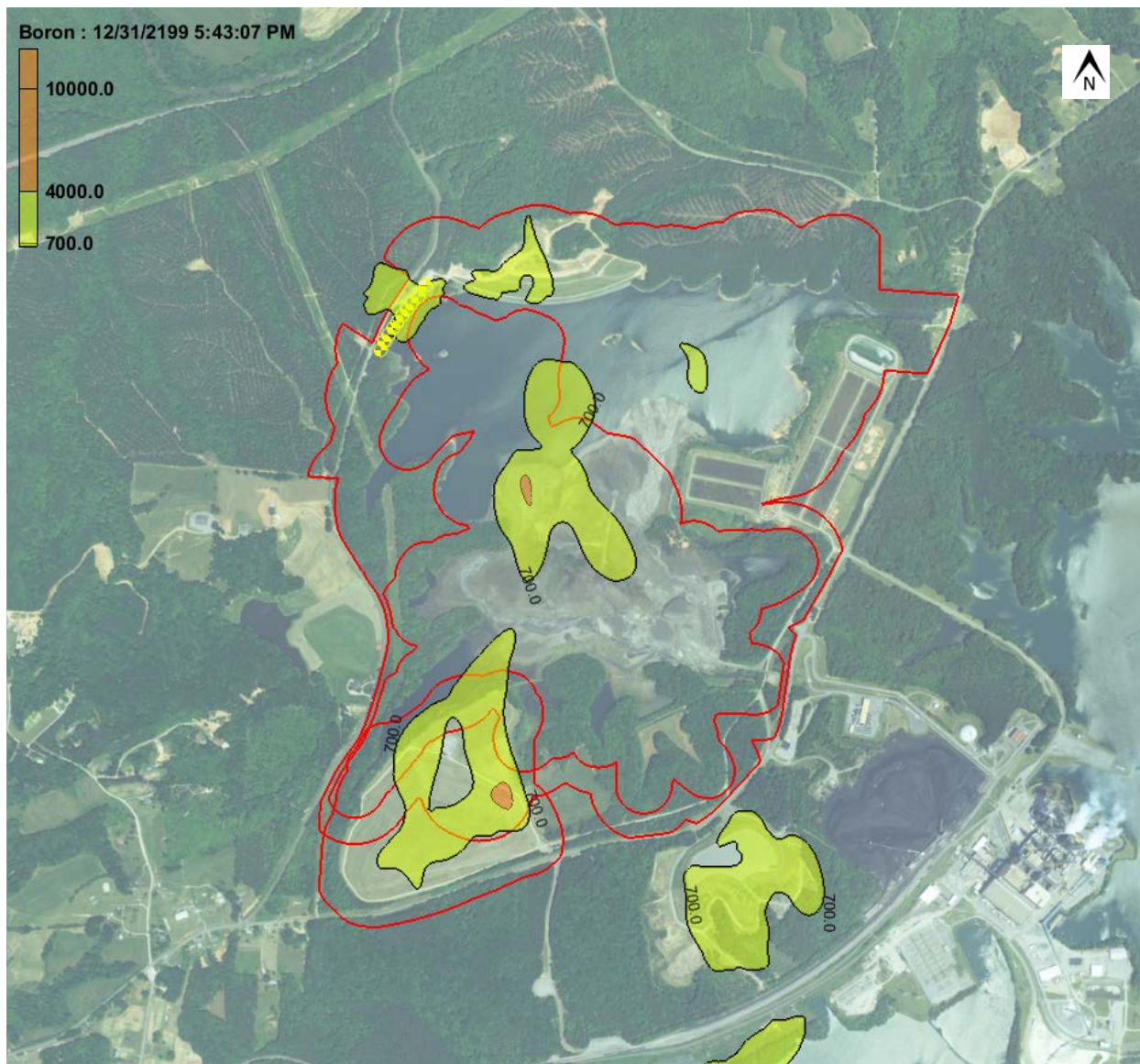


Figure 6-23d. Simulated boron concentrations in the upper bedrock (layer 16) in 2200 for the hybrid scenario with 10 interim action groundwater extraction wells. The outer red line is the current compliance boundary, and the inner red line is the new compliance boundary for the hybrid closure.

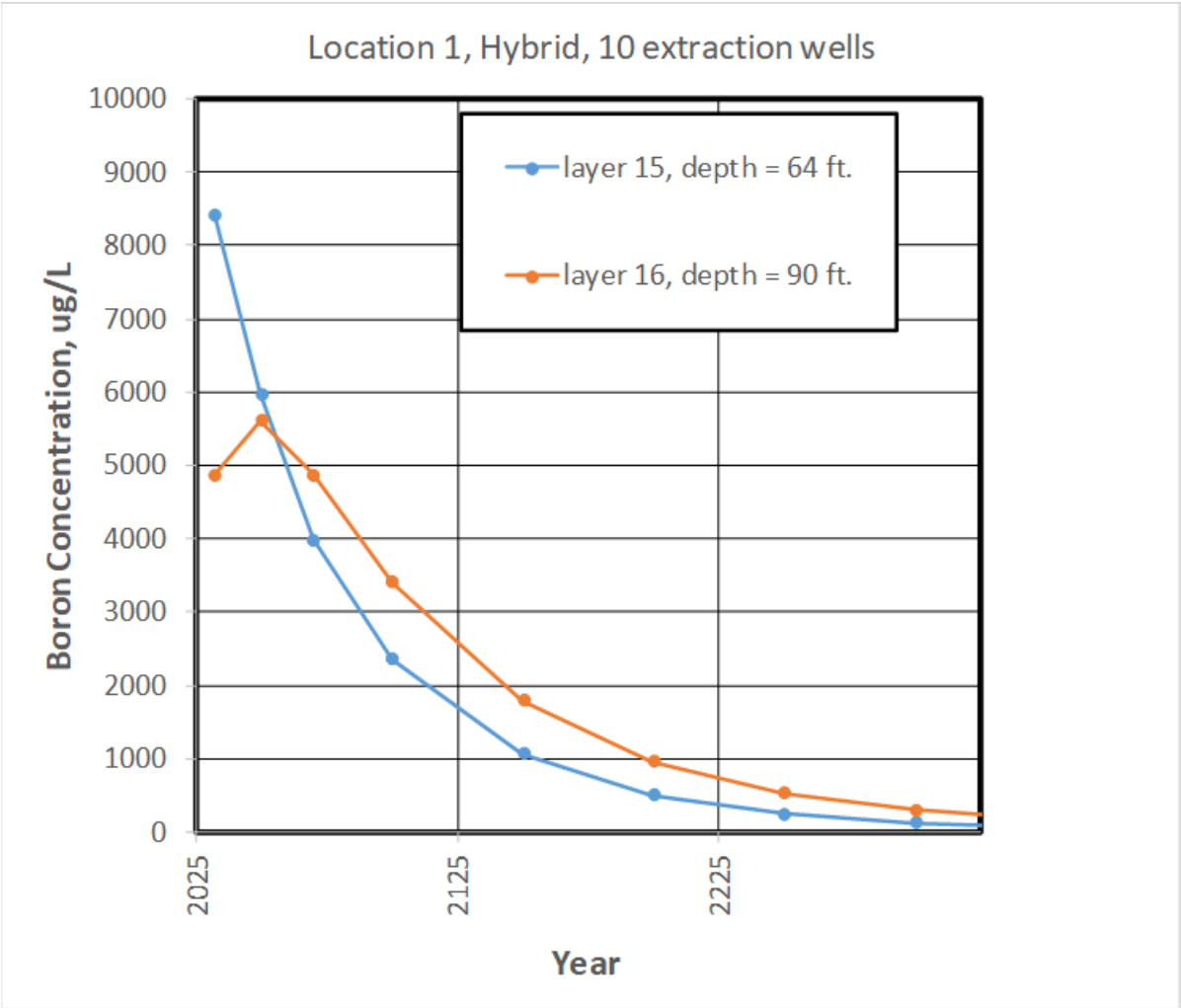


Figure 6-24. Predicted boron concentrations at location 1 along Middleton Loop Road for the hybrid scenario with 10 interim action groundwater extraction wells.

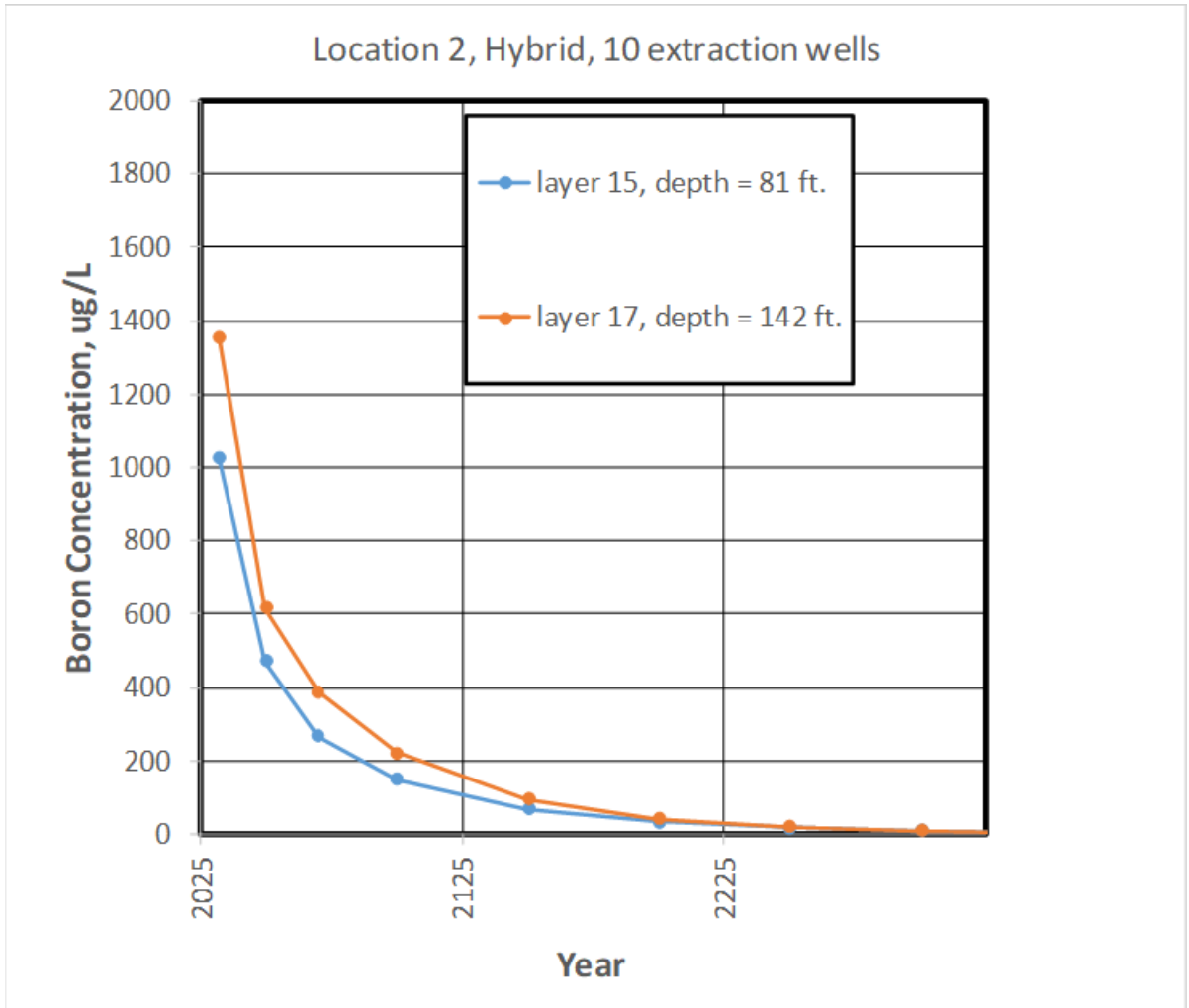


Figure 6-25. Predicted boron concentrations at location 2 below the ash basin dam for the hybrid scenario with 10 interim action groundwater extraction wells.

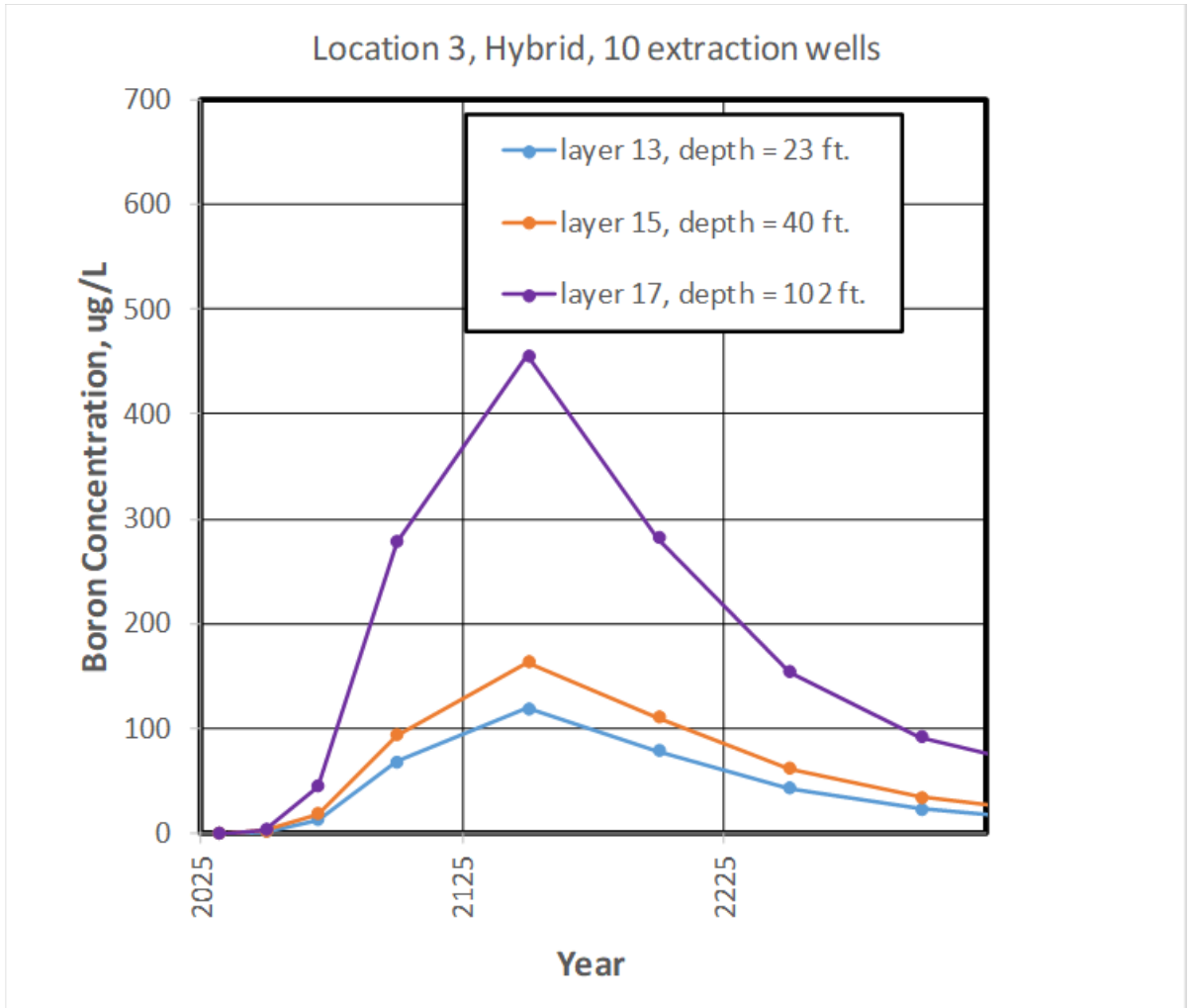
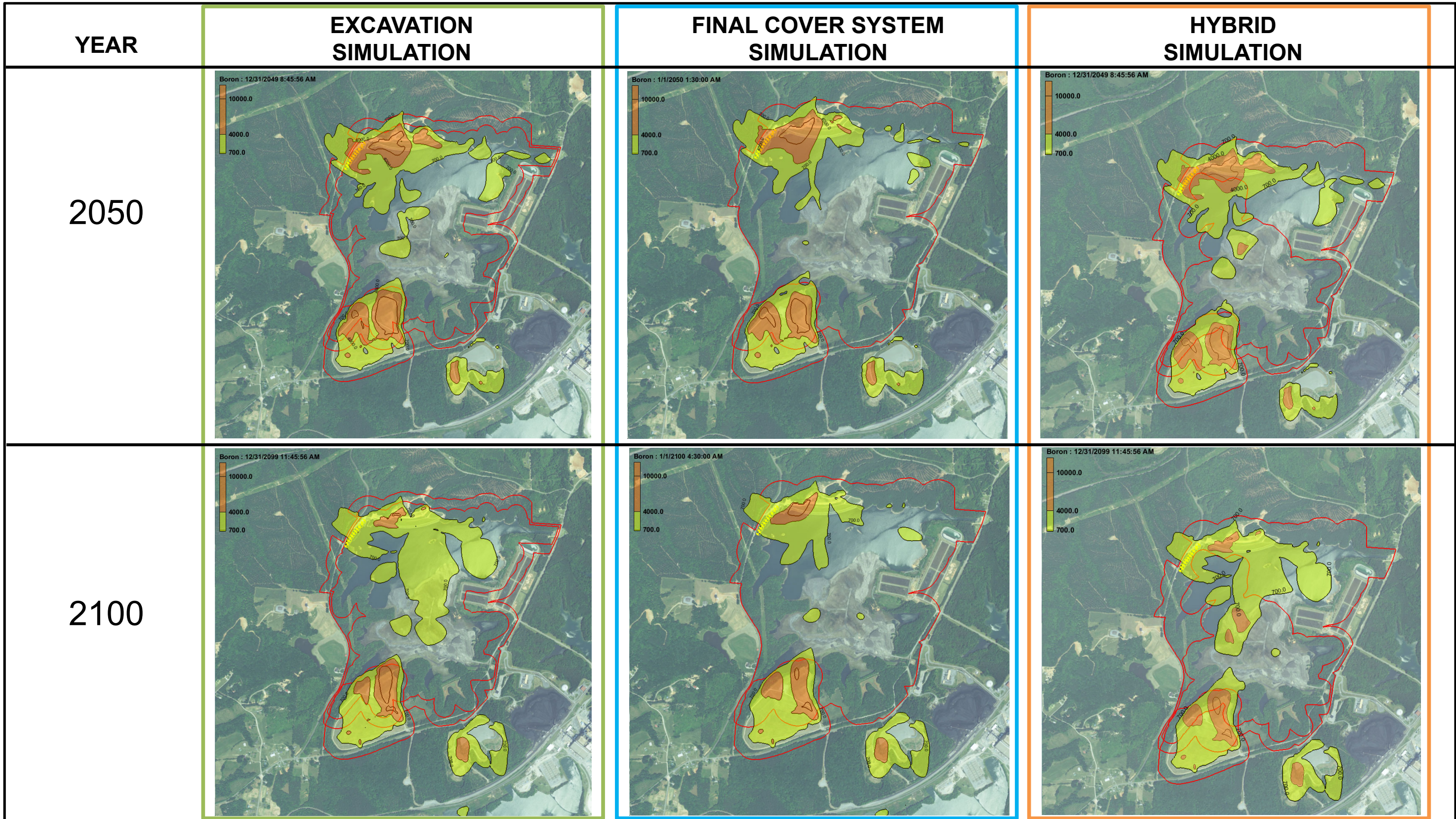


Figure 6-26. Predicted boron concentrations at location 3 near the Dan River for the hybrid scenario with 10 interim action groundwater extraction wells.

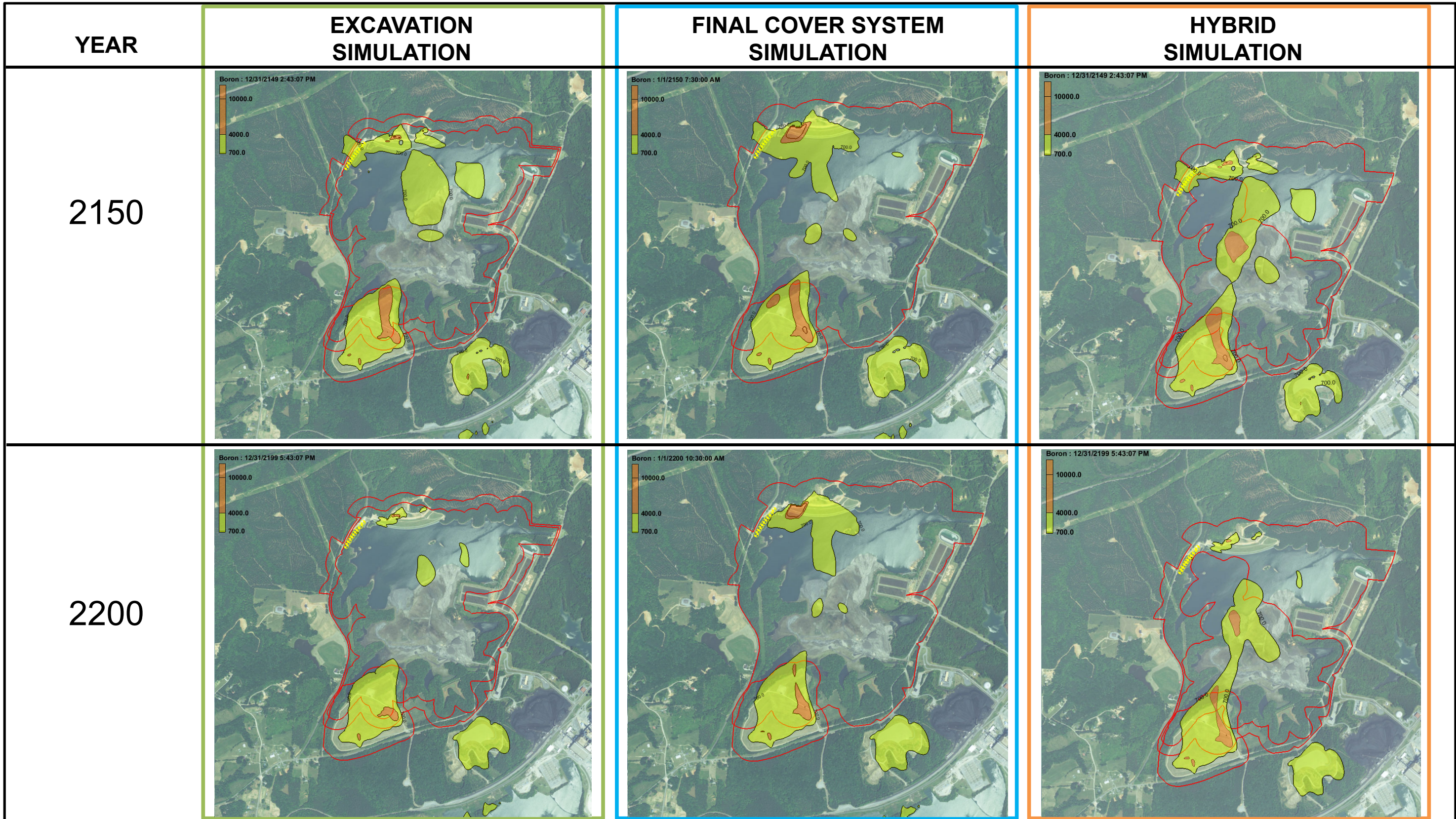


**NOTES:**  
THE START DATES FOR THE THREE MODEL SCENARIOS ARE BASED ON THE COMPLETION DATES FOR THOSE ACTIVITIES. THESE DATES ARE:

- EXCAVATION – YEAR 2032
- FINAL COVER SYSTEM – YEAR 2025
- HYBRID – YEAR 2032

EXISTING COMPLIANCE BOUNDARY AS OUTER RED LINE.  
FUTURE COMPLIANCE BOUNDARY ASSOCIATED WITH BASIN CLOSURE OPTION AS INNER RED LINE.

**FIGURE 6-27**  
**COMPARISON OF CLOSURE OPTIONS FOR THE**  
**TRANSITION FLOW ZONE**  
**MODEL YEARS 2050 AND 2100**  
**BELEWS CREEK STEAM STATION**  
**DUKE ENERGY PROGRESS, LLC**  
**BELEWS CREEK, NORTH CAROLINA**

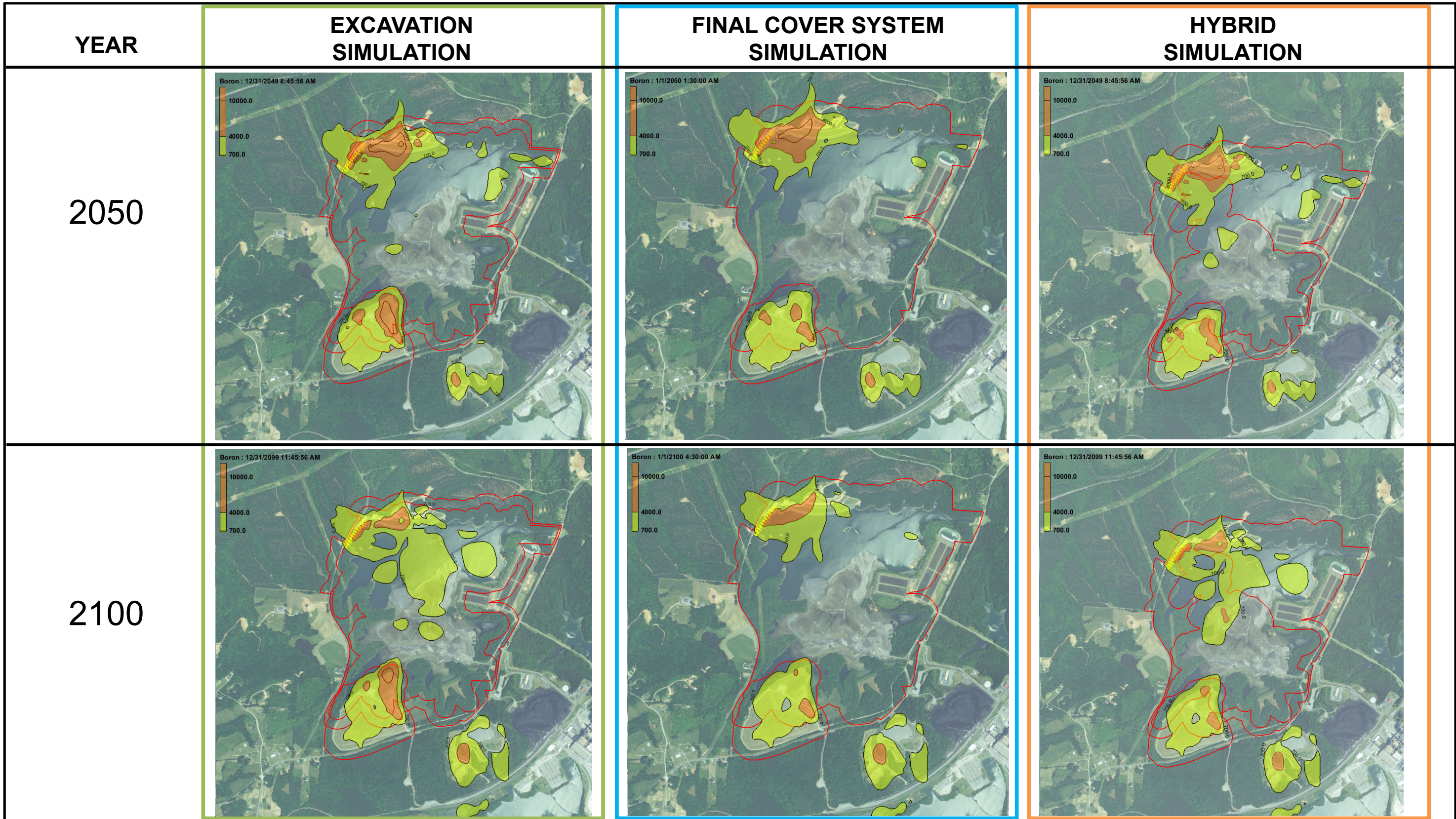


**NOTES:**  
THE START DATES FOR THE THREE MODEL SCENARIOS ARE BASED ON THE COMPLETION DATES FOR THOSE ACTIVITIES. THESE DATES ARE:

- EXCAVATION – YEAR 2032
- FINAL COVER SYSTEM – YEAR 2025
- HYBRID – YEAR 2032

EXISTING COMPLIANCE BOUNDARY AS DARK BLUE LINE.  
FUTURE COMPLIANCE BOUNDARY LIGHT BLUE LINE ASSOCIATED WITH BASIN CLOSURE OPTION.

**FIGURE 6-28**  
**COMPARISON OF CLOSURE OPTIONS FOR THE**  
**TRANSITION FLOW ZONE**  
**MODEL YEARS 2150 AND 2200**  
**BELEWS CREEK STEAM STATION**  
**DUKE ENERGY PROGRESS, LLC**  
**BELEWS CREEK, NORTH CAROLINA**

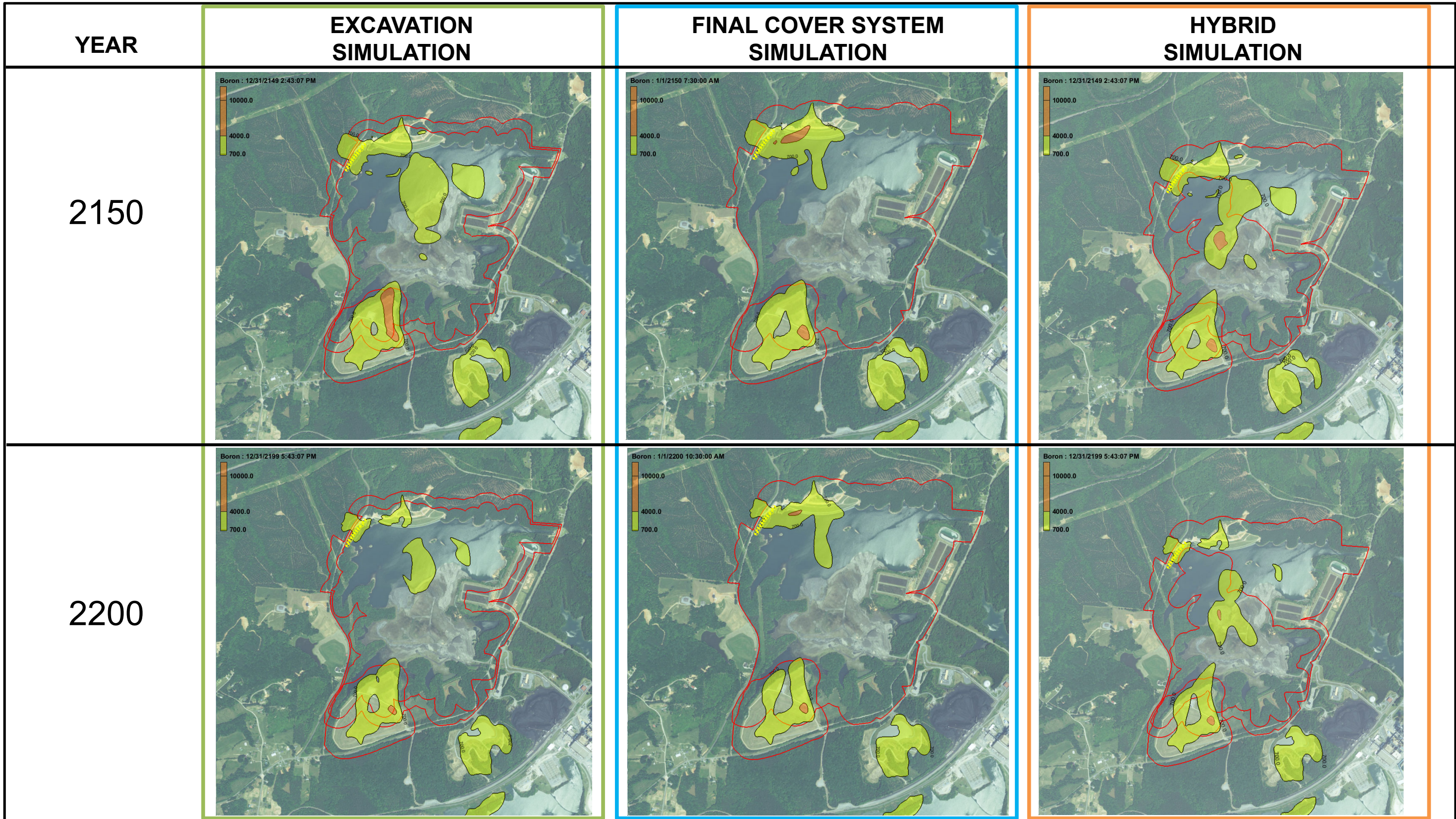


**NOTES:**  
 THE START DATES FOR THE THREE MODEL SCENARIOS ARE BASED ON THE COMPLETION DATES FOR THOSE ACTIVITIES. THESE DATES ARE:

- EXCAVATION – YEAR 2032
- FINAL COVER SYSTEM – YEAR 2025
- HYBRID – YEAR 2032

EXISTING COMPLIANCE BOUNDARY AS DARK BLUE LINE.  
 FUTURE COMPLIANCE BOUNDARY LIGHT BLUE LINE ASSOCIATED WITH BASIN CLOSURE OPTION.

**FIGURE 6-29**  
**COMPARISON OF CLOSURE OPTIONS FOR THE**  
**UPPER BEDROCK FLOW ZONE**  
**MODEL YEARS 2050 AND 2100**  
**BELEWS CREEK STEAM STATION**  
**DUKE ENERGY PROGRESS, LLC**  
**BELEWS CREEK, NORTH CAROLINA**



**NOTES:**  
 THE START DATES FOR THE THREE MODEL SCENARIOS ARE BASED ON THE COMPLETION DATES FOR THOSE ACTIVITIES. THESE DATES ARE:

- EXCAVATION – YEAR 2032
- FINAL COVER SYSTEM – YEAR 2025
- HYBRID – YEAR 2032

EXISTING COMPLIANCE BOUNDARY AS DARK BLUE LINE.  
 FUTURE COMPLIANCE BOUNDARY LIGHT BLUE LINE ASSOCIATED WITH BASIN CLOSURE OPTION.

**FIGURE 6-30**  
**COMPARISON OF CLOSURE OPTIONS FOR THE**  
**UPPER BEDROCK FLOW ZONE**  
**MODEL YEARS 2150 AND 2200**  
**BELEWS CREEK STEAM STATION**  
**DUKE ENERGY PROGRESS, LLC**  
**BELEWS CREEK, NORTH CAROLINA**